

A STUDY OF URANIUM IN GROUND WATER AROUND
GREYHAWK MINE, BANCROFT, ONTARIO

By



DAUD BIN MOHAMAD, B.Sc.

A Thesis

Submitted to the School of Graduate Studies
in Partial Fulfilment of the Requirements

for the Degree

Master of Science

McMaster University

June 1980

STUDIES ON URANIUM IN GROUND WATER

MASTER OF SCIENCE (1980)
(Geology)

McMASTER UNIVERSITY
Hamilton, Ontario

TITLE: A Study of Uranium in Ground Water Around Greyhawk Mine,
Pancroft, Ontario

AUTHOR: Daud Bin Mohamad, B.Sc.

(National University
of Malaysia)

SUPERVISORS: Dr. Henry P. Schwarcz and
Dr. Derek C. Ford

NUMBER OF PAGES: xii, 119

ABSTRACT

The mining operations at the Greyhawk Uranium Mine began in 1956 and were discontinued in 1959. As a consequence of the mining operations, a waste rock pile (pegmatite granite and gabbro) was developed at the site. These rocks have subsequently undergone weathering processes and consequently introduced leachate into the aquifer.

The uranium content and uranium isotope ratio ($^{234}\text{U}/^{238}\text{U}$) of the Greyhawk groundwaters were measured utilising the analytical methods of isotope dilution and alpha-particle spectrometry. Uranium contents range from about 1.2 to as high as 380 ppb. Most samples at deep sampling points ($>7\text{m}$) are usually anomalously high. This suggests that a plume of uranium-rich water possibly emanating from the waste rock source is migrating in the deeper part of the aquifer. The high uranium content in the waters at greater depths may also be attributed to leaching of the buried bedrock surface by acid water of the waste dump. This U-rich water also has distinctly higher $^{234}\text{U}/^{238}\text{U}$ ratios. The samples at the water table closest to the waste rock source also showed quite significant concentration of uranium. Uranium in these waters occurs predominantly as stable and soluble uranyl carbonate complexes; part of the dissolved uranium is taken by the porous medium as it passes through, as shown by high concentrations of leachable uranium on the sediment of the aquifer.

Generally, the Greyhawk groundwaters have a relatively low $^{234}\text{U}/^{238}\text{U}$ ratio which ranges between 0.95 and 1.85. Most samples have U ratios between 1.00 and 1.30. Migration of ^{234}U -enriched water was

observed at intermediate and bottom depths of the aquifer. The spatial distribution of isotope ratios in the aquifer indicates the migrating path of the contaminants emanating from the waste rock source. The enrichment of ^{234}U over ^{238}U is probably due to preferential leaching of ^{234}U from the waste rock as well as from the bedrock.

The thermal neutron activation-delayed neutron counting technique is also applied to the analysis of uranium content in the water. The technique is non-destructive, rapid, moderately accurate and precise and appears satisfactory for uranium prospecting purposes.

The possibility of applying combined fission track and alpha track counting technique to determine isotopic ratios ($^{234}\text{U}/^{238}\text{U}$) is investigated in this programme. The ratios obtained by this technique are promising and generally are in good agreement with those determined on an alpha-particle spectrometry. This technique has a great potential in the determination of $^{234}\text{U}/^{238}\text{U}$ ratio in natural water. However, some improvements on the technique are still needed to make the method more reliable, quantitative and rapid.

ACKNOWLEDGEMENTS

I wish to thank the following people whose assistance throughout this work is appreciated and hereby acknowledged.

1. Dr. Henry P. Schwarcz and Dr. Derek C. Ford who diligently supervised the entire work. Their criticism, suggestions and encouragement were of immense help.
2. Dr. Melvyn Gascoyne for his helpful suggestions and discussion particularly in the analytical procedure.
3. Mr. Alfred Latham for his help with the electrodeposition method of U.
4. Mr. Martin C. Knyf and Mrs. Marija Russell for their help during analytical work.
5. Dr. John A. Cherry of University of Waterloo, for arranging the field trip to Bancroft.
6. Messrs. Eric Veska and W. Clarke of University of Waterloo, for their help in the field, providing hydrogeological data and their helpful discussions and constant friendship.
7. Dr. Marilyn Truscott who provided muscovite and CN85 film for fission- and alpha-tracks analysis.
8. Dr. John Andrews of University of Bath for his helpful suggestion and discussion in the combined fission-track and alpha-track counting technique.
9. Messrs. Peter Earnst and Mike Butler and Dr. Eric Hoffman for their help in irradiation work. Dr. Eric Hoffman did the analysis of U content of rock and water samples by the neutron activation-delayed neutron counting technique.
10. Mr. Jack Whorwood for his help in the preparation of photographic work in this thesis.
11. Mrs. Jackie Hassan for typing the final report.

I wish to thank the Ministry of Environment, Ontario, for performing the major ions and trace metal analyses for some of the water samples. Lastly, but not the least, I wish to thank the Government of Malaysia for awarding me a scholarship (financial support) during my stay in Canada.

TABLE OF CONTENTS

		<u>Page</u>
CHAPTER I.	INTRODUCTION	1
1.1	General Statement	1
1.2	Objectives of this Study	2
1.3	Hydrogeochemistry of Uranium	3
1.4	Mechanisms of Uranium Isotopic Fractionation	5
1.5	Previous $^{234}\text{U}/^{238}\text{U}$ Studies	8
CHAPTER II	THE STUDY AREA	11
2.1	Location	11
2.2	Geology	11
2.2.1	Regional Geology	11
2.2.2	Local Geology	14
2.3	Hydrology	14
2.4	Description of the overburden	17
2.5	Mining Activity and Land Use	17
2.6	Previous Studies of the Greyhawk Mine and the Surrounding Area	18
CHAPTER III	SAMPLING AND ANALYTICAL PROCEDURES	21
3.1	Sampling and Field Procedure	21
3.2	Laboratory Procedure	25
3.2.1	Alpha Spectrometry Technique	25
3.2.2	Neutron Activation-Delayed Neutron Counting and Combined Fission-Track and Alpha-Track Technique	29
3.2.2.1	Thermal Neutron Activation-Delayed Neutron Counting	31
3.2.2.2	Fission Track Measurement	32
3.2.2.2.1	Preparation of Irradiation Sample	32
3.2.2.2.2	Etching and Track Counting	33
3.2.3	Water Chemistry Analysis	36
3.2.4	Soil and Waste Rock Analysis	36
CHAPTER IV	RESULTS AND DISCUSSION	37
4.1	Geochemical Investigation	37
4.2	Radiochemical Investigation	58
4.2.1	Uranium in Water	60
4.2.2	U content in Waste Rock and Soil Samples	75
4.2.3	U Isotopes in Water	77
4.2.4	U Isotopes in Waste Rock and Soil Samples	82

Table of Contents (Cont'd.)

		<u>Page</u>
4.3	Neutron Activation-Delayed Neutron Counting Technique (NA-DNC)	83
4.4	Determination of $^{234}\text{U}/^{238}\text{U}$ Ratio by Combined Fission Track and Alpha Track Counting	84
4.4.1	Theory	84
4.4.2	Fission Track and Alpha Track Results	88
CHAPTER V	SUMMARY	101
APPENDIX I	ELECTROPLATING PROCEDURE FOR U	104
REFERENCES		108

LIST OF TABLES

TABLE		PAGE
1	Chemical and radiochemical composition of Greyhawk ground water (July 1979)	38
2	Chemical and radiochemical composition of Greyhawk ground water (Sept. 1979)	39
3	Chemical and radiochemical composition of Greyhawk ground water (Oct. 1979)	40
4	Chemical composition of Greyhawk ground water	41, 42
5	Trace metal composition of Greyhawk ground water	43, 44
6	U and Th contents in waste rock and soil samples	76
7	Comparison of the results of fission-alpha track and alpha spectrometry analyses (set J)	93
8	Comparison of the results of fission-alpha track and alpha spectrometry analyses (set K)	94
9	Experimental and Calculated values of slope, relative slope and intercept	98

LIST OF FIGURES

FIGURE		PAGE
1	^{238}U Decay Series	6
2	Topography and location of the study area, Bancroft	12
3	Geology and Uranium occurrences, Bancroft, Ont.	13
4	Water table contour map for June 1/79	16
5	Location of sampling sites	22
6	Schematic diagram of the multilevel sampling device	23
7	An actual alpha particle energy spectrum of U in ground water	28
8	A sketch diagram of experimental arrangement of the counting system.	34
9	Selected areas for fission and alpha tracks counting	35
10	Chemical and Radiochemical composition of Greyhawk ground water (site B)	45
11	Chemical and Radiochemical composition of Greyhawk ground water (site J)	46
12	Chemical and Radiochemical composition of Greyhawk ground water (site K)	47
13	Chemical and Radiochemical composition of Greyhawk ground water (site Q)	48
14	Chemical and Radiochemical composition of Greyhawk ground water (site U)	49
15	Chemical and Radiochemical composition of Greyhawk ground water (site T)	49
16	Chemical and Radiochemical composition of Greyhawk ground water (site V)	50
17	Chemical and Radiochemical composition of Greyhawk ground water (site X)	51

List of Figures (Cont'd.)

FIGURE		PAGE
18	Chemical and Radiochemical composition of Greyhawk ground water (site GR9)	52
19	Chemical and Radiochemical composition of Greyhawk ground water (site GR10)	52
20	Chemical and Radiochemical composition of Greyhawk ground water (site GR11)	53
21	Chemical and Radiochemical composition of Greyhawk ground water (site GR4)	53
22	Chemical and Radiochemical composition of Greyhawk ground water (site GR6)	53
23	Three distinct routes of migration of leachate in sandy aquifer, Greyhawk Mine	59
24	A plot of U content versus bicarbonate concentration	62
25	Eh-pH diagram	64
26	A plot of U content versus sulfate concentration	66
27	A plot of U content versus Specific conductance	67
28	Distribution of U in ground waters samples along B-Q cross-section	70
29	Distribution of U in ground water samples along the GR9-GR11 cross-section	71
30	Diagrammatic sketch showing U migration in shallow aquifer, Greyhawk	73
31	A plot of U concentration versus activity ratio in the Greyhawk ground water	78
32	Distribution of U concentration and $^{234}\text{U}/^{238}\text{U}$ ratio of ore bearing ground water	79
33	Distribution of U isotopes $^{234}\text{U}/^{238}\text{U}$ in ground water sampled along the B-Q cross-section	81
34	A histogram of frequency versus % yield	85

List of Figures (Cont'd.)

FIGURE		PAGE
35	A regression curve of $\Sigma N_x / \Sigma N_f$ versus uranium activity ratio (set J)	96
36	A regression curve of $\Sigma N_x / \Sigma N_f$ versus uranium activity ratio (set K)	97
37	Diagram of apparatus for electroplating of U	105

LIST OF PLATES

PLATE		PAGE
1	Waste rock pile of pegmatite granite (pink) and Metagabbro (black) on unconsolidated glacial overburden, Greyhawk Uranium Mine, Bancroft	19
2	Apparatus used for collecting ground water samples at various levels	24
3	Photomicrograph showing fission tracks distribution in etched muscovite (sample Q 4.15)	90
4	Photomicrograph showing cluster of fission tracks in etched in CN85 film (sample U-11.80)	90
5	Photomicrograph showing alpha tracks distribution in etched muscovite (sample B-5.7 July)	91
6	Photomicrograph showing cluster of alpha tracks in etched CN85 film (sample U-11.80)	91

CHAPTER I

INTRODUCTION

1.1 General Statement

Ranges of uranium concentrations in natural waters of the world have been tabulated by Rogers and Adams (1970). In sea waters, uranium content is almost constant, ranging from 1 to 4 ppb. However, uranium content in fresh water is highly variable, depending on local conditions such as rock types, flowrate of water, evaporation, physiochemical conditions of the environment, etc. (Barker and Scott, 1958; Cohen, 1961; Lopatkina, 1964; Langmuir, 1978). Fix (1956) has suggested that the background uranium value in the U.S. streams is about 0.1 ppb. In uraniumiferous areas, he found that uranium ranges from 1 to 10 ppb in surface waters and 1 to 120 ppb in ground waters.

Radioactive disequilibrium of two uranium isotopes, U-234 and U-238, was first discovered by V. V. Cherdyn'tsev and co-workers in 1955 during an investigation of the $^{234}\text{U}/^{238}\text{U}$ ratio in secondary minerals. Subsequently, this disequilibrium characteristic was used to solve specific problems in carbonate and lake geochronology, uranium ore genesis, soil evolutionary processes, earthquake prediction and evaluation of regional hydrogeology. However, intensive studies of these problems only began a few years ago, especially in the U.S. and the Soviet Union.

In general, the $^{234}\text{U}/^{238}\text{U}$ activity ratio of water and secondary uranium-bearing minerals is greater than unity due to the selective leaching of ^{234}U from weathering rocks. The activity ratio of $^{234}\text{U}/^{238}\text{U}$

2

in ground water varies from about 0.5 to 19.94 (Osmond and Cowart, 1976) and in river waters ranges from 1.00 to 2.00 (Thurber, 1965; Cherdyntsev, 1971). The ocean, a reservoir that receives water from lakes and streams has a fairly constant activity ratio of about 1.14 (Thurber, 1962). In addition, strong fractionation of these two isotopes was also observed in deep oil-brines (8 to 10: Kronfeld et al., 1975); in waters of granite massifs (1.5 to 6.5), in lake water (1.2 to 1.3) and spring water (1.03 to 1.40) and bone sample (1.2 to 1.6) (Cherdyntsev, 1971) and limestone cave deposits (0.93 to 2.44: Cherdyntsev, 1965; Thompson et al., 1975).

1.2 Objectives of this Study

The principal objective of this study is to investigate any variation of the uranium content and its isotopic ratio ($^{234}\text{U}/^{238}\text{U}$) with depth in shallow ground water in granular deposits. To achieve this, the Greyhawk Mine, Ontario, was chosen as the investigation site and various geochemical, radiochemical and hydrogeological studies have been made. The studies were carried out using multilevel ground water samplers installed in the sandy overburden. Ground water samples were collected from selected intervals and analysed for chemical and radiochemical constituents as well as geochemical conditions (pH, specific electrical conductance, bicarbonate alkalinity, dissolved oxygen and temperature). Major cations and anions measured included Ca^{2+} , Mg^{2+} , Na^+ , Cl^- , SO_4^{2-} , etc. While uranium was analysed by the alpha spectrometry technique. The uranium present in this water is presumably derived from pegmatitic and gabbroic waste rocks which had been piled up adjacent to the abandoned Greyhawk Mine about two decades ago. A few samples of waste rock and

core soil were analysed for their uranium content and U isotope ratio.

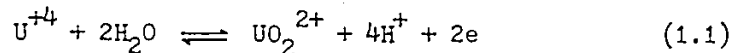
The water table and ground surface elevations as well as other hydrogeologic parameters were surveyed so that quantitative and qualitative interpretations of the chemical and radiochemical results could be made within the hydrogeologic framework. It was hoped from this programme too, that an improved understanding of migration of uranium in the natural environment could be developed.

As a part of this study, a new technique to determine uranium isotopic ratio ($^{234}\text{U}/^{238}\text{U}$) has been developed utilizing alpha and fission tracks. This method proved to be useful in obtaining a first estimate of the uranium isotopic ratio.

In addition, waste rocks and core soil samples were also analysed for uranium and thorium by neutron activation-delayed neutron counting and instrumental neutron activation techniques, respectively. Furthermore, analyses of total uranium content in water samples were also performed by the neutron activation-delayed neutron counting. This method is fairly cheap, rapid and accurate and appears satisfactory for uranium prospecting purposes.

1.3 Hydrogeochemistry of Uranium

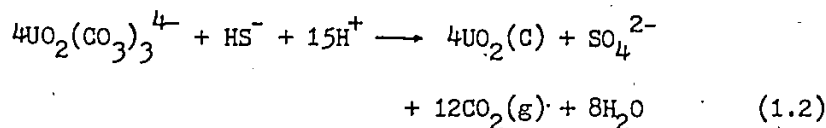
Uranium is an element showing changes from one oxidation state to another in geologic environments. The possible valence states of uranium are +2, +3, +4, +5, and +6, but only the +4 and +6 valence states are of geologic interest. The transition from +4 to +6 has a redox potential within normal range for geologic environments.



$$E^0 = 0.32 \text{ to } 0.33 \text{ volts (Hostetler and Garrels, 1962).}$$

The primary source of uranium in the geochemical cycle is the weathering of felsic igneous rocks where it is present almost entirely as U(IV). During surficial weathering processes uranium is oxidised to soluble uranyl ions, UO_2^{2+} . Hostetler and Garrels (1962) showed that in the presence of CO_2 and at low temperatures and pressures, uranium is soluble in either the 4-valent (U^{+4}) or the 6-valent (UO_2^{2+}) state, depending on the pH and Eh of the solution. In oxidising environments and ground water systems, uranium transport occurs mainly as U(VI) species, commonly as UO_2^{2+} or in the form of the highly stable complexes such as fluorides UO_2F^+ , phosphates $UO_2(HPO_4)_2^{2-}$, hydroxyl UO_2OH^+ ; $(UO_2)_3(OH)_5^+$, silicate $UO_2SiO_3(OH)_3^+$, sulphate $UO_2SO_4^0$, carbonates $UO_2CO_3^0$; $UO_2(CO_3)_2^{2-}$; $UO_2(CO_3)_3^{4-}$ and organic complexes. The most significant uranyl complexes in natural waters between pH 4 to 10 are uranyl carbonates and uranyl phosphates (Langmuir, 1978). These complexes greatly increase the solubility and mobility of uranium in surface and ground waters.

On the other hand, in reducing ground water environments, the mobile uranyl species, U(VI), are reduced to U(IV) and hence precipitate as uraninite or coffinite. Concurrently, oxidation of the more abundant species such as iron and sulphur occurs.



Moreover, uranium in solution can also be removed by sorptive materials such as zeolite, clays, limonites and organic matter (Dement'yev and Syromyatnikov, 1968; Doi et al., 1975; Andreyev and Chuvachenko, 1964). As a result of precipitation and sorption processes, uranium content in natural waters may decrease drastically.

1.4 Mechanisms of Uranium Isotopic Fractionation

The activity ratio of U-234 and U-238 should be unity in closed geological systems older than one million years, according to the radioactive decay series as shown in Figure 1.

At secular equilibrium, the rate of decay of ^{234}U is equal to that of parent ^{238}U (Eqn. 1.3), and hence the ratio of their activities is equal to one (Eqn. 1.4).

$$N_1\lambda_1 = N_2\lambda_2 \quad (1.3)$$

and $N\lambda = A$

$$\text{Therefore, } \frac{A_1}{A_2} = \frac{\lambda_1 N_1}{\lambda_2 N_2} = 1 \quad (1.4)$$

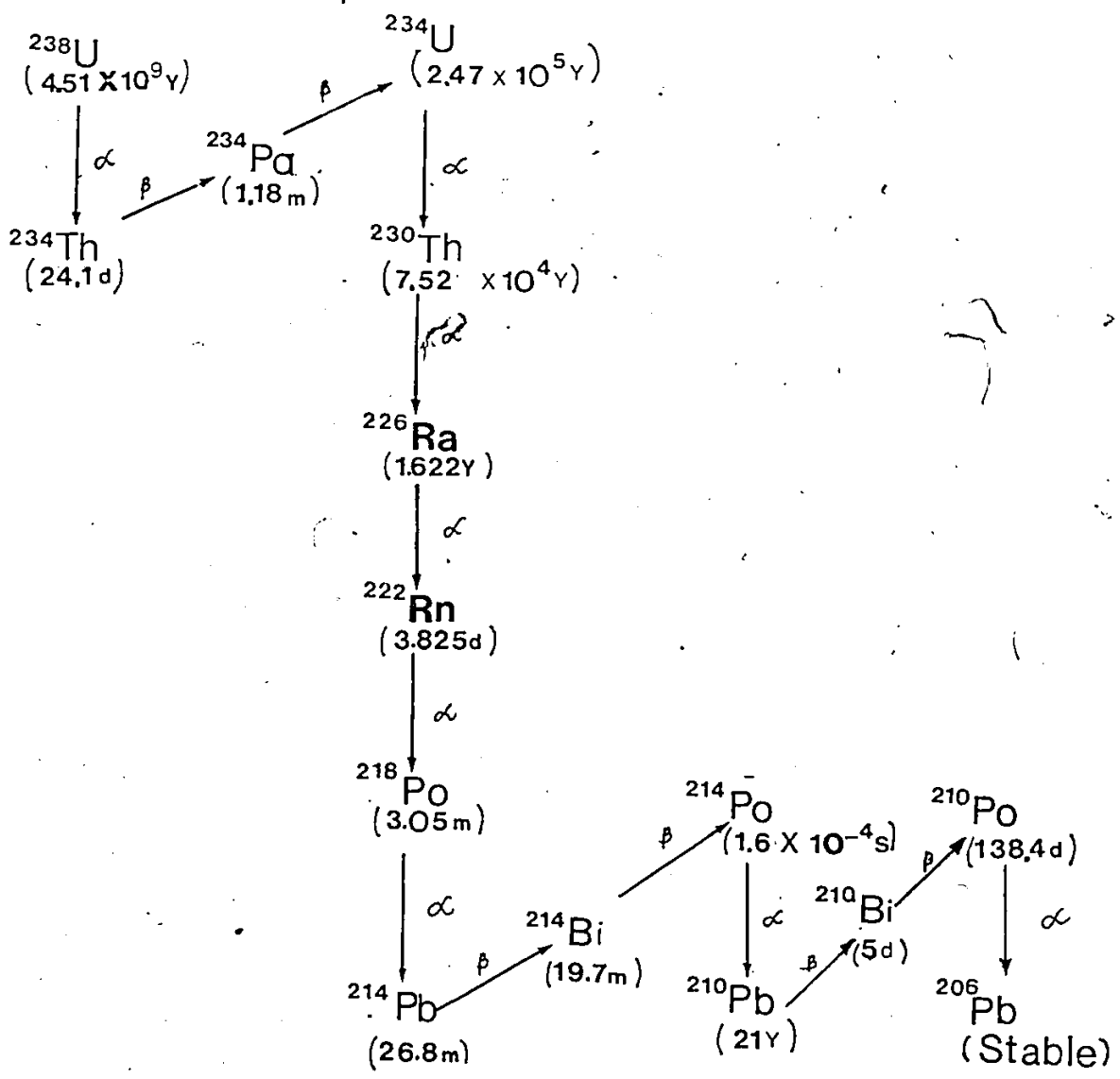
where, N_1 and N_2 = no. of ^{238}U and ^{234}U atoms respectively

λ_1 and λ_2 = decay constant of ^{238}U and ^{234}U atoms respectively

A_1 and A_2 = alpha activity of ^{238}U and ^{234}U atoms respectively.

However, in open systems that are exposed to weathering and ground-water circulation, ^{238}U and ^{234}U may be separated and a state of disequilibrium is established (i.e. $A_1 \neq A_2$). As noted, such disequilibrium has been observed in various water bodies (Cherdyntsev, 1955; Thurber, 1962; Dooley et al., 1964; Chalov et al., 1966; Rosholt et al., 1963; Kaufman et al., 1968; Kronfeld and Adam, 1974; Wakshal and Yaron, 1974; Osmond and Cowart, 1974). Consequently, several laboratory and

Fig. I - ²³⁸U Decay Series.



6

7

field studies have been done by the above workers and others to improve the understanding of the mode of ^{238}U and ^{234}U fractionation.

Generally, two mechanisms of uranium isotopic fractionation are believed to be involved, resulting in the enhancement of $^{234}\text{U}/^{238}\text{U}$ ratio in aqueous environment. The two mechanisms are:

- (i) Preferential leaching of the ^{234}U atoms; and
- (ii) Direct alpha recoil of ^{234}Th across a solid/liquid boundary.

During the three-stage decay of ^{238}U to ^{234}U (Fig. 1), the high energy particles liberated cause bond breakage, microfractures and displacement of ^{234}U atoms in weakly-bonded or interstitial sites (Cherdyn'tsev et al., 1955; Rosholt et al., 1963, 1964; Dooley et al., 1964; Chalov and Merkulova, 1966). At these sites, the daughter ^{234}U is more exposed to the oxidising agents than the parent ^{238}U and thus a high activity ratio should be expected in association with the more oxidising environments. Additionally, stripping of two electrons from ^{234}U atom occurs concurrently during the decay process. Therefore the ^{234}U attains the soluble +6 valence more readily than the tetravalent ^{238}U . Hence, fractionation of ^{234}U takes place due to the more oxidised state from the time of transition and thus no oxidising agent is essential. These two factors, consequently, contribute to the increased mobility and preferential leaching of ^{234}U with respect to ^{238}U .

Laboratory leaching experiments by Chalov and Merkulova (1966), have shown that solutions contained about 1.3 times ^{234}U compared to that of parent ^{238}U . However, $^{234}\text{U}/^{238}\text{U}$ alpha activity disequilibrium as great as 1200% has been recorded by Kronfeld (1973) in natural waters, thus a leaching mechanism alone would not be sufficient to explain this

phenomenon. Therefore, the process responsible for a disequilibrium state as high as 3x or greater required mechanisms other than the preferential leaching of ^{234}U atom. Kigoshi (1971) suggested that the main source of excess ^{234}U in ground water is due to the alpha recoil of ^{234}Th nucleus following ^{238}U decay, thereby enriching the solution in ^{234}U . This is based on his studies on zircon powder suspended in diluted nitric acid or sodium carbonate solution where progressive increases in the amount of ^{234}Th were observed in the aqueous phase. Fleischer and Raabe (1978) also observed a similar result. Hence, it is established that an excess of ^{234}U in ground water may also be supplied by the α -recoil of ^{234}Th originating from the solid surfaces of sand or clay particles; the excess may be directly related to aquifer porosity and the age of the water.

1.5 Previous $^{234}\text{U}/^{238}\text{U}$ Studies

Investigation of uranium isotopic disequilibrium in natural environments began about 25 years ago. As noted, it was first reported by Cherdyntsev and Co-workers (1955) in secondary minerals and later confirmed by several others (Chalov et al., 1959, 1964; Dooley et al., 1964; Rosholt et al., 1966).

Thurber (1962) used uranium disequilibrium for dating corals, though it gives a large error limit ($\pm 35\%$). Other marine carbonates have also been dated by this method (Cherdyntsev, 1965). Researchers at McMaster University have widely employed uranium-series disequilibrium for dating of cave deposits (speleothem), (Schwarcz, 1978). Chalov and Co-workers (1966, 1970) have applied it to arrive at absolute ages of closed basins in Russia. Cherdyntsev, Thurber and many others noted

that, this technique may be useful for dating geologic events within the Pleistocene; however its main disadvantage is the difficulty in estimating the initial excess of ^{234}U .

Wide ranges of $^{234}\text{U}/^{238}\text{U}$ ratio have been reported from a variety of natural water. Kronfeld and Adam (1973) found an activity ratio as high as 12.3 in the Trinity aquifer, Texas. They attempted to use excess ^{234}U to derive the absolute age and the flow rate of the water. Kaufman et al., (1969) have applied disequilibrium studies as an aid to hydrogeologic investigations of the Floridan aquifer. Variations in isotopic activity ratios and concentrations were found to be related to the regional hydrogeologic framework. Groundwaters depleted by as much as 50% have also been reported from the Floridan aquifer (Kaufman et al., 1965). Thurber (1962, 1965); Koide et al., (1965); Umemoto (1965) and Cherdyntsev (1971) have reported that the activity ratio of uranium was constant for all open oceans (A.R = 1.14). Osmond and Cowart (1976) used the concentration and isotopic ratio of uranium to calculate the uranium residence time in the oceans and obtained values of 500,000 and 220,000 years respectively. Thompson et al., (1975) studied the $^{234}\text{U}/^{238}\text{U}$ ratios in limestone cave seepage waters and speleothem from West Virginia. They reported that $^{234}\text{U}/^{238}\text{U}$ ratios in the waters vary significantly from month to month and their average values differ from that of the speleothem which they are depositing. Also, it was found that the degree of ^{234}U enrichment in seepage waters varied from site to site even though they are only several meters apart. Gascoyne (1979) also observed a similar situation in cave waters from Kentucky, West Virginia, the Canadian Rockies and the Craven area of Northern England.

Uranium disequilibrium has also been used in prospecting for uranium ore deposits by studying the changes in uranium concentration as well as isotopic ratios in groundwaters (Coward and Osmond, 1977). Doble and Co-workers (1964) applied disequilibrium to the problem of uranium ore genesis. Rosholt et al., (1965) observed that altered ore bodies have excess ^{234}U , while unaltered ores usually show deficiency of ^{234}U .

CHAPTER II

THE STUDY AREA

2.1 Location

The study area is located at the abandoned Greyhawk Mine ($45^{\circ} 01' 51''\text{N}$; $77^{\circ} 53' 48''\text{W}$), approximately 4 km. southwest of Bancroft, Faraday Township, Ontario. It encompasses about 20,000 sq. meters and is readily accessible by a gravel road that exits south from highway 28. The country around the Greyhawk Mine is hilly with most land falling between 360 and 430 m above sea-level. The study site is generally flat (elevation, 419 m a.s.l.). Figure 2 shows topography and location of the study area.

2.2 Geology

2.2.1 Regional Geology

The general geology of the Greyhawk Mine and its surrounding area (Faraday-Cardiff Townships) is reported in detail by Satterly (1956); Lang (1962); Griffith (1967) and Hewitt (1957, 1959). The area lies in the Grenville Province of the Canadian Shield. Bedrock formations are all of Precambrian age, consisting of two main rock types: (i) The Grenville metasediments to the south (mainly marble, paragneiss and amphibolite), and (ii) Plutonic rocks to the north (mainly granite, syenite and gabbro). They are separated by a narrow band of syenitic rocks and nephelene gneiss. Figure 3 shows the geology of the area.

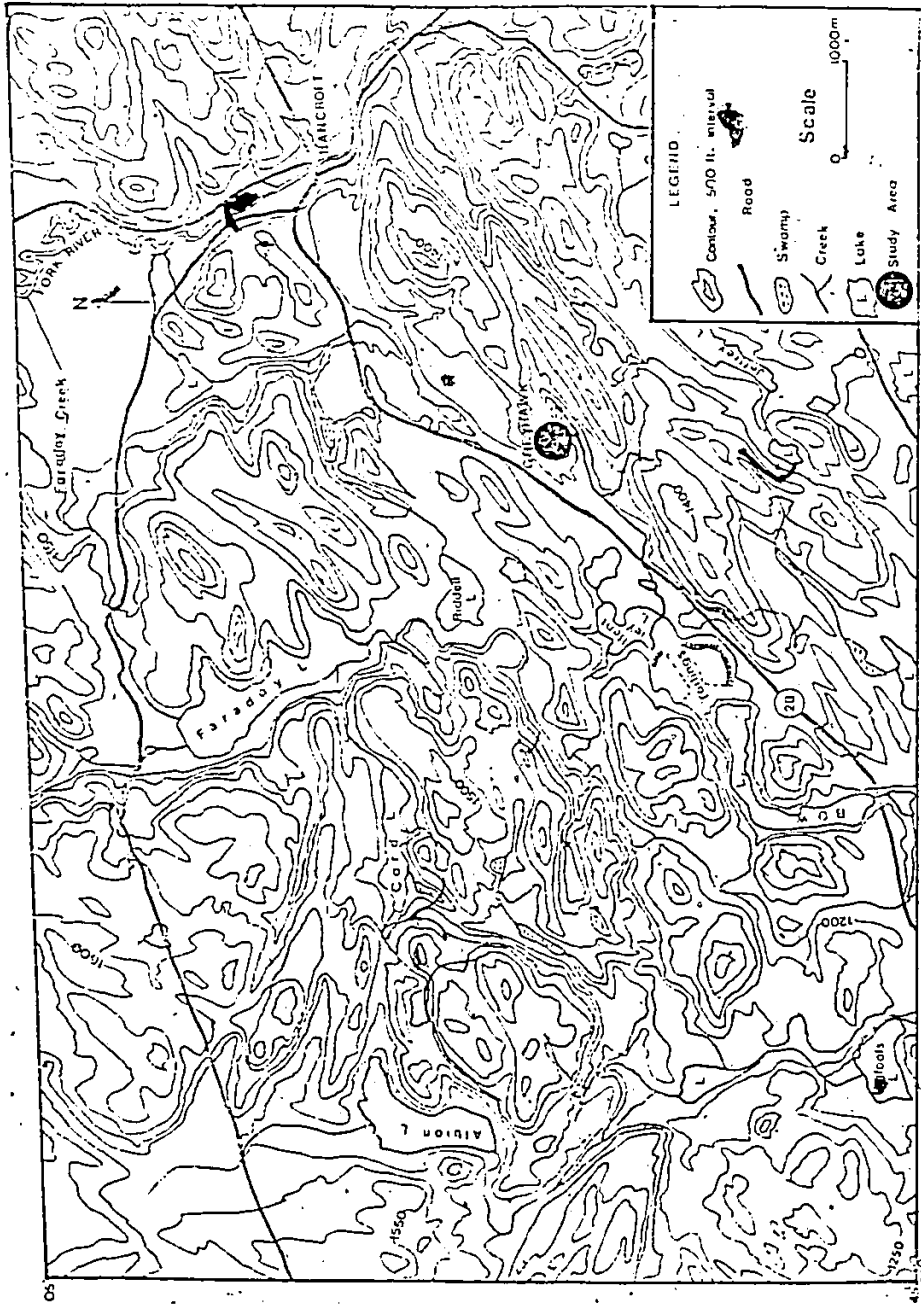


Fig.2 Topography And Location of The Study Area, Bancroft.

Handwritten scribbles at the bottom of the page.

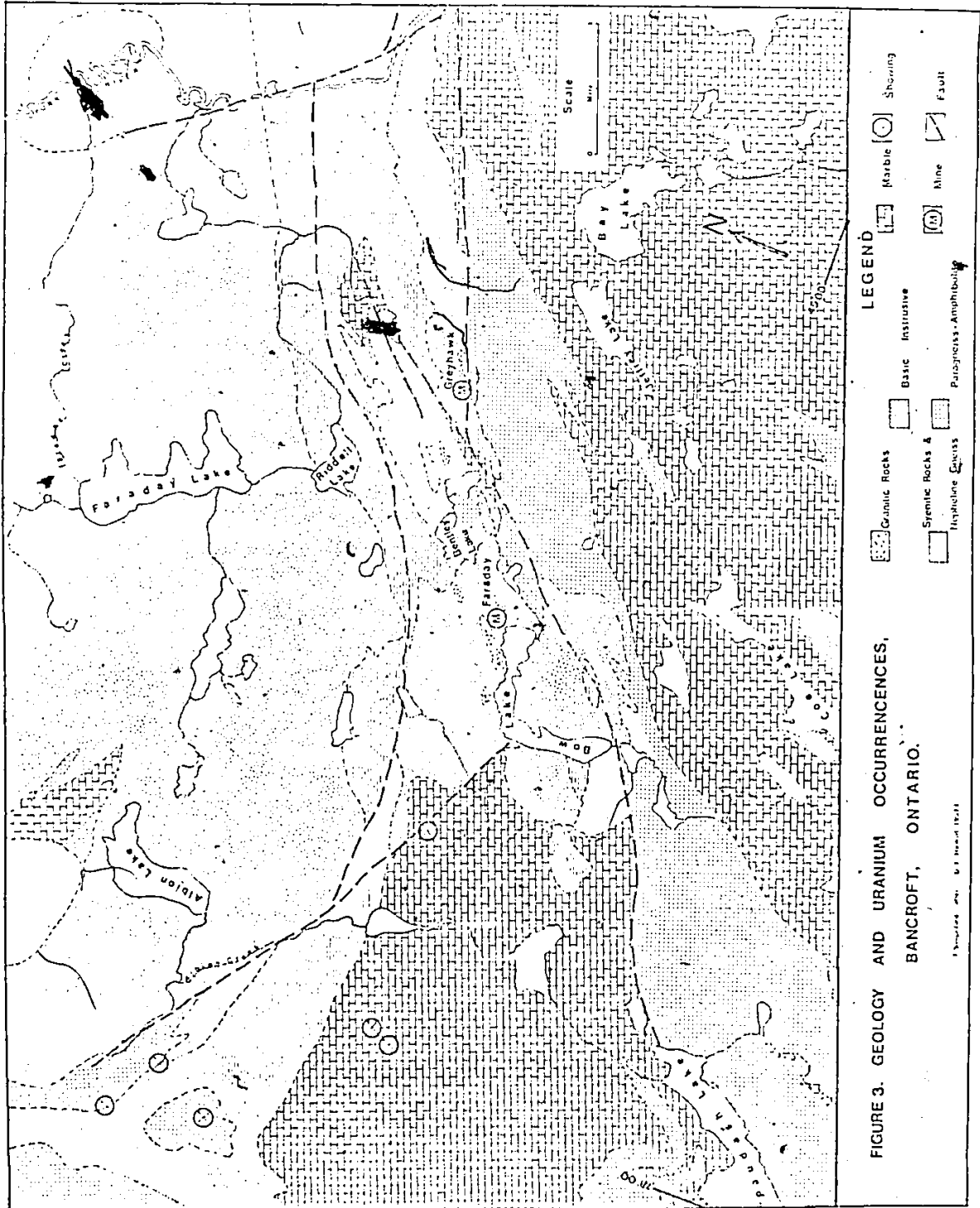


FIGURE 3. GEOLOGY AND URANIUM OCCURRENCES, BANCROFT, ONTARIO.

Revised by B. H. H. H. H. H.

LEGEND

- Granite Rocks
- Basic Intrusive
- Sienitic Rocks & Amphibole Gneiss
- Marble
- Mine
- Fault

The Grenville metasediments are the oldest rocks in the area. They were intruded by gabbro and diorite, followed by nephelene syenites and granites which were emplaced during the Grenville Orogeny. Strong structural deformation accompanied this orogeny; the principal structural features of the area were formed at this time. After the last period of Precambrian mountain building the whole area was eroded to a peneplain of low relief. During Pleistocene times the area was glaciated; glacial till and fluvioglacial deposits of sand and gravel cover much of the bedrock.

2.2.2 Local Geology

The terrain surrounding the Greyhawk Mine is underlain by diorite, metagabbro, amphibolite, paragneiss and marble (Hewitt, 1959). The plutonic rocks that outcrop at the study site consist mainly of pegmatitic granite and intruding metagabbro (Lang, 1962). The metagabbro bodies strike north east and pegmatite dikes sometimes follow joint directions in the host rocks. The uranium ore is found in porphyroblastic leucogranite pegmatite and commonly occurs in magnetite-rich or quartz-rich pegmatites. The radioactive minerals include uraninite (UO_2), uranothorite, allanite, pyrochlore, betafite and others (Hewitt, 1959; Lang, 1962).

2.3 Hydrology

The surface water drainage for the area is towards the southwest, draining into Bow Lake which borders Madawaska Uranium Mine (Fig. 2). A detailed hydrogeology survey of the study area has been carried out by W. Clarke, Department of Earth Sciences, University of

Waterloo. Water-level measurements were made on several occasions during the study period (May to Sept. 1979) during which it was observed that the water table fluctuated from almost one meter below ground surface in the early summer to about two meters below ground surface by the early fall. The ground water flow directions were not changed throughout the study period.

Basically, the ground water flow system in the area can be divided into two components. In the eastern half of the study area, the ground water flow is controlled largely by the free-water elevation in an adjoining swamp. The water flows primarily in a south-westerly direction through the aquifer and discharges at the lower free-water elevation below a beaver dam.

In the central and north-western parts the flow pattern is more complex, recharge water here enters the aquifer from the swamp to the east of the study area and also from the north west. Nevertheless, both components discharge into the same low-lying area below the beaver dam, (Fig. 4). Ground water velocities were calculated by the Darcy Equation:

$$v_n = \frac{K}{n} \cdot \frac{dh}{dl} \quad (2.1)$$

Where, K = Coefficient of Permeability
(ranging from 5.0×10^{-4} to 5.0×10^{-3} cm/s)

n = Porosity
(0.33)

$\frac{dh}{dl}$ = Hydraulic gradient along B-Q
(4.6×10^{-3})

It is found that velocity ranges from 2.2 to 22m/yr. K and n values were estimated based on previous experience with similar materials (H. Veska et al., 1978).

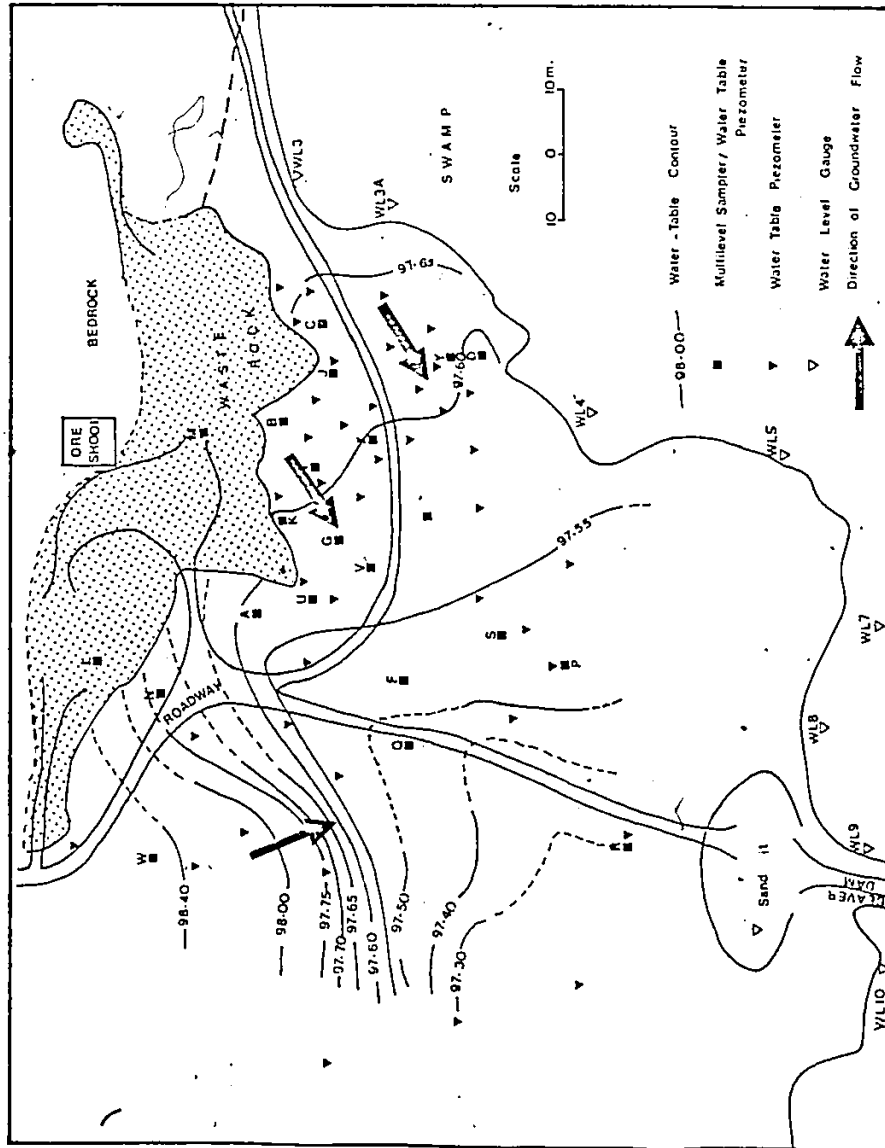


FIGURE 4. WATER - TABLE CONTOUR MAP FOR JUNE 1/79 (after B. Clarke).

2.4 Description of the Overburden

Continuous and split-spoon core samples were collected from several locations in order to obtain a good understanding of the composition of the aquifer. The cores were taken at six locations to depths of about 2.5 meters, using a Cobra vibrator to drive aluminum tubes into the ground. The tubes were cut longitudinally and the stratigraphy was revealed in a relatively undisturbed state. The samples were found to be highly heterogeneous. The dominant material was a medium to fine sand, with frequent intervals of coarse sand and occasional intervals of very fine sand or silt. The upper part normally consisted of a brown coarse sand with occasional laminated banding (5 cm) of fine sand. Medium sand occurred between 4 to 7 meters and below 7 meters there was generally a mass of grey, silty, fine sand.

Chapman and Putman (1951) noted that more than half of the total area of Southern Ontario was submerged for a time during or immediately after the retreat of the last glacier. Therefore, the sediments here are probably deposited following the event. The deposits themselves are stratified and generally free of stones, these features may indicate that the deposits are derived from lacustrine sediments.

2.5 Mining Activity and Land Use

Mining operations began at the Greyhawk in 1956 and were discontinued on April 8, 1959, owing to lack of enough funds to mine ore of acceptable grade. The uranium ore at Greyhawk was shipped for treatment to the nearby Madawaska Mill. The ore (800,000 tons) had an average grade of 0.095% U_3O_8 (Canadian Mines Handbook, 1958).

As a result of mining operations, two separate piles of waste rocks have developed. Respectively, these consist mainly of granite pegmatite and gabbroic rocks. The waste rocks were piled up about two meters high on unconsolidated glacial overburden adjacent to the outcrop (Plate 1). The size of the waste debris varies from boulder size to small granular dimensions.

Vegetation around the area consists of tall grass, bushes and deciduous trees. The land use is generally for recreation and wild life, with a few cottages built in its vicinity.

2.6 Previous Studies of the Greyhawk Mine and The Surrounding Area

There have been many geological investigations of the area since the early fifties. This area attracted geologists because it contains many known uranium occurrences. Published studies, etc. mainly emphasised the geology and uranium mining activity. The area has been mapped geologically by Adams and Barlow (1910), Satterly (1957), and Hewitt (1957, 1959). Reports on mining operations of the Greyhawk Mine were filed annually by the Ontario Department of Mines, especially in the fifties and early sixties.

Chamberlain (1964) studied the hydrogeochemistry of uranium in the Bancroft-Haliburton region and, using U concentrations in surface waters, successfully to outline the many known uranium occurrences and deposits that together form the belt of uranium mineralization. Creeks, lakes and swamps exhibited a systematic variation in uranium content; 1.7 to 1.5 to 1.1 ppb, respectively.

As a result of the intensive uranium mining operations in Bancroft area, an investigation of radiological water pollution was carried out by



Plate 1. Waste rock pile of pegmatite granite (pink) and Metagabbro (black) on unconsolidated glacial overburden, Greyhawk Uranium Mine, Bancroft.

the Ontario Water Resources Division in 1965. It was reported that the waters had a mean Ra-226 concentration of less than 3 pCi/l. However, the groundwater of the Greyhawk mine that discharges southwest to a stream flowing into Bow Lake contained about 106 pCi/l of Ra-226 (Ont. Water Res., 1965).

Morse (1971) applied the principles of Ra-226 analysis to outlining favourable areas for uranium prospecting at Bancroft and compared this method with those using radon and uranium. Sediments and water samples were collected from lakes and streams and analysed for uranium, radium and radon. His study showed that there is a positive correlation of the location of high values of uranium, radium and radon with the contact between plutonic rocks and metasedimentary rocks, along which known uranium deposits are concentrated. The water downstream from the Greyhawk Mine had a high content of both radon (90 to 250 pCi/l) and uranium (1.6-2.7 ppb).

Recently, the Ministry of Environment had reported that Bentley Creek which received much of its recharge from the Greyhawk area contained between 1 to 50 ug/l of uranium and 1 to 7 pCi/l of Ra-226. As far as the author is aware, no uranium isotopic work has been carried out in the study area prior to the present investigation.

CHAPTER III

SAMPLING AND ANALYTICAL PROCEDURES

3.1 Sampling and Field Procedure

Ground water samples at various levels were collected from 17 stations on three occasions (July, September and October 1979). Sample localities are shown in Figure 5. At these locations water samples were taken at various levels where the piezometer tips are represented by their depth below ground surface (eg. B5.7 is the tip 5.7 meters below ground surface). Multilevel sampling devices were installed in the summer of 1978 (stations A to G and I) and from the period of June through August, 1979 (J to Y and GRS'-4,6,9,10,11).

The sampling device consists of a number of polyethylene tubes contained inside a polyvinyl chloride (PVC) pipe that is installed in the aquifer. Each tube protrudes through the wall of the pipe at a different elevation where it serves as a point water sampler and piezometer. The tip of each tube is enclosed in a fine-meshed-steel screening. For a more detailed description the reader is referred to Picken et al., 1978. A schematic diagram of the multilevel sampling device is shown in Figure 6.

Prior to sampling, a volume equivalent to or greater than that initially in the sampling tube was drained and discarded. This was done by connecting a 1-litre Erlenmeyer flask to the polyethylene tube. The flask was evacuated with either a hand pump or a portable peristaltic pump, run by a 12V D.C. battery (see plate 2). All water samples were

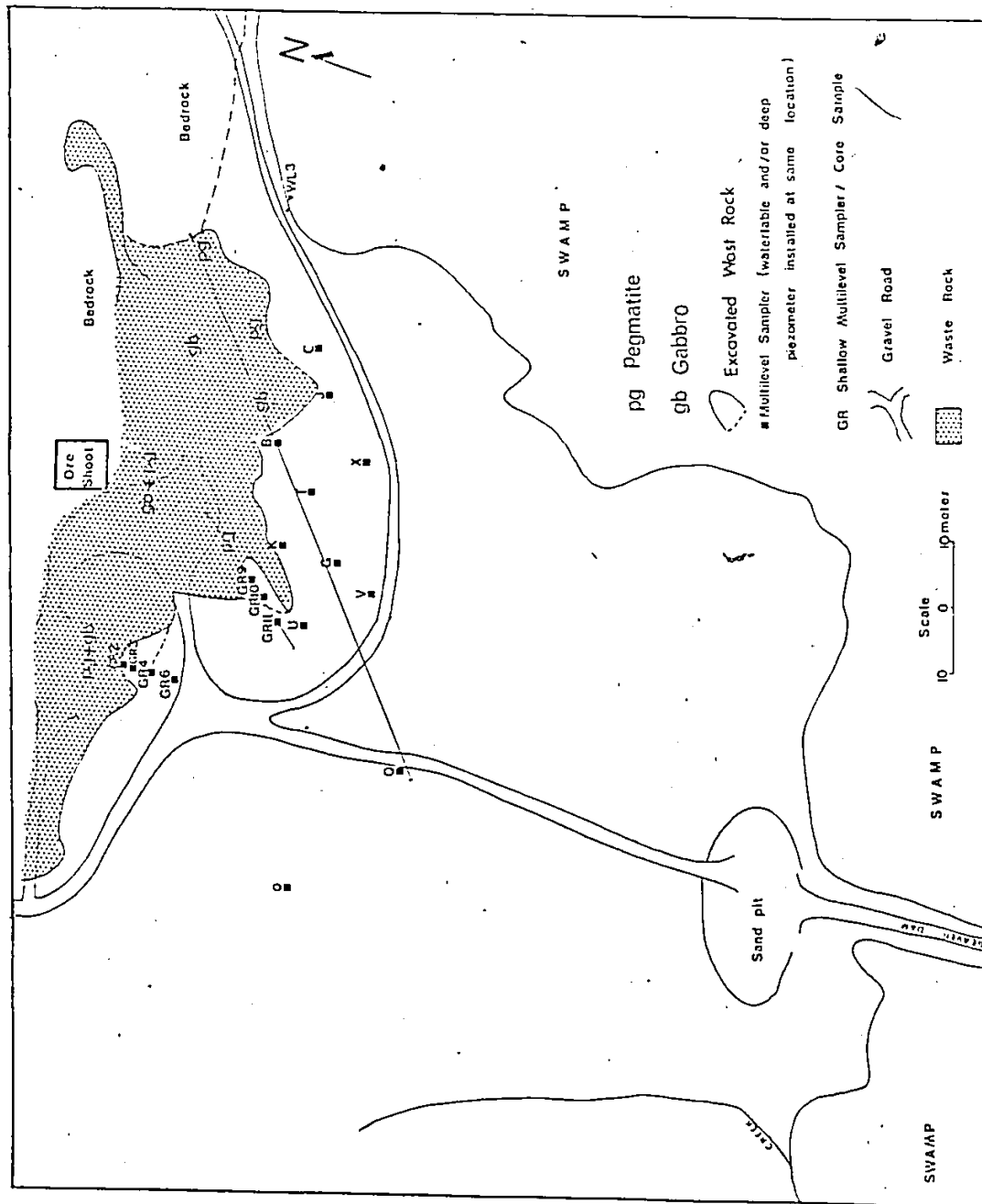


FIGURE 5. LOCATION OF SAMPLING SITES, GREYHAWK MINE, BANCROFT.

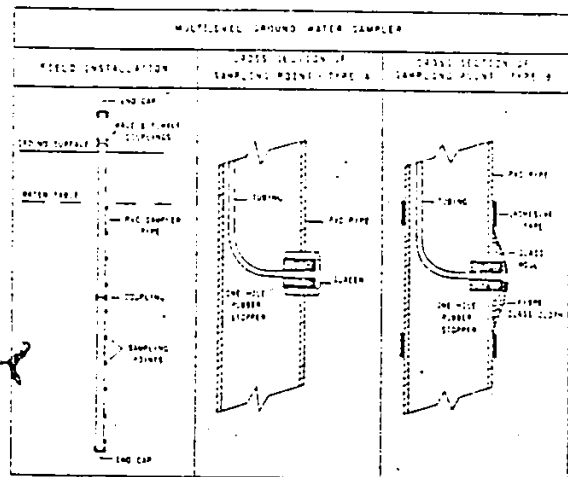


Fig. 6. Schematic diagram of the multilevel sampling device.
(after Pickens et al., 1978)



Plate 2. Apparatus used for collecting ground water samples at various levels.

filtered in the field using 0.45μ filter paper because they seemed to contain a fairly substantial amount of suspended sediments (predominantly silty sand). Two samples were collected in polyethylene bottles from each site for radiochemical analyses (U content and U isotope). These water samples were acidified with conc. HNO_3 to obtain a pH of about 1 in order to prevent precipitation or sorption of cations during storage (Robertson, 1968).

The specific electrical conductance, bicarbonate alkalinity, dissolved oxygen and pH of ground water samples were measured soon after collection. The bicarbonate alkalinity was determined by a potentiometric titration method using $0.01\text{NH}_2\text{SO}_4$ acid as titrant. For each site, 300 mls of water sample was collected in BOD glass bottles for dissolved oxygen analysis using the Azide Modification Method (A. P. H. A., 1975). Also, about 250 mls of unacidified water from some sites were taken for major cation and anion analyses (analysed by the Ministry of Environment, Canada).

3.2 Laboratory Procedure

The ground water samples were analysed for their uranium content and isotopic ratio utilizing the two analytical techniques:

- (i) Alpha Spectrometry Technique (isotope dilution and isotope ratio) and
- (ii) Neutron Activation-Delayed Neutron Counting (NA-DNC) and Combined Fission-Track and Alpha-Track Technique.

3.2.1 Alpha Spectrometry Technique

In general, determination of uranium concentration and its activity ratio in water entails three major steps (Veselsky, 1974).

- (i) Preconcentration of uranium from the water samples.
- (ii) Separation of uranium from other elements.
- (iii) Final purification of uranium and preparation of counting sources for alpha spectrometry.

(i) Preconcentration

To two-litre water samples, about 3 mls of iron chloride solution (100-200 mg of iron) and a known quantity of ^{232}U spike (to give a comparable activity with the sample) are added. The resulting solution is shaken periodically for several days to allow ^{232}U traces to equilibrate with uranium in the sample. Uranium forms stable complexes with carbonate species and this might cause poor yield in the chemical extraction. Therefore, the sample is degassed for about one hour to rid it of CO_2 which is present as HCO_3^- ions in the solution. Ammonium hydroxide is added to the sample until a brown precipitate, $\text{Fe}(\text{OH})_3$, is formed. Uranium and many other elements, such as thorium are coprecipitated with the ferric hydroxide. After the precipitate has settled, the floc is separated from the supernatant liquid by decanting and centrifuging. The hydroxides are dissolved in 9N HCl (about 20-50 mls) and the excess of iron is extracted with isopropyl ether.

(ii) Separation

To separate uranium from interfering elements, the 9N HCl solution is passed through an anion resin (AG11-X8, 100-200 mesh chloride form, Bio-Rad laboratories) column (5mm internal diameter and 15 to 20 cm length) that has been preconditioned with 9N HCl acid. Uranium and iron are absorbed on the anion resin in a strong hydrochloric environment. whereas thorium, radium and various alkalies and alkaline earth elements

are not. Uranium is then desorbed with 0.1N HCl (60 mls) and evaporated slowly to dryness.

If the uranium residue appears fairly substantial and brown in colour, it is boiled to dryness under reflux with 2 ml concentrated HNO_3 /HCl to remove organic materials that may be derived from the sample, ether or decomposed resin. If the residue is still brown or red, one more ether extraction is performed by dissolving the residue in a little 9NHCl acid. The sample is then transferred into a centrifuge tube and about an equal volume of ether is added. It is then squished for one minute with a Pasteur pipette. The aqueous layer is separated into a 100 ml beaker and evaporated to dryness again. A clear residue is usually obtained after this treatment.

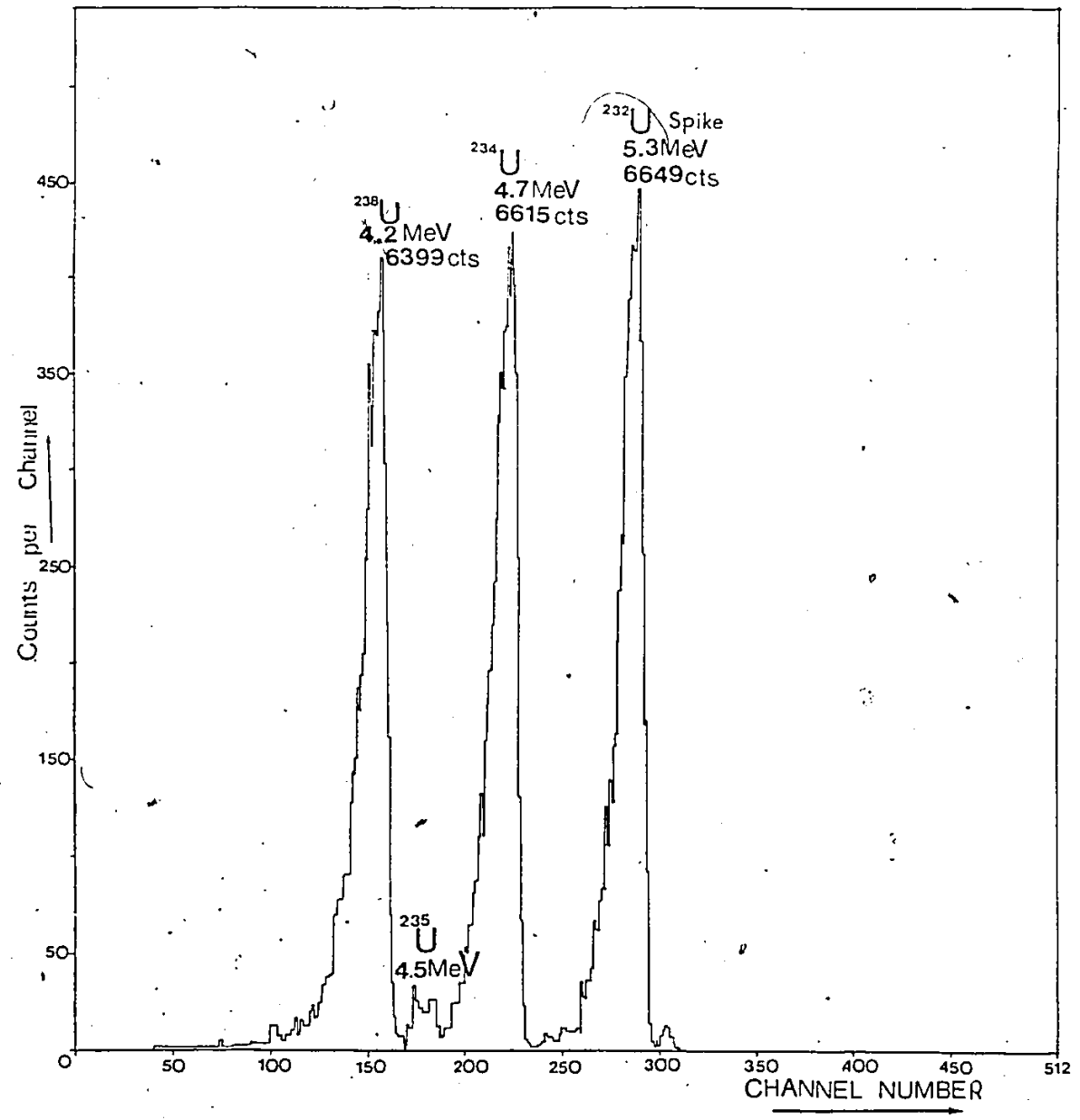
(iii) Purification, Electroplating and Counting

The residue is dissolved in 5 ml of electrolyte, evaporate to almost dryness and then taken up again in about 50 to 60 ml electrolyte. Electroplating is carried out at 12V and a current of about 0.8 Amps. onto a clean, stainless steel disc which has an exposure area of 380 mm². The details of the electroplating procedure is given in Appendix 1.

The activities of the uranium isotopes are determined on an alpha spectrometer. Eg. Figure 7 shows an actual alpha particle energy spectrum for sample GR4-114. A detailed description of the equipment can be found in Thompson (1973a). Uranium concentration and uranium activity ratio ($^{234}\text{U}/^{238}\text{U}$) of the water samples are determined from the alpha spectra using equations 3.1 and 3.2, respectively.

$$\text{U Concentration } U_w = \frac{^{238}\text{U}}{^{232}\text{U}} \times B \times \frac{V_{sp}}{V_w} \quad (3.1)$$

Fig. 7. An Actual Alpha Particle Energy Spectrum of Uranium in Groundwater.



U Activity Ratio ($^{234}\text{U}/^{238}\text{U}$):

$$A.R = \frac{^{234}\text{U}}{^{238}\text{U}} \quad (3.2)$$

where, U_w = Conc. of uranium in water (ug/l)

^{232}U = observed activity for ^{232}U (Cts./min.)

^{234}U = observed activity for ^{234}U (Cts./min.)

^{238}U = observed activity for ^{238}U (Cts./min.)

$B = ^{238}\text{U}$ equivalent spike activity constant
(22.7 ug/l = 17 dpm)

V_{sp} = volume of spike added to water sample (mls)

V_w = volume of water sample (litres).

A more detailed description of the calculation is obtained in Gascoyne (1977a, 1979).

3.2.2 Neutron Activation-Delayed Neutron Counting (NA-DNC) and Combined Fission-Track and Alpha-Track (FT-AT) Technique

The main objective here is to develop a new method for determination of $^{234}\text{U}/^{238}\text{U}$ ratio in natural waters. A litre of filtered water sample was collected for this purpose. Uranium was extracted from the sample by coprecipitating it on $\text{Fe}(\text{OH})_3$, without addition of ^{232}U spike. The rest of the procedure for U-extraction is carried out in similar way as described above.

Thermal neutron activation followed by delayed neutron counting is applied to the analysis of the uranium content of the ground water samples. From the analyses carried out by this technique it was hoped to determine:

- (i) the efficiency of coprecipitation of uranium with $\text{Fe}(\text{OH})_3$ from water samples, and

(ii) the uranium content in the water samples quickly and with a good precision.

Delayed neutron counting has been used extensively to measure U and Th contents in a variety of geological materials (Amiel, 1962; Amiel et al., 1967; Gale, 1967; Cumming, 1974). Basically, the technique depends on the fact that fissionable nuclides such as U and Th yield some fission products which continue to emit "delayed" neutrons in their subsequent decay to stable nuclides.

The half-lives of the delayed neutron-emitting precursors range from a fraction of a second to just under a minute (Amiel, 1962). These neutrons can be detected and counted with good discrimination even in the presence of large amounts of other radiations. This makes the technique highly specific and sensitive. The theory underlying the technique and analytical procedure are given in Amiel, (1962), Millard (1974), Cumming (1974), and Boulanger (1976).

This technique is non-destructive (in the sense that damage to the samples is limited to that caused by the short exposure to nuclear reactor radiations) and therefore allowing the same samples to run several times. Furthermore, after allowing any N^0 -induced radiation to cool, the samples can be used for the determination of $^{234}\text{U}/^{238}\text{U}$ ratio by the combined fission-track and alpha-track technique (described in the next section).

The feasibility of uranium determination using induced fission tracks in a suitable detector was first shown by Price and Walker (1963). Since then, many applications of the basic procedure have been reported (Fleischer and Lovett, 1968; Fisher and Bostrom, 1969; Hashimoto, 1971).

Fission track studies utilise either spontaneous or induced fission of heavy elements (eg. U). ^{235}U can be induced to fission by exposure to thermal neutrons. The fission fragments thus produced move in various directions leaving tracks of damage on an atomic scale in the material through which they pass. The tracks can be preserved in many non-conductive solid materials (eg. muscovite) and they are revealed by etching. The tracks can then be counted. The number of tracks produced for any given irradiation condition is proportional to the total uranium content of the material since the $^{238}\text{U}/^{235}\text{U}$ ratio (137.6) is essentially constant in nature with the exception of the Oklo "fossil reactor".

On the other hand, much work on uranium alpha tracks has not been done until the present time. Huang and Walker (1967) observed α -recoil tracks in muscovite and phlogopite. Isotopes of U and Th decay by emission of alpha particles. These energetic alpha particles impart a significant amount of recoil energy which damage the surrounding area of the crystal. These α -recoil tracks are preserved in some materials (detectors). The tracks can be enlarged by etching and can then be counted.

In brief, the final $^{234}\text{U}/^{238}\text{U}$ ratio is obtained from a regression curve of alpha track density/fission track density versus $^{234}\text{U}/^{238}\text{U}$ ratio. This will be discussed in chapter 4.

3.2.2.1 Thermal Neutron Activation-Delayed Neutron Counting

The precipitate, $\text{Fe}(\text{OH})_3$, was separated from the supernatant liquid by decanting and centrifuging. The sample was washed with about 2 x 10 ml of deionised water, transferred to a petri dish and dried overnight in the oven at about 70°C . A blank sample, $\text{Fe}(\text{OH})_3$, consists of

all the reagents used in the coprecipitation method is also prepared in the same manner. The dried sample was then kept in a plastic vial and irradiated at McMaster University nuclear Reactor, currently operating at a power of 2 MW with a thermal flux of 5.0×10^{12} neutrons/cm²/sec. The analytical sequence consists of 30 sec. irradiation, 10 sec. delay and 30 sec. count. The uranium content was calculated by comparison with standard samples which has undergone an identical irradiation/delayed/counting history.

3.2.2.2 Fission Track Measurement

3.2.2.2.1 Preparation of Irradiation Sample

After allowing for any N⁰-induced radiation to cool (usually about one week), a routine uranium extraction was carried out as described previously. Also, a few standards of known uranium isotopic ratio were prepared (standards with $^{234}\text{U}/^{238}\text{U}$ ratios of: 1.00, 1.40, and 1.85).

A thin muscovite layer was placed in contact with the sample (using scotch tape). Two sets of samples (J and K) were prepared. Each set contains about 15 samples and 4 standards and these were sandwiched with aluminum foil. The samples for each set were chosen in such a way that the uranium contents are comparable with the standards. Irradiations of sets J and K were performed in the RIFLS-9E position at 42 and 51 cm below the lid, respectively. Different neutron fluences were selected in order to attain a reasonable number of tracks. The estimated total fluence used for sets J and K were 8×10^{11} n/cm² and 8×10^{12} n/cm² respectively.

3.2.2.2 Etching and Track Counting

After about a week of cooling, the muscovite detectors were etched with 49% HF acid for about 20 minutes at room temperature. After etching, the detectors were washed with deionised water a few times (6 to 7 times are usually sufficient), and finally with a little ethanol. They were then dried. Fission tracks were observed under an optical microscope at 320x magnification. A grid and the tracks were then projected on a TV screen and counting of track density was done visually. Figure 8 shows the arrangement of the counting system used.

Counting of tracks was carried out by fixing the microscope stage in a given position and all tracks in the field of view bounded by the square were counted. If the tracks cross the line they were only counted if the beginning of the tracks fell within the square; this can be accessed by adjusting the fine focus control so that a clear visibility of tracks is obtained. When the counting in one field was completed, the stage was moved to the next boundary and the counting process was then repeated. The tracks were usually counted for 4 or 5 stripes depending on the track density; each stripe consists of 50 squares (1 square = 0.0506 mm^2). They usually contained greater than 10,000 tracks in 200 or 250 squares; the selected area for track counting is shown in Figure 9.

3.2.2.3 Alpha Track Measurement

Cellulose nitrate film (CN85) was mounted in contact with the samples for a period of 21 and 42 days for sets J and K respectively. It was found that sufficient numbers of alpha tracks had been accumulated during these periods. The films were then etched with 6.25N NaOH solution at $30 \pm 1^\circ \text{C}$ for a period of 12 hours. Finally they were washed with

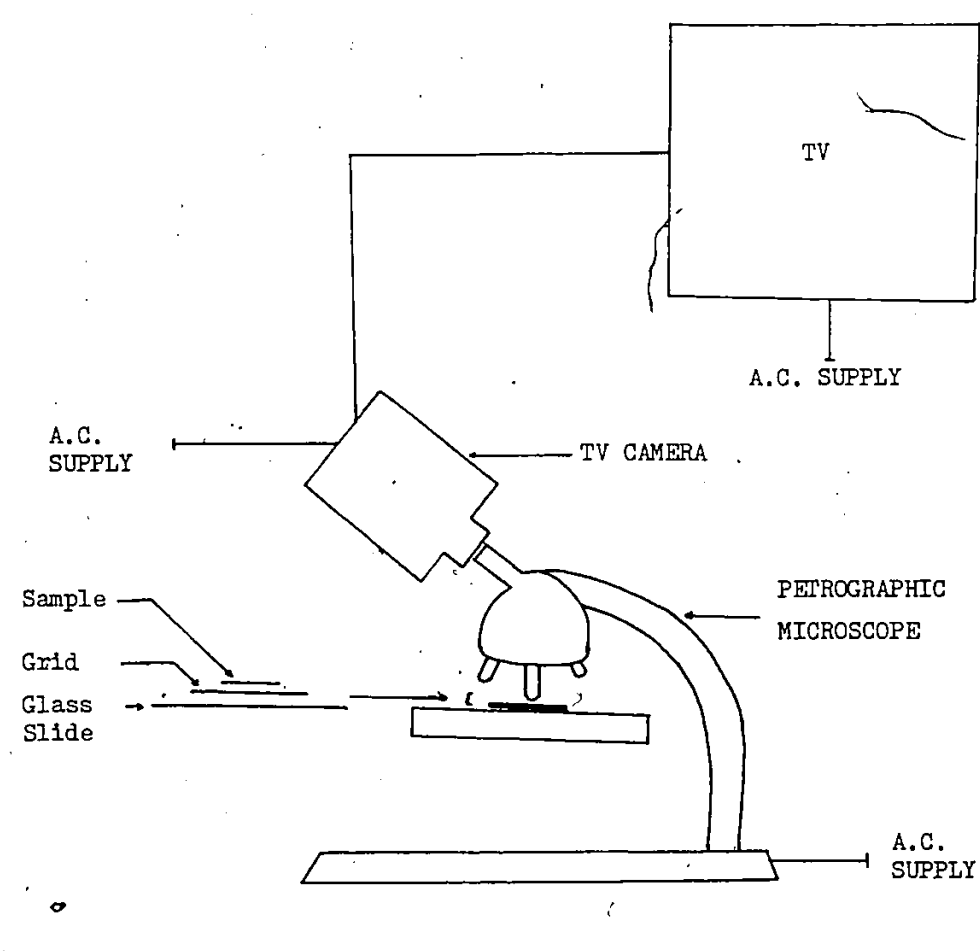
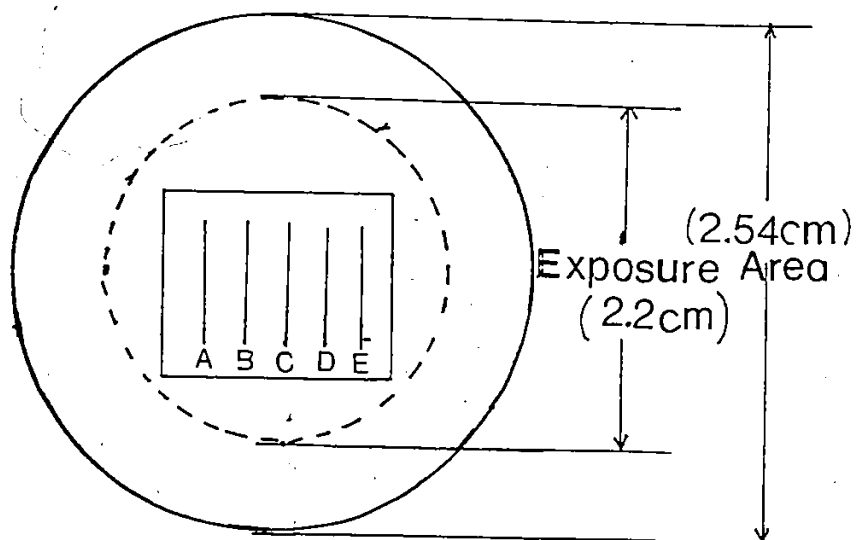


Fig. 8: A sketch diagram of experimental arrangement of the counting system.

FIG.9.
SELECTED AREAS FOR FISSION AND
ALPHA TRACKS COUNTING.



ABCD and E - stripes for counting of track.
Each stripe consists of 50 squares
1 square = 0.0506mm^2

deionised water and air-dried. Counting of track density was carried out in the same way as for fission tracks.

3.2.3 Water Chemistry Analysis

The chemical constituents analysed in the laboratory included Ca, Mg, Na, K, SO_4 , F, Si, Mn, Fe, Zn, total P, Cu, Ni, Pb, As, Cl and Mo. These analyses were done by the Dept. of Chemistry, University of Waterloo and by the Ministry of Environment, Canada. The major cations were determined using conventional methods as described by ALPHA-AWWA-WPCF (1975). Ca^{2+} , Mg^{2+} , Na^+ and K^+ were analysed on a Perkin-Elmer-305 Atomic Absorption Spectrometer. Sulphate was measured by U.V. spectrophotometry and chloride measurements were done potentiometrically using specific ion electrodes.

3.2.4 Soil and Waste Rock Analysis

Approximately 15 gm of soil sample was placed in a 250 ml pyrex beaker and wetted with distilled water. One ml of ^{232}U spike and 3 mls of iron hydroxide solutions were added. 50 mls of concentrated HCl was slowly added. The sample was then left to stand overnight. It was then boiled on a hot plate for 20 mins. The acid solution was filtered and the residue discarded. The solution was then diluted to about 500 mls. The remainder of the procedure is the same as that previously described for water.

One gram of powdered rock sample was placed in a teflon bomb. 1 ml of ^{232}U spike solution, about 8 ml HF and 2 ml conc. HNO_3 were added. It was then heated on a hot plate for about 6 hours. The solution was then poured into a polyethylene bottle containing boric acid solution and iron carrier. The remaining chemical procedure is the same as described above.

CHAPTER IV

RESULTS AND DISCUSSION

4.1 Geochemical Investigations

Bicarbonate alkalinity, pH and specific electrical conductance were measured in all multilevel water samples taken in the test holes. Major cations and anions were determined from only a few of the ground water samples (analysed by the Ministry of Environment, Ontario. As a consequence, computation of the soluble ion balances is not practicable. Results of the analyses are given in Tables 1, 2, 3, 4 and 5.

Bicarbonate concentrations in the ground water samples ranged from 3 to 295 mg/l, with most of them containing less than 80 mg/l. This range (3 to 295 mg/l HCO_3^-), is surprisingly wide. At the low end (3 to 30 mg/l HCO_3^-), it suggests waters practically deprived of soluble weathering products whilst at the high end it compares with most conduit ground waters in carbonate rocks. This is a remarkable range for what is a small geographical area.

Figures 10 to 22 show the profiles of bicarbonate concentrations in the ground water. It can be seen that the high bicarbonate values are usually found at the deep sampling sites. A distinct feature is that sites closest to the edge of the waste pile (K, B and J) show high bicarbonate even at the water table surface (70 to 100 mg/l) and a trend for concentration to double with depth to the limits of the test holes; sites a little further downstream (V and X) display only 15 to 30 mg/l bicarbonate at the water table but greater proportional increase with

Table 1 -- Chemical and Radiochemical Composition of Greyhawk Ground waters for July 1979.

Location	pH	Alkalinity (mg/l HCO ₃)	Specific Conductance (uS/cm)	Uranium Concentration (ppb)			Yield(%)	234U/238U
				α-Spect.	232U Re- covery(%)	NA-DNG		
J 1.15	6.3	80	180	10.08 ± 1.01	7	7.12 ± 0.413	74	1.24 ± 0.13 1.28 ± 0.08+
2.15	6.0	86	465	6.40 ± 0.62	10	-	-	1.22 ± 0.14
2.65	5.9	81	260	-	-	12.84 ± 0.21	-	1.21 ± 0.10+
11.85	7.5	170	550	44.23 ± 0.52	8	44.17 ± 0.52	100	1.50 ± 0.12 1.45 ± 0.03+
K 1.72	6.5	70	260	-	-	9.24 ± 0.17	-	1.07 ± 0.06+
2.72	6.3	42	260	-	-	7.89 ± 0.18	-	1.16 ± 0.10+
3.72	5.2	70	460	65.58 ± 2.92	19	-	-	0.95 ± 0.03
0 7.7	6.5	77	520	48.10 ± 3.78	10	-	-	1.41 ± 0.09 1.43 ± 0.04
Q 2.65	5.9	12	-	-	-	1.18 ± 0.05	-	1.00 ± 0.11
4.15	6.0	22	-	3.82 ± 0.35	10	-	-	1.82 ± 0.04+
15.43	7.2	100	-	-	-	-	-	-
B 2.2	6.5	110	535	82.85 ± 5.64	11	51.82 ± 0.61	63	1.27 ± 0.05
5.7	6.9	74	535	-	-	89.53 ± 1.00	-	1.30 ± 0.05+
C 8.6	6.8	143	475	45.06 ± 3.48	8	43.23 ± 0.53	96	1.16 ± 0.08

+ Unspiked runs

* Yield(%) of uranium coprecipitated onto Fe(OH)₃

NA-DNG Neutron Activation-Delayed Neutron Counting

Table 2 -- Chemical and Radiochemical Composition of Greyhawk Ground waters for September 1979
Uranium Concentration (ppb)

Location	pH	Alkalinity (mg/l HCO ₃)	Specific Conductance (uS/cm)	232U Re-		NA-DNC	Yield(%)	234U/238U
				α -Spect.	covery(%)			
B 2.7	6.6	160	680	33.49 ± 1.34	26	22.18 ± 0.42	66	1.15 ± 0.05
3.7	6.0	43	430	8.71 ± 0.42	15	6.65 ± 0.18	76	1.15 ± 0.06
4.7	6.2	62	310	14.10 ± 0.53	26	-	-	1.37 ± 0.04
5.7	6.5	74	535	23.83 ± 0.91	27	24.33 ± 0.43	100	1.22 ± 0.05
7.7	6.7	78	290	117.33 ± 2.75	38	28.96 ± 0.61	25	1.40 ± 0.02
G 5.8	6.0	22	375	8.41 ± 0.24	42	3.55 ± 0.13	42	1.07 ± 0.03
K 1.72	-	-	-	14.50 ± 0.42	16	11.62 ± 0.26	80	1.17 ± 0.03
4.60	5.1	70	545	3.95 ± 0.12	26	3.67 ± 0.13	93	1.13 ± 0.04
8.30	7.0	164	670	39.83 ± 1.40	30	38.94 ± 0.66	98	1.05 ± 0.03
M 5.93	6.4	38	445	10.19 ± 0.35	46	9.12 ± 0.29	89	1.10 ± 0.04
Q 5.85	5.9	22	220	*3.50 ± 0.75	18	-	-	1.24 ± 0.11
15.43	7.4	-	410	27.06 ± 0.79	17	24.19 ± 0.36	89	1.27 ± 0.06+
T 3.29	5.8	40	210	8.07 ± 0.27	13	2.96 ± 0.11	36	1.04 ± 0.05
4.86	6.35	80	315	9.84 ± 0.35	19	8.92 ± 0.22	91	1.03 ± 0.04
5.60	5.9	54	220	11.15 ± 0.55	6	7.48 ± 0.19	67	1.21 ± 0.06
7.91	6.2	48	320	8.52 ± 0.33	10	7.48 ± 0.19	88	1.02 ± 0.04
10.72	7.1	203	490	357.75 ± 14.20	21	340.11 ± 4.92	95	1.43 ± 0.02
U 3.29	5.25	11	280	10.84 ± 0.33	40	2.15 ± 0.10	20	1.25 ± 0.04
4.86	5.4	13	410	3.58 ± 0.12	25	2.42 ± 0.10	68	1.08 ± 0.04
6.37	5.3	11	340	2.17 ± 0.11	76	1.77 ± 0.07	82	1.23 ± 0.08
7.91	5.1	9	390	2.08 ± 0.07	38	2.01 ± 0.07	98	1.09 ± 0.04
11.80	7.6	220	480	380.21 ± 9.77	28	374.29 ± 5.48	98	1.18 ± 0.01
V 3.24	5.6	38	140	1.20 ± 0.06	40	-	-	1.20 ± 0.08
8.89	6.3	56	240	9.40 ± 0.25	31	-	-	1.07 ± 0.02
16.59	7.6	295	400	8.81 ± 0.21	37	5.64 ± 0.13	64	1.35 ± 0.03

+ Unspiked runs; * Yield(%) of uranium coprecipitated onto Fe(OH)₃;
NA-DNC Neutron Activation-Delayed Neutron Counting.

Table 3 -- Chemical and Radiochemical Composition of Greyhawk Ground water for October 1979

Location	pH	Alkalinity (mg/l HCO ₃)	Specific Conductance (uS/cm)	Uranium Concentration (ppb)				Yield(%) [*]	234U/238U
				α-Spect.	232U Re- covery(%)	NA-DNG	238U		
GR9-	6.1	23	210	49.94 ± 0.44	52	25.05 ± 0.44	50	1.07 ± 0.02	
2.57	5.5	9	245	8.60 ± 0.23	64	-	-	1.12 ± 0.03	
2.82	3.2	-	500	1.80 ± 0.07	41	-	-	1.58 ± 0.06	
GR10-	5.6	16	220	6.07 ± 0.16	61	5.18 ± 0.15	85	1.19 ± 0.03	
2.65	5.2	9	210	4.77 ± 0.10	44	2.54 ± 0.09	56	1.30 ± 0.02	
2.90	5.8	7	360	-	-	1.83 ± 0.09	-	-	
GR11-	5.9	16	150	3.22 ± 0.11	45	3.40 ± 0.14	100	1.36 ± 0.04	
2.65	5.85	31	120	2.04 ± 0.07	42	0.91 ± 0.06	45	1.08 ± 0.04	
2.90	6.2	31	100	1.50 ± 0.05	48	0.98 ± 0.05	65	1.36 ± 0.05	
GR4-	4.8	3.2	760	22.31 ± 0.54	43	22.94 ± 0.36	100	1.03 ± 0.02	
1.64	4.95	3.0	750	27.62 ± 0.73	24	-	-	1.00 ± 0.02	
GR6-	5.5	12.4	590	9.51 ± 0.23	58	7.48 ± 0.16	80	1.10 ± 0.02	
1.89	5.4	9.1	420	5.45 ± 0.21	47	4.89 ± 0.13	90	1.13 ± 0.05	
2.14	5.5	15.3	450	5.99 ± 0.20	52	5.34 ± 0.14	89	1.17 ± 0.04	
U-	-	-	-	2.86 ± 0.11	27	-	-	1.63 ± 0.08	
2.52	5.2	8	270	2.39 ± 0.06	50	2.13 ± 0.08	89	1.20 ± 0.03	
4.06	5.5	10	350	2.00 ± 0.15	17	1.59 ± 0.07	80	1.57 ± 0.14	
7.14	5.5	10	440	5.80 ± 0.23	48	4.87 ± 0.13	84	1.16 ± 0.05	
8.89	7.5	210	480	319.41 ± 7.31	22	-	-	1.16 ± 0.01	
X-	5.8	15	140	4.05 ± 0.21	52	-	-	1.56 ± 0.09	
4.06	6.1	54	310	19.68 ± 0.56	36	-	-	1.39 ± 0.03	
7.14	6.5	120	375	107.00 ± 2.86	35	-	-	1.71 ± 0.03	

+ Unspiked runs

* Yield(%) of uranium coprecipitated onto Fe(OH)₃

NA-DNG Neutron Activation-Delayed Neutron Counting

Table 4 (Cont'd.)

Location	SO ₄ ²⁻ (mg/l)	CL ⁻ (mg/l)	NO ₃ ⁻ (mg/l)	Na ⁺ (mg/l)	K ⁺ (mg/l)	Ca ²⁺ (mg/l)	Mg ²⁺ (mg/l)	Si (mg/l)	F (mg/l)	P (mg/l)
K-										
1.22	62	1.0	-	16.0	2.8	31.1	2.0	3.2	0.1	-
9 1.72	69	6.0	1.8	3.0	2.8	-	-	-	-	-
2.72	124	1.0	0.1	2.0	2.9	54	4.0	-	-	-
3.22	167	1.3	-	3.1	3.6	60	5.0	2.7	0.1	-
3.72	36	2.0	0.1	2.0	1.4	29	5.0	-	-	-
4.22	290	1.0	-	3.5	4.4	99	5.7	3.7	0.2	-
4.60	214	3.0	0.3	11.0	2.2	90	13.0	-	-	-
U-										
✓ 2.52	3									
3.29	10									
✓ 4.06	12									
4.86	18									
5.63	16									
6.37	-									
✓ 7.14	15									
7.91	15									
✓ 8.89	27									
✓ 11.80	8									

- N.B.: 1. All water samples were sampled on Oct. 29 and 30/79 except for the samples indicated by a (+) mark which were sampled on July 9 and 10/79.
2. All samples were analysed by the Ministry of Environment, Ontario.

✓ Analyses for alkalinity, etc. also given in Table 1 or 3 for these samples.

Table 5 -- Trace Metal Composition of Greyhawk Ground water

Location	Mn mg/l	Al mg/l	Fe mg/l	Zn mg/l	Pb mg/l	Ni mg/l
GR1-						
5	0.04	0.54	0.13	0.29	0.03	0.02
6	0.07	0.70	0.04	0.08	0.03	0.02
GR2-						
4	0.30	0.16	0.25	0.49	0.03	0.02
6	0.07	0.91	0.08	0.10	0.03	0.02
GR4-						
✓ 1.14	0.89	11.0	0.17	0.38	0.03	0.13
✓ 1.64	1.50	16.0	0.50	0.37	0.03	0.21
B-						
+ ✓ 2.50	0.70	-	1.80	0.04	0.08	0.02
+ ✓ 5.68	0.02	-	0.04	0.05	0.08	0.02
K-						
1.22	0.09	-	0.04	0.86	0.08	0.02
1.72	0.02	0.04	0.04	0.21	0.03	0.02
2.72	0.02	0.03	0.02	0.11	0.04	0.02
3.22	0.03	-	0.04	0.54	0.08	0.02
3.72	1.70	0.02	1.90	0.41	0.03	0.02
4.60	0.05	-	0.04	0.35	0.08	0.02
8.03	0.45	0.02	0.04	0.06	0.03	0.02
O-						
2.40	0.06	0.04	0.15	0.12	0.08	0.02
2.90	0.56	-	0.66	0.14	0.08	0.02
3.90	0.40	0.04	2.10	0.04	0.03	0.02
4.90	0.63	-	0.71	0.45	0.08	0.02
5.40	0.09	0.02	0.92	0.05	0.03	0.02
5.80	0.06	0.02	1.20	0.06	0.03	0.02
7.70	0.52	0.02	6.40	0.04	0.03	0.02

.../

Table 5 (Cont'd.)

Location	Mn mg/l	Al mg/l	✓ Fe mg/l	Zn mg/l	Pb mg/l	Ni mg/l
Q-						
+ ✓ 2.65	0.21	-	0.04	0.21	0.08	0.02
+ ✓ 4.15	1.20	-	0.31	0.20	0.08	0.02
+ 5.85	1.20	-	1.51	0.34	0.08	0.02
P-						
1.50	0.21	-	0.14	0.05	0.08	0.02
2.00	0.13	-	0.04	0.05	0.08	0.02
Y						
3.29	0.25	0.02	0.25	0.16	0.03	0.02
4.83	0.48	0.02	1.40	0.42	0.03	0.02
7.14	0.13	0.02	0.28	0.32	0.03	0.02
7.91	0.11	0.02	0.23	0.14	0.03	0.02
14.45	0.10	0.02	0.08	0.03	0.04	0.02

N.B.: 1. The chemical constituents which were analysed to be constant throughout all the analysed water samples were:

Cu	0.01 mg/l
Cr	0.02 "
Cd	0.05 "
As	0.01 "
Mo	0.04 "

2. All samples were analysed by the Ministry of Environment, Ontario.
 3. All water samples were sampled on Oct. 29 and 30/79, except for the samples indicated by a (+) mark which were collected on July 9 and 10/79.
- ✓. Analyses for alkalinity, etc. also given in Table 1 or 3 for these samples.

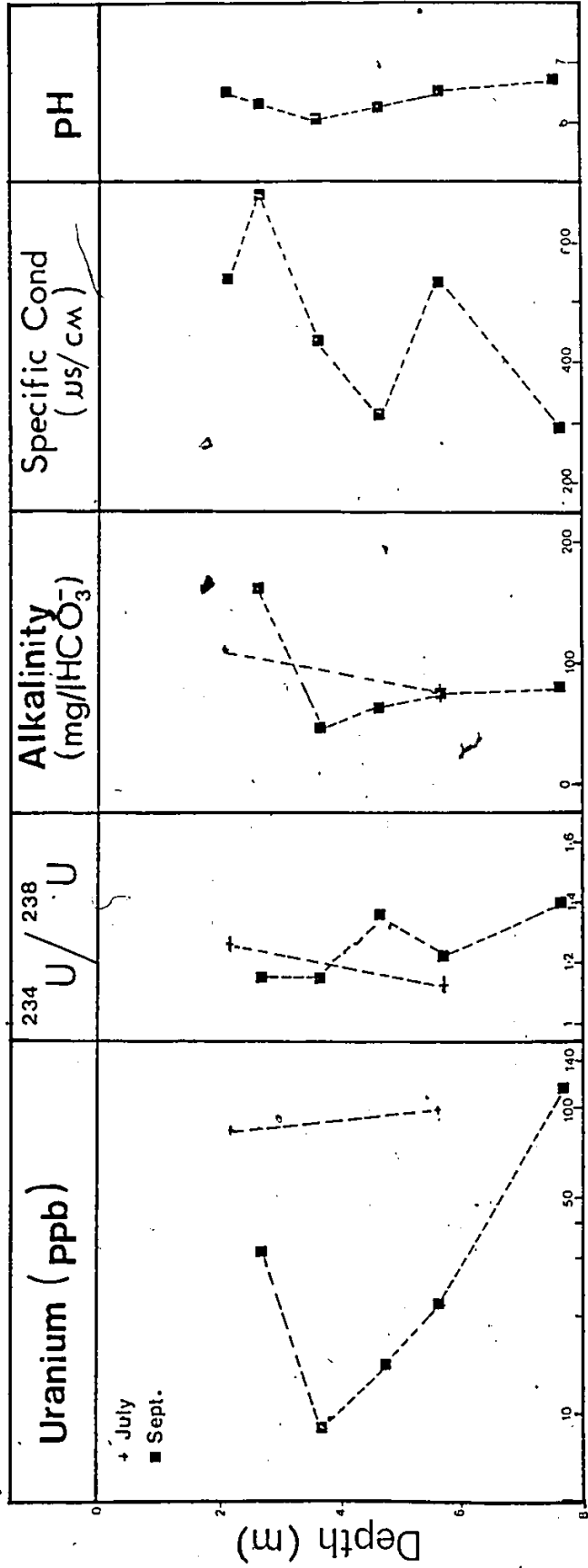


FIG. 10. CHEMICAL AND RADIOCHEMICAL COMPOSITION OF GREYHAWK GROUNDWATER AT VARIOUS LEVELS FOR SITE B.

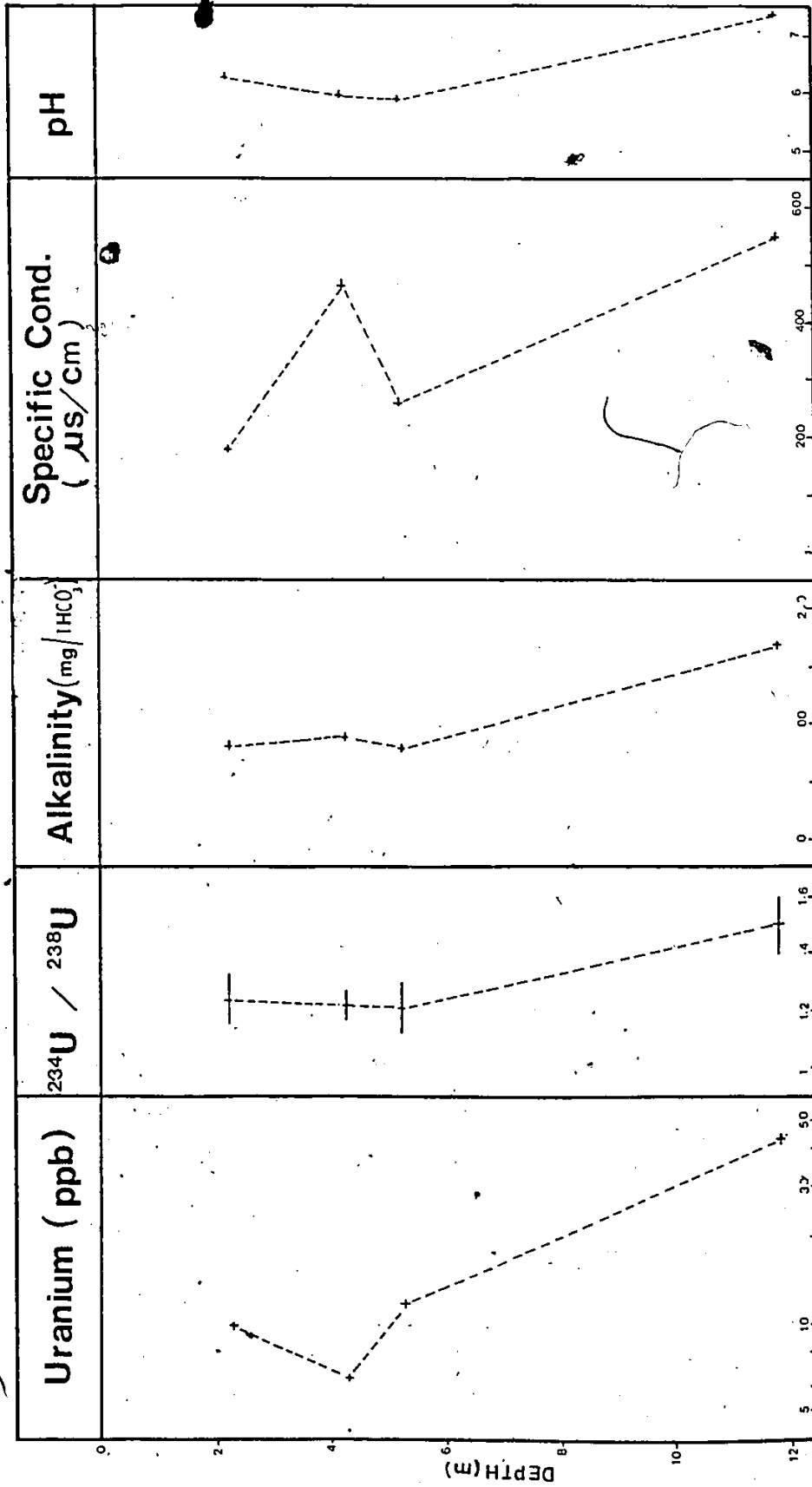


FIG. 11. CHEMICAL AND RADIOCHEMICAL COMPOSITION OF GREYHAWK GROUND WATER AT VARIOUS LEVEL FOR SITE J (Sampled in July 1979).

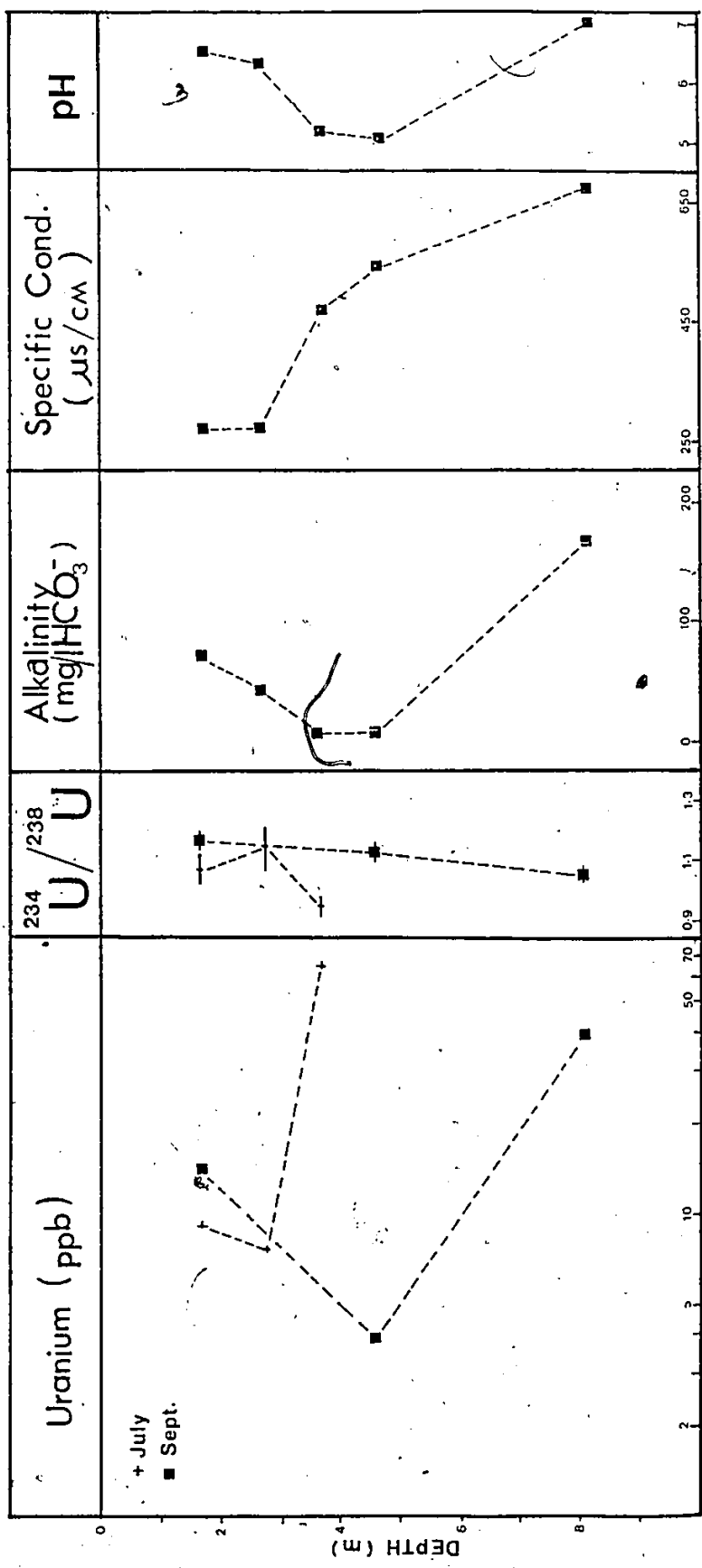


FIG. 12. CHEMICAL AND RADIOCHEMICAL COMPOSITION OF GREYHAWK GRONDWATER AT VARIOUS LEVELS AT SITE K.

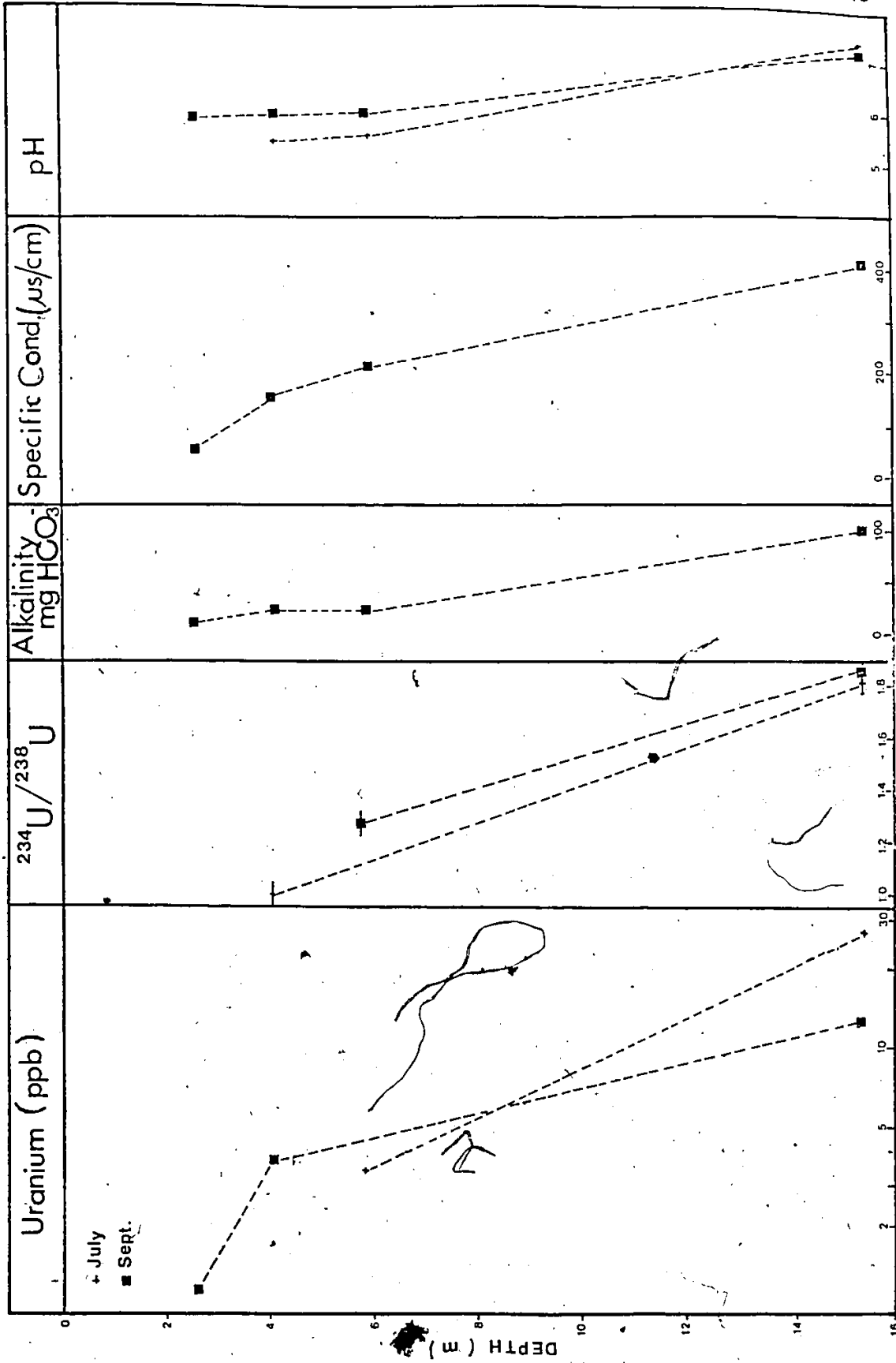
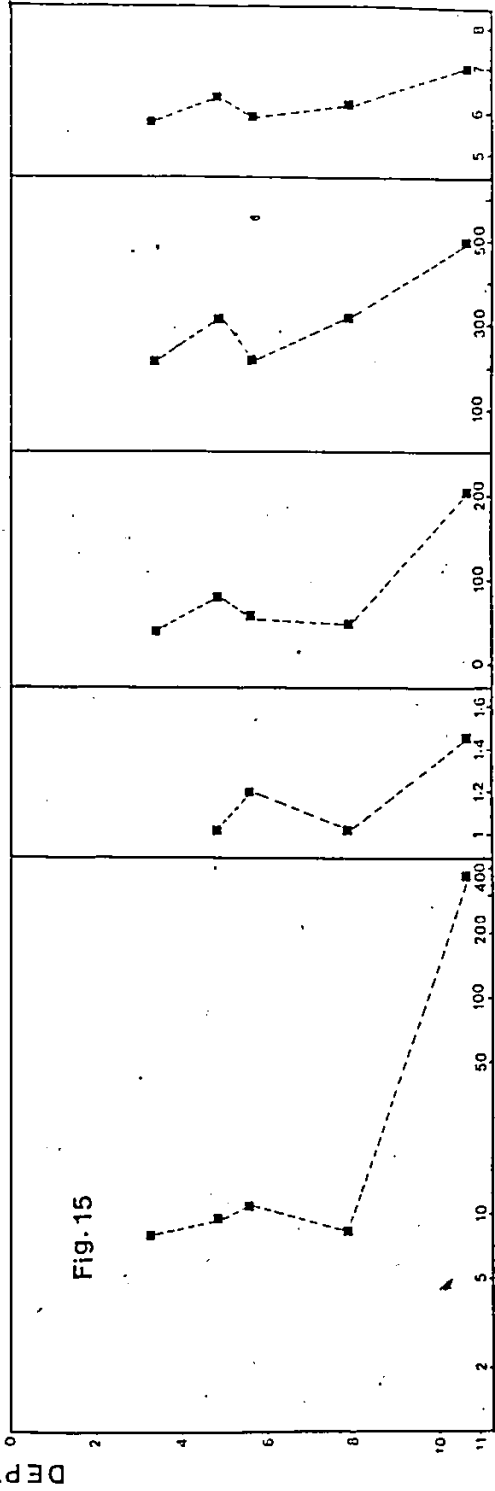
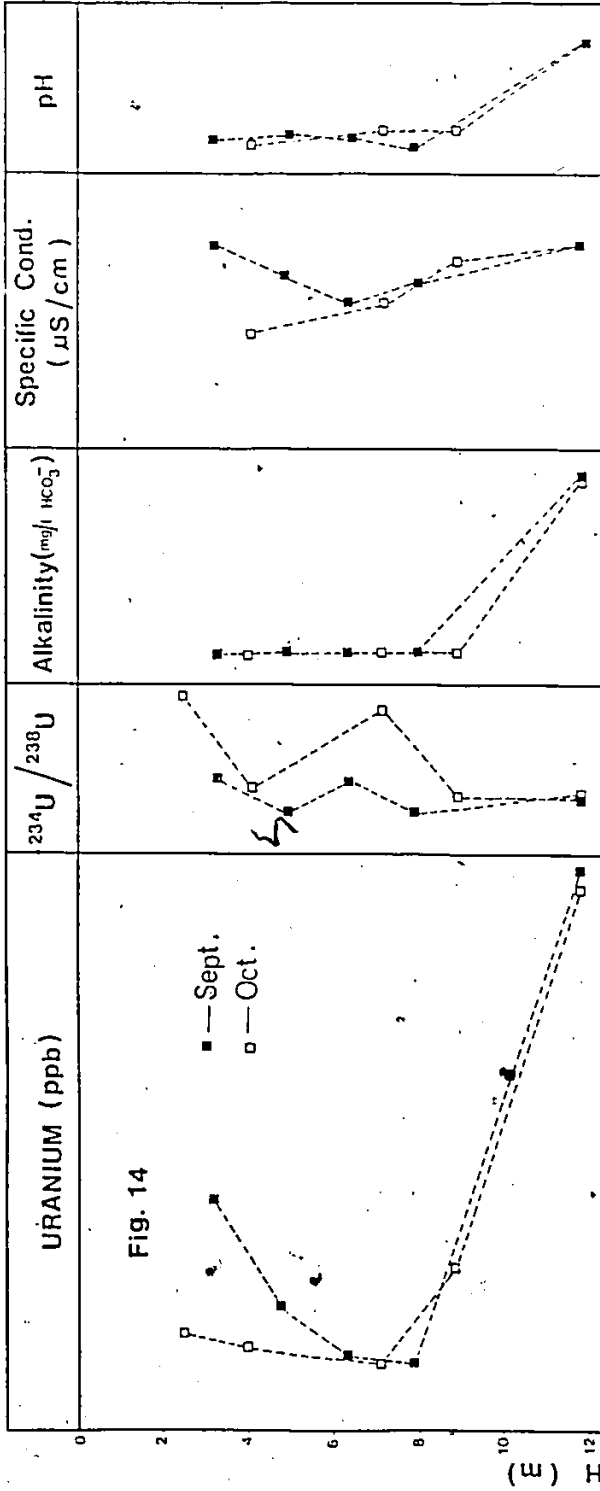


FIG. 13. CHEMICAL AND RADIOCHEMICAL COMPOSITION OF THE GREYHAWK GROUNDWATER AT VARIOUS LEVELS FOR SITE Q.



Figs 14, 15. Chemical and Radiochemical Composition of Greyhawk Ground water at Various levels For Sites U and T Respectively.

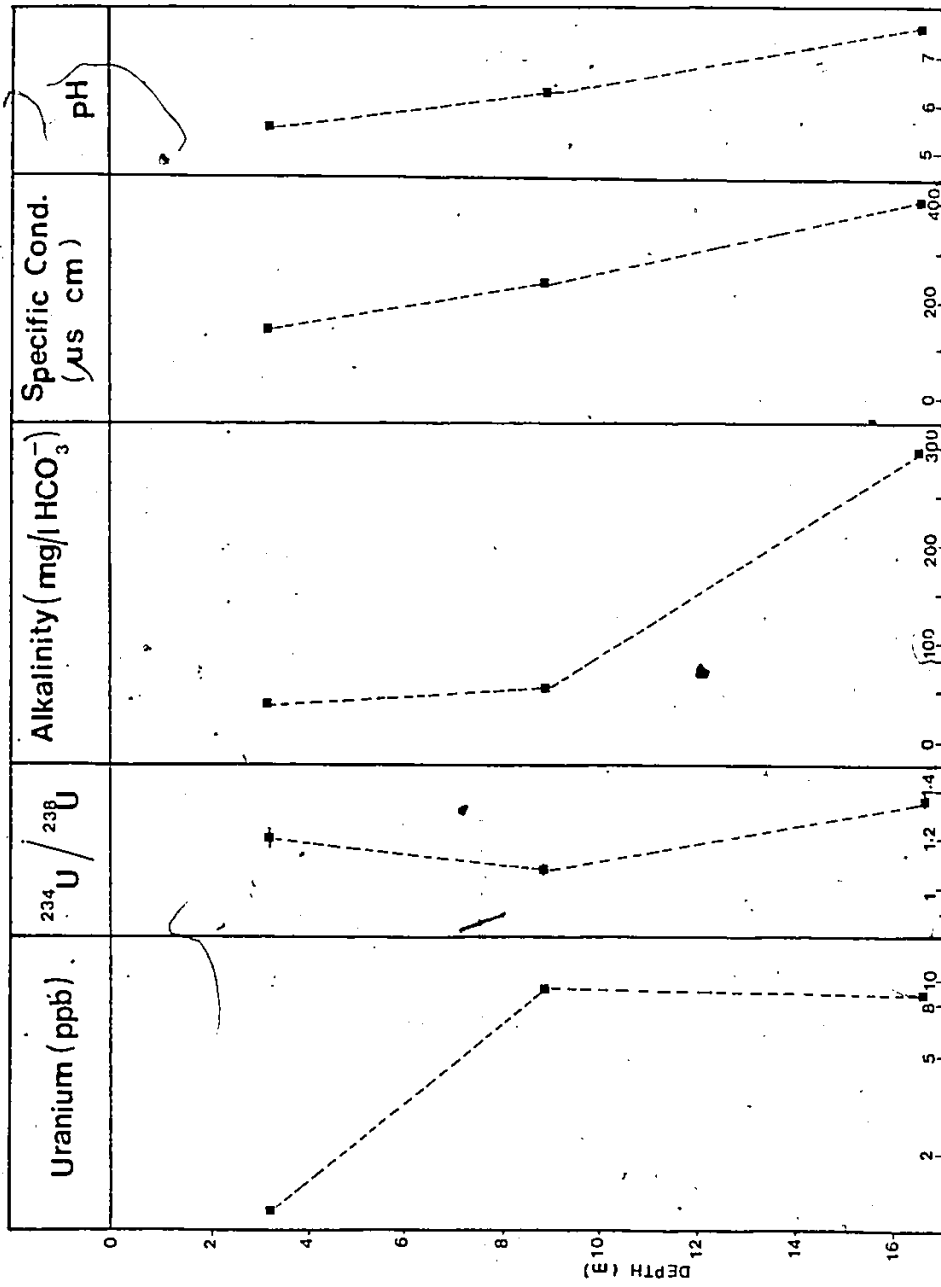


FIG. 16. CHEMICAL AND RADIOCHEMICAL COMPOSITION OF GREYHAWK GROUNDWATER AT VARIOUS LEVELS FOR SITE V.

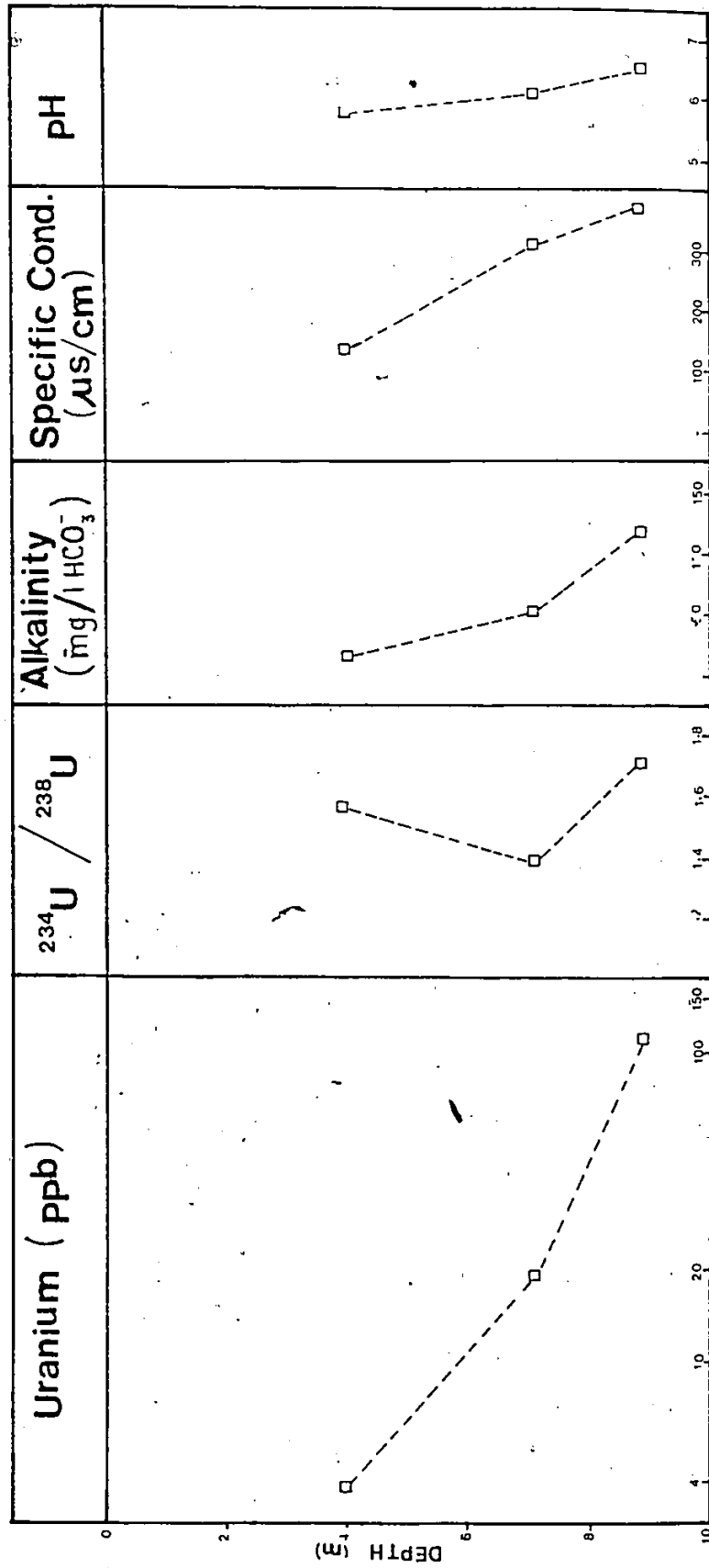
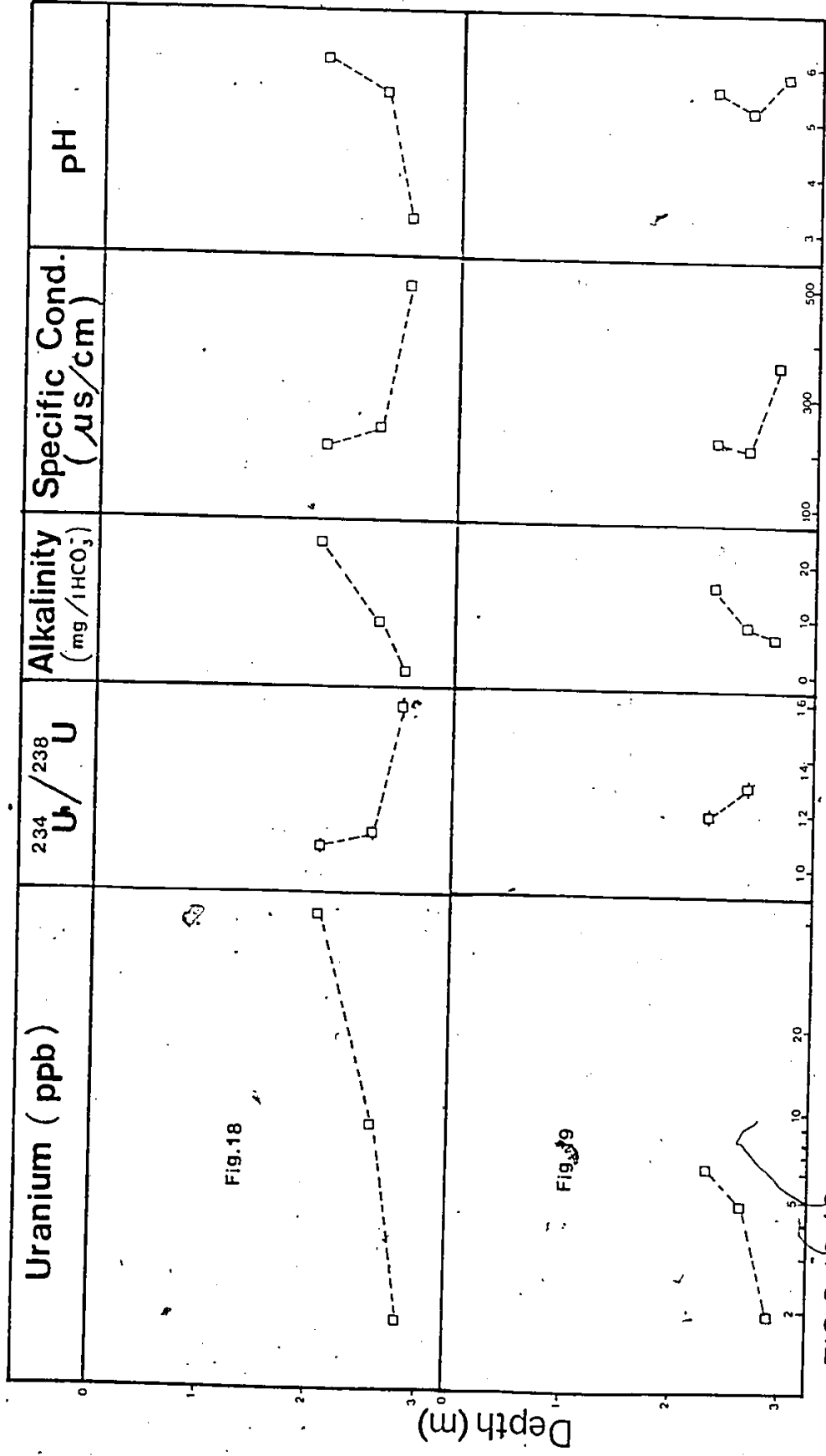
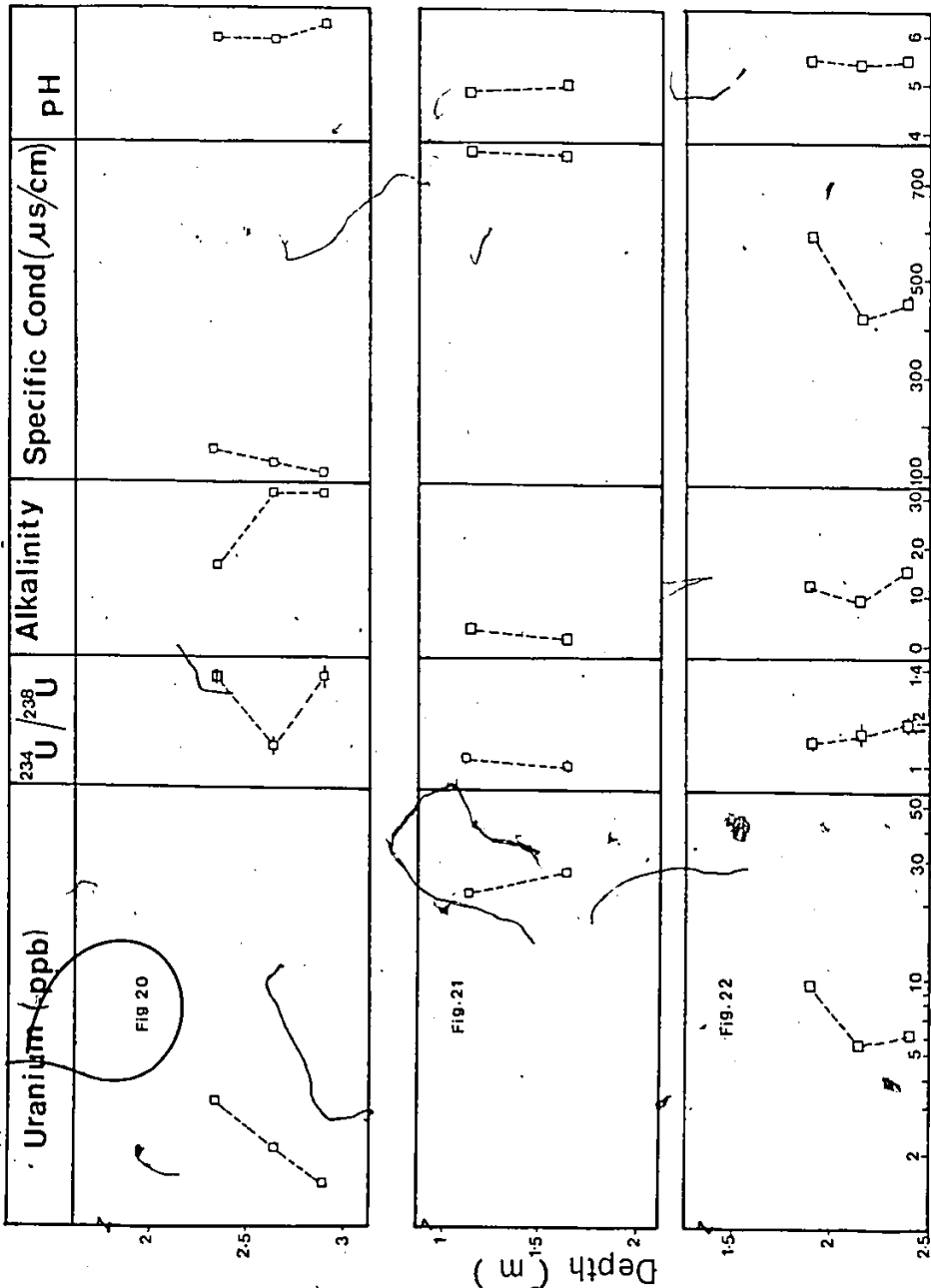


FIG.17. CHEMICAL AND RADIOCHEMICAL COMPOSITION OF GREYHAWK GROUNDWATER AT VARIOUS LEVELS FOR SITE X.



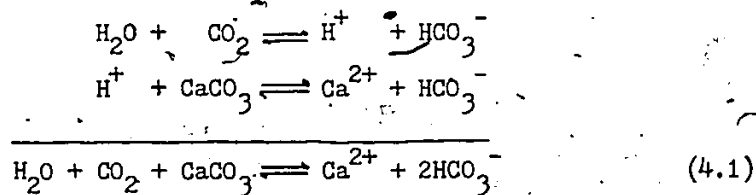
FIGS. 18, 19. CHEMICAL AND RADIOCHEMICAL COMPOSITION OF GREY HAWK GROUNDWATER AT VARIOUS LEVELS FOR SITES GR 9 AND 10 RESPECTIVELY.



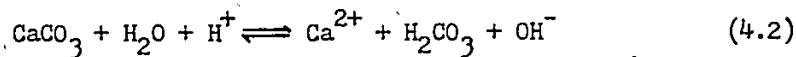
FIGS 20, 21, 22: CHEMICAL AND RADIOCHEMICAL COMPOSITION OF 'GREY HAWK' GROUNDWATER AT VARIOUS LEVELS AT SITES GRS'11, 4 AND 6 RESPECTIVELY.

depth, about 10 times. This is an initial suggestion of a plume of hard water descending within the aquifer as it flows from the waste pile. However, water samples taken from sites GR9, GR10 and GR11 contained low bicarbonate concentration even though they were located close to the waste pile; here, it is supposed that conditions had not stabilized at the time of sampling after the disturbance of the clearing operation of the waste pile. In general, bicarbonate hardness at the water table everywhere at the undisturbed sites closest to the pile are sufficiently low to indicate that negligible HCO_3^- is being produced by weathering of the aquifer sand in the vadose zone. It was found that these sands contain negligible carbonate material. It is supposed, therefore, that the bicarbonate content in the waters is produced from dissolution of carbonate minerals such as dolomite and calcite that are associated with the metagabbro and perhaps from dissolution of nearby marble. Additionally, it may be produced by solution at the bedrock surface and in fissures and joints within the rock. Furthermore, part of HCO_3^- may be produced from the oxidation of organic matter. The reactions for calcite and dolomite dissolution are represented as follows:

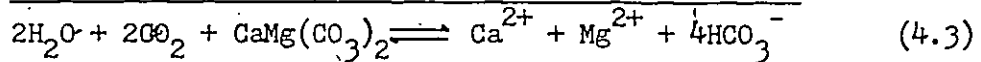
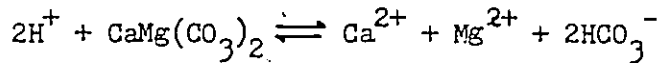
Calcite Dissolution Reaction:



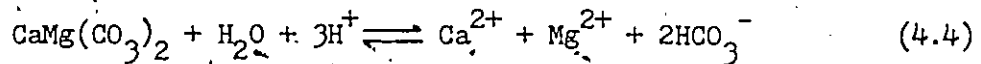
Also,



Dolomite Dissolution Reaction:



Also,



The most likely mechanism for producing an acid medium (eqs. 4.2 and 4.4) is oxidation of pyrite (will be discussed below); pyrite was found to be associated with the metagabbro. The source of H^+ ions may also be attributed to acid rain and snow.

The electrical conductance of the ground water samples ranged from 50 to 680 $\mu\text{S}/\text{cm}$. The majority of the determinations are above 200 $\mu\text{S}/\text{cm}$. Figures 10 to 22 show the distribution. No very strong trends for the specific electrical conductance are observed. The variation is complex, especially for shallow water samples. However, high values are usually observed for waters near the waste rock and at the deep sites. Also, there is some trend to gradual decrease in conductance values as the water flows away from the waste rock. The complexity of the conductance patterns, is probably caused by the following factors:

- (i) Complex flow patterns and variation in hydraulic conductivity resulting from the non-uniform nature of the aquifer sands.
- (ii) The presence of varying source areas (which are not adequately identified; eg. differing composition at different places on the waste rock pile, and
- (iii) Effect of the activity during the time the mine was in operation.

pH values, in general, varied from 5.0 to 7.6, except for site GR9-2.82 (pH = 3.2). The higher pH values always appear at deep sampling sites. There is an evident relationship with bicarbonate concentration; high pH values are also associated with high conductance values.

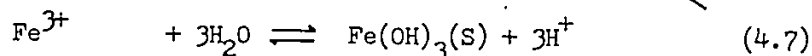
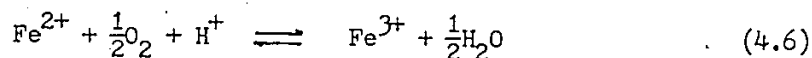
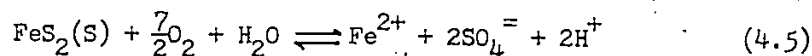
Dissolved oxygen values vary from 0.6 to 10 mg/l with most being in excess of 3 mg/l. These values suggest that the Eh would be in excess of a few hundred mV. However, based on the reduced appearance (grey) of the soil samples collected about 2.5 m below ground surface during the drilling programme, Eh values near zero or in the negative range would have been expected. Moreover, water sample from site V-16.59 contained H₂S gas which is certainly an indication of a reducing environment. The validity of the dissolved oxygen results is therefore questionable.

The laboratory analyses of Mg, K, Cl, F, Si, Zn, total P, Cu, Ni, Pb, As and Mo show the concentrations of these constituents to be relatively constant over the site. Other parameters, including Mn and Fe showed some variability; Fe varies from < 0.04 to about 2.0 mg/l whereas Mn varies from < 0.02 to 1.70 mg/l.

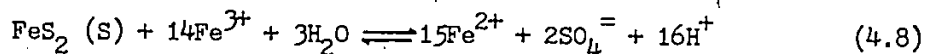
The other variability was observed in the Ca²⁺ and SO₄⁼ data. For the few water samples analysed in detail, Ca²⁺ ranged from 21.4 to 99 mg/l and SO₄⁼ from 3 to 350 mg/l (Table 4). High Ca²⁺ and SO₄⁼ values usually occurred at sites near the waste rock as well as in samples taken at greater depths. However, the ability to map discrete sulphate plumes emanating from the waste rock is, at this point, quite uncertain due to very little data available.

Significant concentrations of SO₄⁼ which occur in the ground water may be produced from the oxidation of pyrite that takes place during the

weathering of the waste rock. Pyrite was found in association with the waste rock (metagabbro). During and after the mining operation pyrite is exposed to air and water; the suggested reactions of pyrite oxidation (Stumm and Morgan, 1970) are



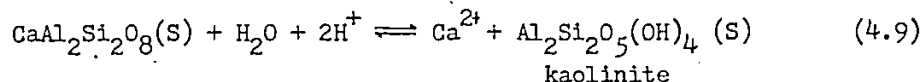
The oxidation of the pyrite to sulphate (eqn. 4.5) releases dissolved ferrous iron and acidity into the water. Subsequently, the dissolved ferrous iron undergoes oxygenation to ferric iron (eqn. 4.6) which then hydrolyses to form insoluble "ferric hydroxide" (4.7), releasing more acidity to the ground water. Ferric can also be reduced by pyrite itself, as in eqn. 4.8 below, where sulphide is again oxidised and acidity is released along with additional ferrous iron which may re-enter the reaction cycle via (4.6).



As a result, pyrite is recognised as the major source of $\text{SO}_4^{=2-}$ and acid water at the study site.

On the other hand, high Ca^{2+} concentration in the waters is probably a result of dissolution of dolomite and calcite which occur in association with the metagabbro and also perhaps from the nearby marble (mentioned earlier). Moreover, anorthite ($\text{CaAl}_2\text{Si}_2\text{O}_8$) which is a common feldspar in the gabbro is generally regarded as being quite leachable relative to K-feldspar and the more sodic plagioclase feldspars. It may be another source of Ca^{2+} besides calcite and dolomite. The anorthite

reaction is



The source of H^+ ion is presumably from the oxidation of pyrite.

In general, leachate from the waste rock which is migrating in the Greyhawk aquifer could be transported in three distinct routes as shown in Figure 23:

- (a) In shallow ground water zone;
- (b) along the bedrock surface; and
- (c) Leachate with high H^+ content (from pyrite oxidation) may possibly be migrating through rock fissures and joints and concurrently dissolving carbonates and other minerals as it passes.

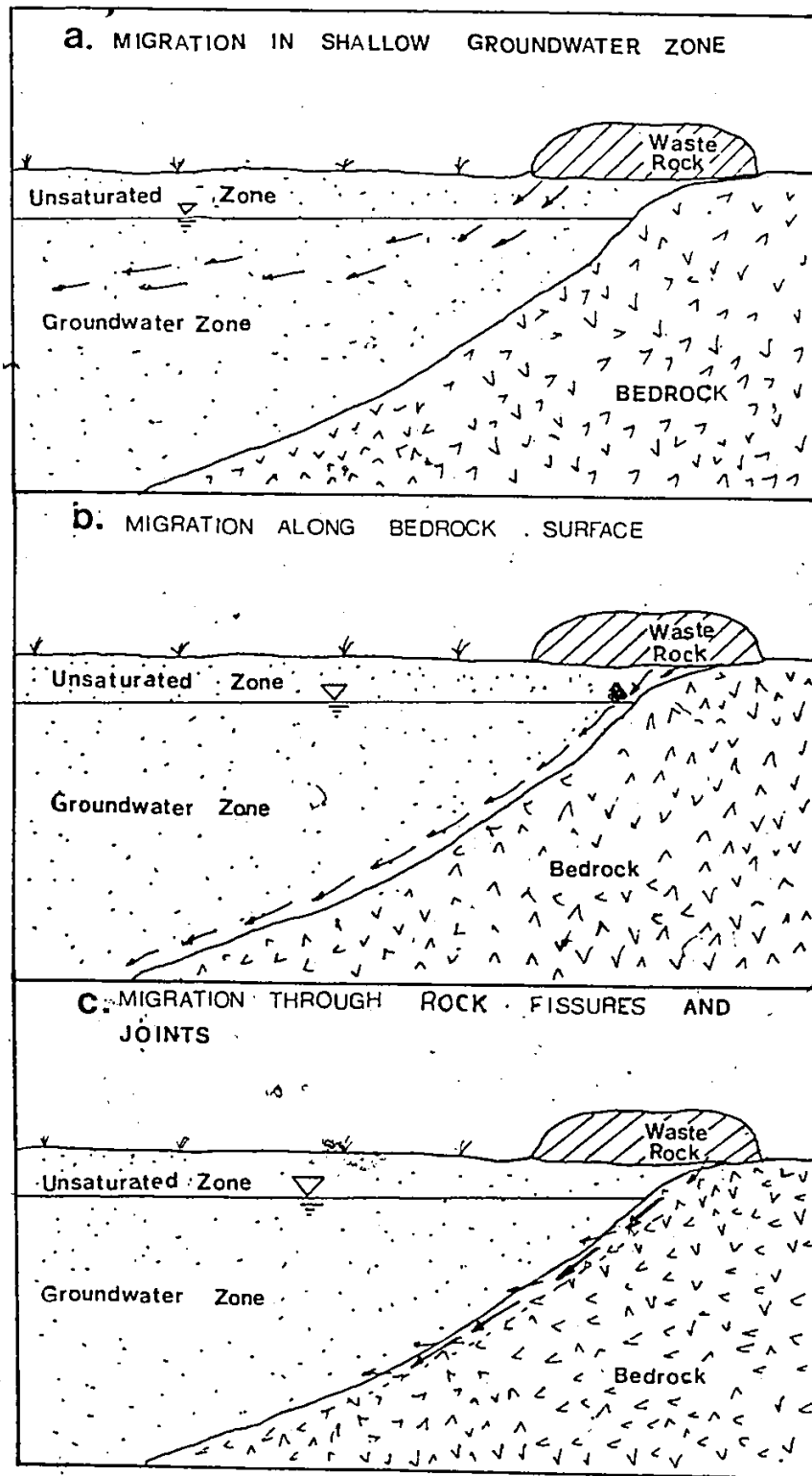
The high conductance values and bicarbonate concentrations at greater depths may be explained by a combination of the last two hypotheses.

In summary, the Greyhawk ground waters can generally be classified into two types with respect to their geochemical constituents. Firstly, the shallow ground water, with low electrical conductance which, perhaps, may imply low total dissolved solids (TDS). Secondly, the deeper ground-water, with a much higher electrical conductance with calcium, sulphate as well as bicarbonate being a primary constituent. At shallow depths leachate from the waste rock and with high conductance may be distributed in a complex manner.

4.2 Radiochemical Investigations

Ground water samples were analysed for their uranium content and isotopic ratio ($^{234}\text{U}/^{238}\text{U}$) by the alpha spectrometry method. The results of analyses are given in Tables 1, 2 and 3.

FIG. 23. THREE DISTINCT ROUTES OF MIGRATION OF LEACHATE IN SANDY AQUIFER, GREYHAWK MINE.



The chemical yields for uranium ranged from about 10% to 76%, with most of the determinations clustered between 30 to 50%. This lies within the range of the majority of analyses cited as in the literature. The errors shown with each analysis are from the counting statistics; most of them fell within $\pm 5\%$.

4.2.1 Uranium in Water

The concentration of uranium in ground waters from the Greyhawk Mine ranged from 1.20 ppb to as high as 380 ppb. The majority of the determinations however, fell between 10 and 50 ppb. Most of the water samples at deepest sampling positions showed significant concentrations of uranium; for example, sites B, T, U and X contained 117, 357, 380 and 107 ppb of uranium, respectively. However, sites V and Q are the exception, with only 8 ppb and 27 ppb U, respectively. The low concentration of uranium at depth at V is attributed to a strongly reducing environment found there, as shown by the presence of H_2S gas in the water sample. Low uranium content at site Q is most probably due to its greater distance from the waste rock source. Nevertheless, significant concentrations of uranium generally occur in the deep ground water zone (Tables 1, 2 and 3). Also, water samples near the water table were found to contain quite high uranium content (mostly above 10 ppb). This may be influenced by the dissolved oxygen (hence Eh) and CO_2 availability near the water table. Also, as noted by Langmuir (1978) uranium is more soluble as p_{CO_2} increases in the water. Sites GR9, GR10 and GR11 clearly showed this situation.

The distribution of uranium concentration in the groundwater samples at various levels are shown in Figures 10 to 22. In most cases, uranium content tends to decrease with depth to about 4 to 6 meters below

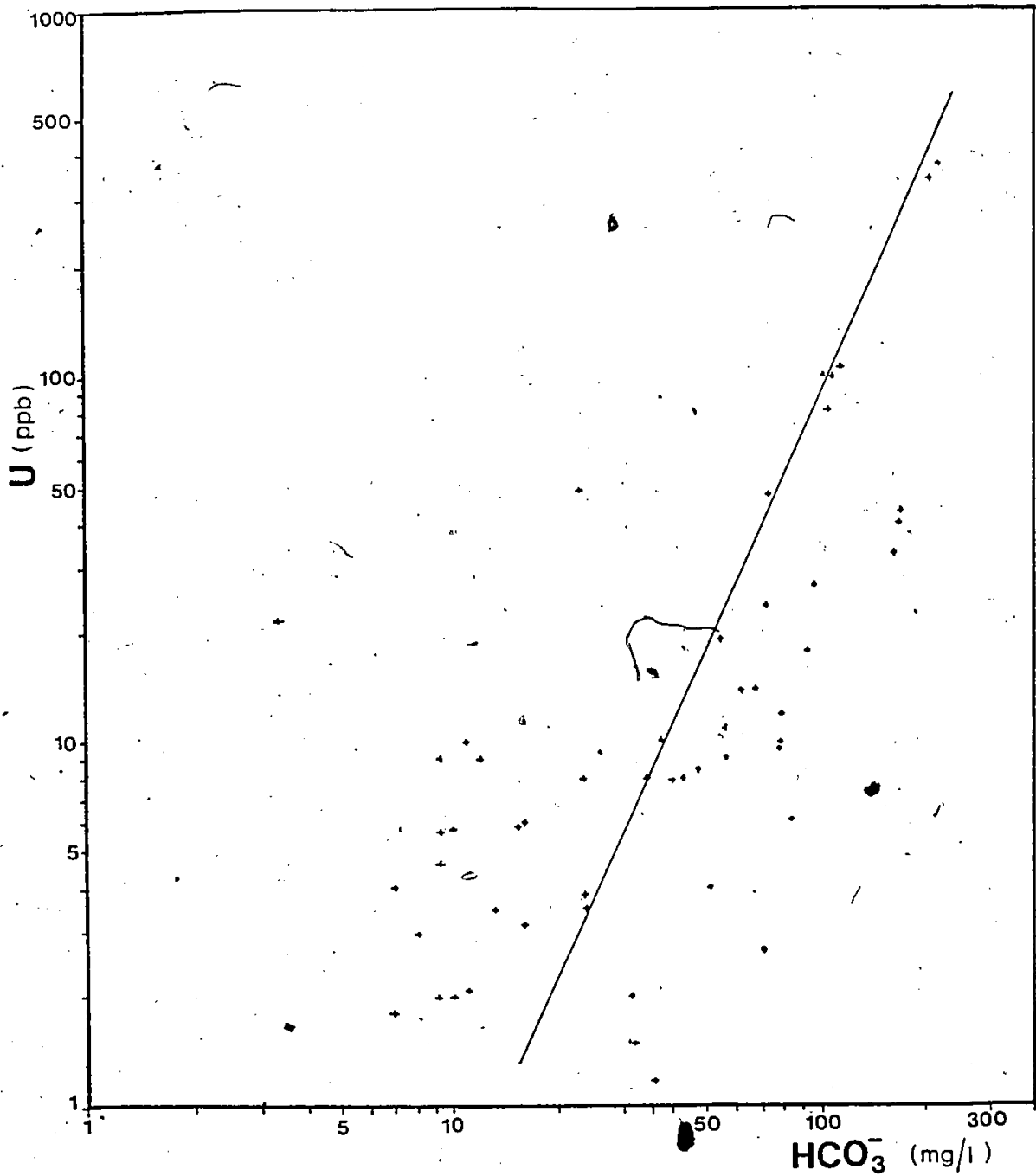
the ground surface and then to increase from there downwards. This pattern occurs repeatedly at most of the sites, eg. B (Fig. 10), J (Fig. 11), K (Fig. 12) and U (Fig. 14); the exception is site V (Fig. 16).

The increase in uranium content from about 6 m downward probably represents the front of a uranium-enriched water mass expanding downwards into the aquifer by diffusion.

The geochemical parameters of the ground waters were examined statistically to provide a more rigorous estimate of possible correlations with uranium abundance. The data set consisted of partial or complete analyses of geochemical and radiochemical parameters. The predominant anions (HCO_3^- and SO_4^{2-}) present in the Greyhawk ground waters were emphasised, and were plotted against uranium content as these ions presumably combine with uranium ions to form stable and soluble complexes.

Figure 24 is a plot of uranium content against bicarbonate concentration for the samples. It shows a fair positive correlation; the 'r' value is 0.57. As can be seen, the uranium content in the water tends to increase as the bicarbonate concentration increases. Also, the individual sites (Figs. 11 to 22) show this trend in detail. Site U-11.80 which has the second highest value of bicarbonate concentration, contains the highest concentration of uranium (380 ppb). However, site V-16.59 is an exception; although the water sample contained the highest measured concentration of bicarbonate, it had only 8 ppb of uranium. Probably this is due to the existing reducing conditions which are more favourable for the precipitation of uranium species. Here, the carbonate complexes may be broken down and uranium precipitates (Kronfeld and Adams, 1974).

FIG. 24.A PLOT OF URANIUM CONTENT VERSUS BICARBONATE CONCENTRATION IN GREYHAWK GROUNDWATER.

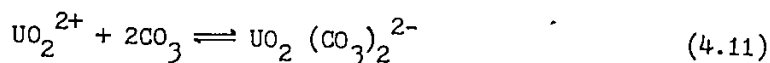


The general relationship shown on Figure 24 is probably the result of the formation of very stable and soluble anionic uranyl carbonate complexes. Carbonate species are available from the dissolution of calcite and dolomite and also from the dissolved CO_2 . Uranyl carbonate complexes may be formed as follows:

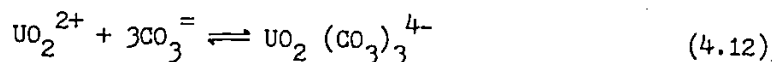
(i) Uranyl carbonate



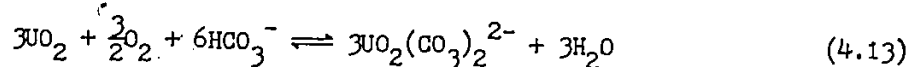
(ii) Uranyl di-carbonate



(iii) Uranyl tri-carbonate



Langmuir (1978) has shown that uranyl carbonate complexes; UO_2CO_3^0 , $\text{UO}_2(\text{CO}_3)^{2-}$ and $\text{UO}_2(\text{CO}_3)_3^{4-}$ are stable at pH 5.0 to 6.8, 6.8 to 8.0 and greater than 8.0, respectively (see Figure 25). Hostetler and Garrels (1962) also noted that the carbonate ions are stable enough to tie up considerable concentrations of uranium even under slightly reducing conditions. Therefore, under pH (5.0 to 7.6) conditions observed at the Greyhawk groundwater, the uranyl carbonate complexes are expected to occur predominantly as uranyl carbonate and dicarbonate complexes. These complexes are relatively soluble and mobile because of the neutral or anionic form. The relationship shown in Fig. 24 suggests that uranium is mobilised as uranyl carbonate complexes during the dissolution of the waste rock and bedrock. The probable reaction involved is



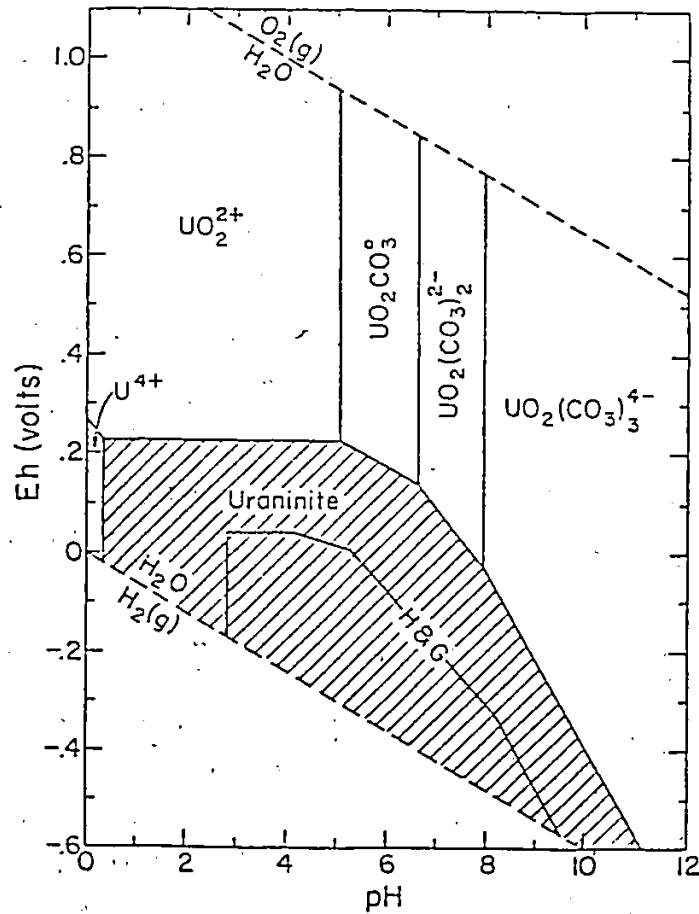


Figure 25: Eh-pH diagram in the U-O₂-CO₂-H₂O system at 25°C for $P_{\text{CO}_2} = 10^{-2}$ atm. Uraninite, UO₂(c), solution boundaries are drawn at 10^{-6} M (0.24 ppm) dissolved uranium species. "H & G" denotes the boundary of the uraninite stability field according to Hosterler and Garrels (1962).

(After Langmuir, 1978)

Furthermore, it is known that oxidising conditions promote the mobility of uranium in ground water (Vinogradov, 1959).

A relationship between uranium content and sulphate concentration is shown in Figure 26, derived from the 22 water samples for which both sulphate and radiochemical data are available. There is a relatively poor correlation ($r = 0.47$); some samples of high sulphate content are relatively rich in uranium but some are not. The complexing reaction for the formation of soluble uranyl sulphate complex is shown below:



Langmuir (1978) has shown that uranyl sulphate is only soluble in acidic environments of pH below 4. Therefore, due to the higher pH of most of the Greyhawk ground waters, conditions are unfavourable for the formation of uranyl sulphate complex. The uranyl sulphate complex may not represent an important component in the Greyhawk ground waters.

Figure 27 relates uranium content and the electrical conductance of the ground water samples. As can be seen, there is a tendency toward an increasing concentration of uranium with an increase in electrical conductance. However, the correlation is poor compared to the other two plots, Figures 24 and 26. Some samples of high electrical conductance are relatively rich in uranium but others are not. The probable reason for this is the heterogeneity of sand thus resulting in the variation of hydraulic conductivity and complex flow pattern. Therefore, the distribution of dissolved constituents may not be uniform.

Concentrations of phosphate in the Greyhawk ground water are low, <0.005 ppm (Table 4). Thus, uranyl phosphate complexes are not expected even though phosphate is supposed to form stable complexes with uranium

Fig- 26. A Plot of Uranium Content versus Sulphate Concentration in the Greyhawk Groundwater.

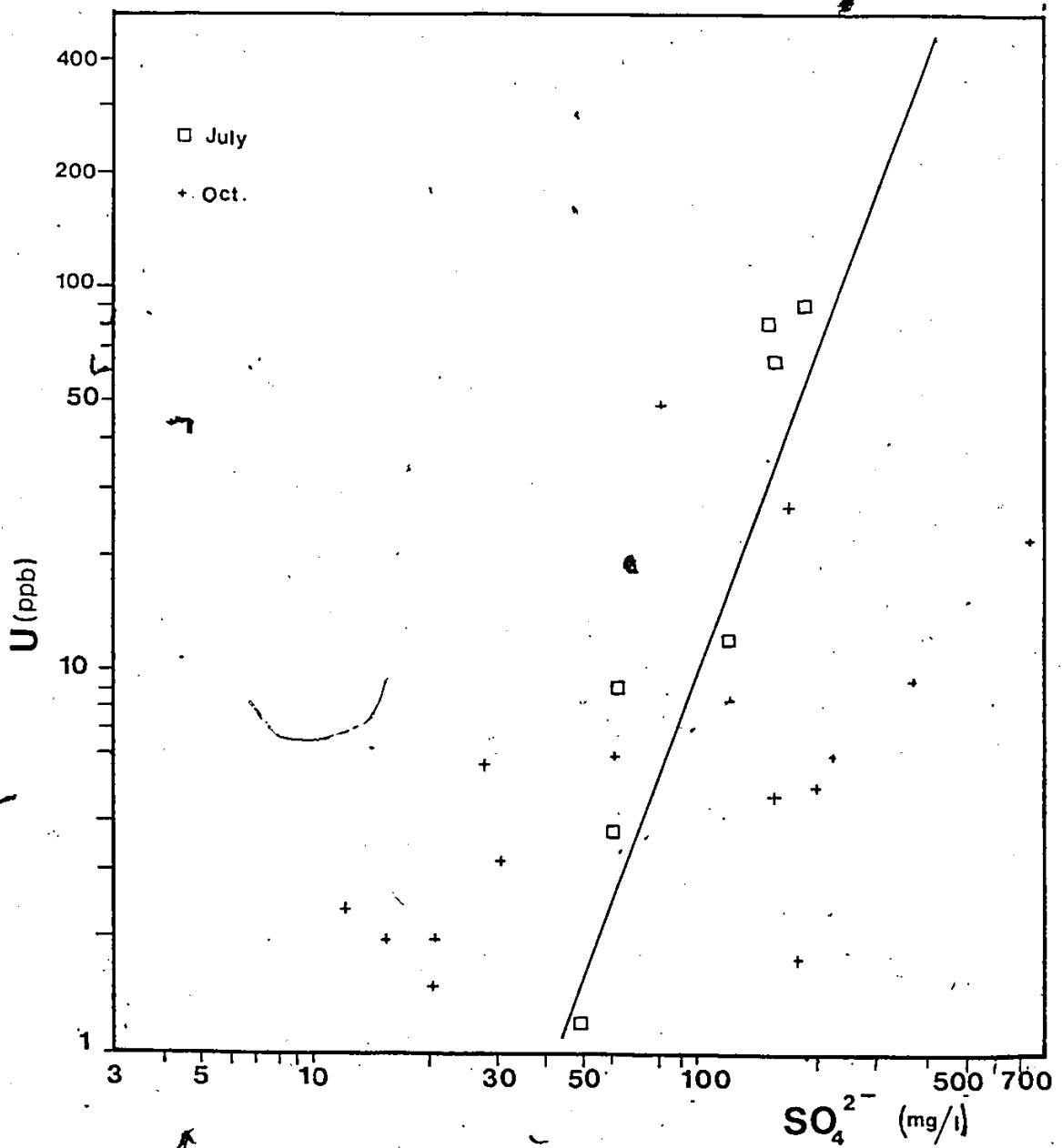
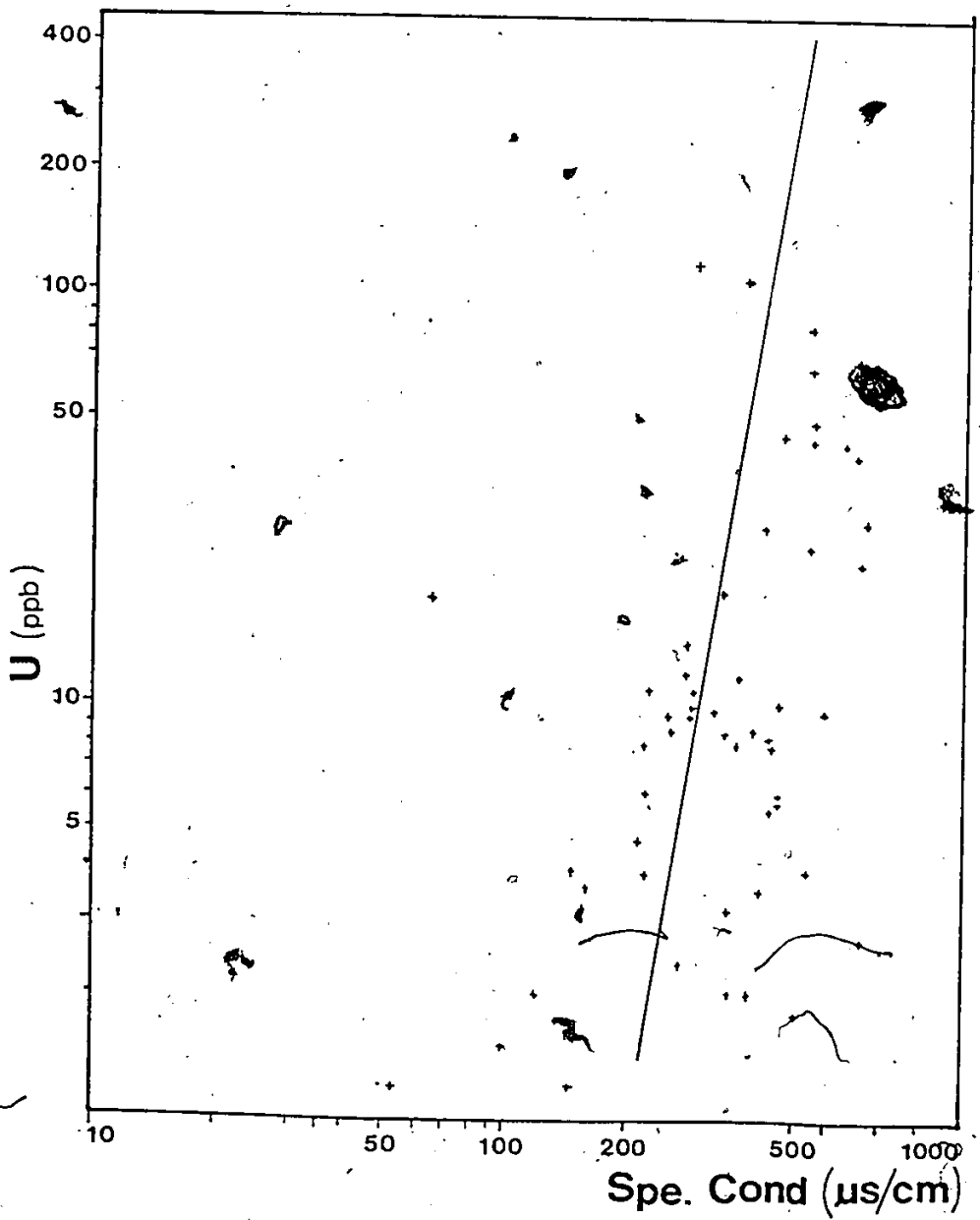


Fig.27. A Plot of Uranium Content versus Specific Conductance in the Greyhawk Groundwater.



over a particularly large pH range (4 to 10). Langmuir (1978) noted that uranyl phosphate complex, $UO_2(HPO_4)_2^{2-}$, is stable for a typical ground water with PO_4 concentration of 0.1 ppm. Uranium content was not compared with Cl^- concentration because the latter is fairly constant throughout the waters (1 to 3 ppm).

Initially, an attempt was made to determine the mode of chemical speciation of the elemental uranium in these ground water samples. Unfortunately, the validity of the dissolved oxygen results is very doubtful and hence the Eh values of the waters could not be determined with accuracy. On the other hand, from the sandy nature of the soil and the shallow depth of the aquifer, the majority of the Eh values of the waters are expected to be of somewhat positive value. Langmuir (1978) has shown that uranium is most soluble in ground waters at Eh value above 0.2V (see Fig. 25). Furthermore, various studies have indicated that in permeable media, uranium mobility is not only a function of redox conditions but also of pH and carbonate and sulphate availability (Lisitsin, 1962; Hostetler and Garrels, 1962). At the pH conditions of the Greyhawk ground water (mostly 5.0 to 7.6), uranium may well be in uranyl carbonate complexes. Moreover, Hostetler and Garrels (1962), Langmuir (1978) and many others have shown that uranium is transported as a uranyl carbonate complex ($UO_2CO_3^0$) at pH 5 to slightly acid, as a uranyl di-carbonate complex $UO_2(CO_3)_2^{2-}$ in about neutral solutions and as a uranyl tri-carbonate complex in basic solution.

The migration of dissolved uranium in the ground water has been studied here with emphasis on the occurrence and processes that control its migration. Two cross-sections along B-Q and GR9-GR11 were made to

visualise more clearly whether a significant zone of uranium contaminated ground water exists at the site. These cross-sections were taken along the ground water flow direction because the velocity and direction of migration of contaminant in the aquifers are influenced by the hydro-geologic parameters and in particular by the ground water velocity and direction.

Figure 28 shows a long section, B-Q. Significant concentrations of dissolved uranium occur in the ground water zone near the water table (33 ppb) and the deep sampling point (117 ppb) at site B. An anomalously high uranium content was found at the deep location at site T (357 ppb). Nevertheless, the concentrations of uranium for most of the sites clustered around 10 ppb with the exception of Q 15.43 (27 ppb). As can be seen, in moving down from the waste rock source, uranium content in the waters decreases abruptly by a large factor. It appears that a plume of uranium-rich water is migrating along the bedrock surface.

The distribution pattern of uranium in shallow wells along GR9-GR11 is shown in Figure 29. A plume from the pegmatitic waste rock is observed. Two trends are readily identified:

- (i) Uranium content tends to decrease with depth, and
- (ii) to decrease with distance from the waste rock source.

A model is proposed to explain the distribution pattern and migration process of uranium in the Greyhawk ground water. It is illustrated in Figure 30. The model delineates the three major stages involved in the transportation and precipitation of uranium in ground water, i.e.

- (a) mobilization of uranium by weathering,
- (b) transportation by circulating water and

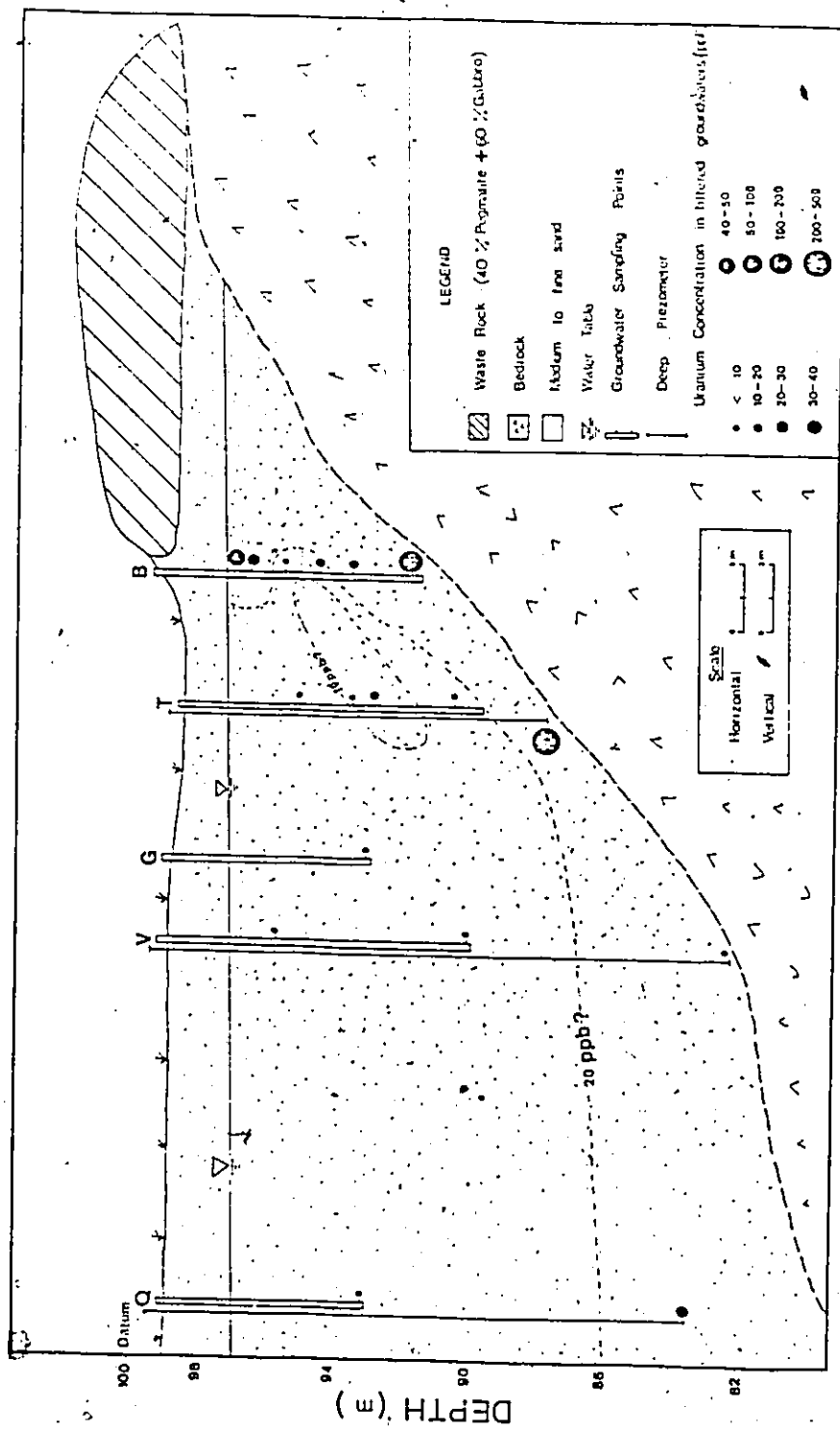


FIG. 28. DISTRIBUTION OF URANIUM IN GROUNDWATERS SAMPLED ALONG B-Q CROSS-SECTION.

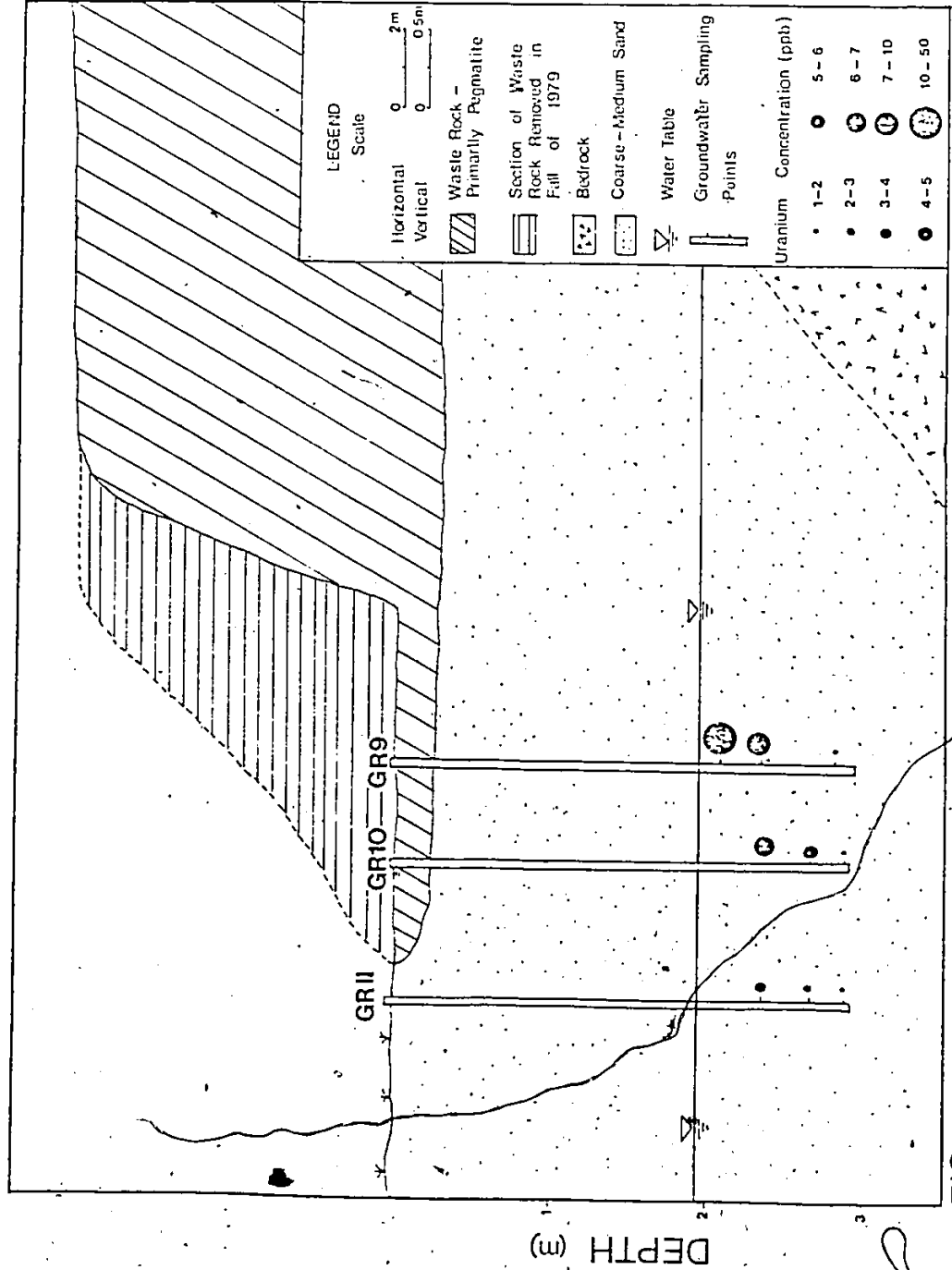


FIG. 29. DISTRIBUTION OF URANIUM IN GROUNDWATER ALONG THE GR9-GR11 CROSS-SECTION.

7

R

1. Rain and Snowmelt

Conditions: $P_{CO_2} = 10^{-3.5}$ atm.

PH = 5.0 to 6.0

2. Weathering of waste rock:

Uranium minerals are leached by percolating water.

Infiltration of leachate into the aquifer.

Uranium migration in the form of carbonate and sulphate complexes.

3. Dissolution of bedrock by the action of circulating water:

Uranium concentration at greater depths may be increased as a result of this process.

4. Migration of uranium in shallow subsurface groundwaters with the influence of:

(a) mixing (i.e. hydrodynamic dispersion)

(b) geochemical reactions (adsorption and desorption etc.).

5. Precipitation of uranium may occur here due to lowering of Eh of the water, (presence of H_2S gas; Eh = -100 to -500 mV).

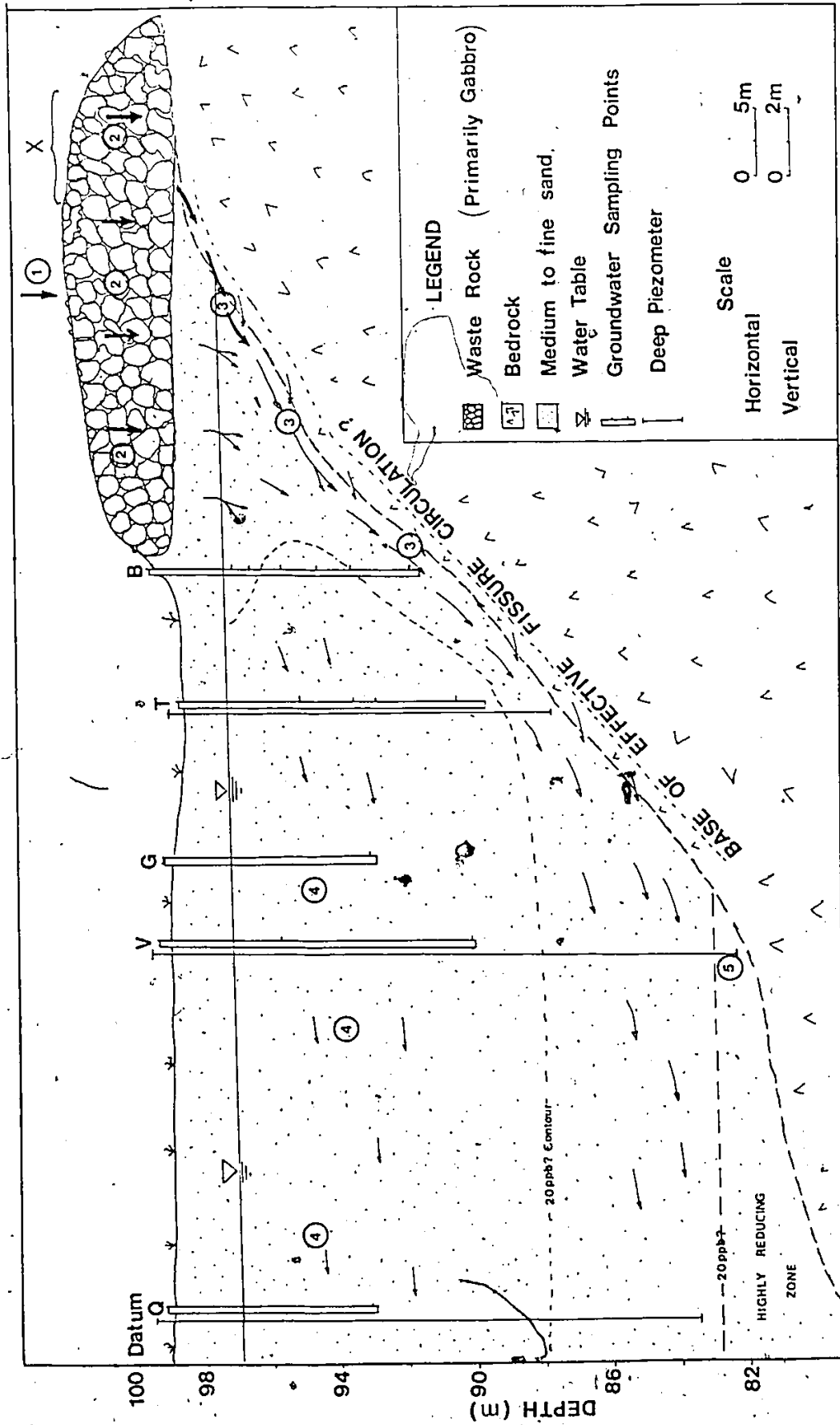


FIG. 30. DIAGRAMMATIC SKETCH SHOWING URANIUM MIGRATION IN SHALLOW AQUIFER, GREYHAWK.

(c) deposition and adsorption during transportation.

This model can be used to explain several features of uranium distribution in the Greyhawk ground water, for example:

(i) The model describes the mobile uranium species which are liberated from the waste rock and bedrock through dissolution and are carried in solution mainly as uranyl carbonate complexes. Uranium is subsequently removed from solution by adsorption on the sands of the aquifer and perhaps also on secondary oxides of iron and manganese and by precipitation that is caused by lowering of the Eh of the water. These processes form the prime geochemical mechanisms that caused the retardation or reduction of the uranium content in the waters.

Lowering of Eh in the lower part of the aquifer is presumably caused by decaying of organic matter. Bacterial sulphate introduced from weathered pyrite leads to formation of dissolved sulphide (HS^- , H_2S) (Thode et al., 1951; Goldhaber et al., 1978). Upon encountering reducing conditions, uranium became reduced to the tetravalent state and precipitated (Reynolds et al., 1978). Krauskopf (1967) in Grisak and Jackson (1978) noted that in such environment redox potential (Eh), may vary between -100mV and -500 mV. The presence of H_2S gas at site V-16.59 is a clear indication of such an environment. Uranium is expected to precipitate as uraninite or coffinite (Langmuir, 1978) at this site and consequently decreases its content considerably in the water (8 ppb).

(ii) Two assumptions are suggested to explain the anomalously high uranium content at deep sites.

(a) Assuming that the spatial flux of uranium from the rock pile is constant, then, in area X, where the pile is on the bedrock,

uranium may be concentrated in basal ground water.

(b) Assuming that the bedrock is rich in uranium, then, leaching of the bedrock surface by the acid water would result in an increase of uranium content in the water at deep sites.

(iii), Assuming that near stagnant water nearly comprises a basal reducing zone as shown in Fig. 30, then, a stronger plume thus indicated in Fig. 30 descends to the rock surface, descends along it, is diffused and reduced but still enriched to 27 ppb at Q 15.43. Therefore, a plume with a contour at the 20 ppb position may be defined.

(iv) There may be mixing of U-rich or U-poor water from other sources. This may be applied to site Q 15.43 which is supposed to be the meeting point of two ground water flow systems in the aquifer (see Fig. 4). Also, uranium content in the water may be reduced by simple dilution process (i.e. from rain and snowmelt).

4.2.2 Uranium Content in Waste Rock and Soil Samples

The waste rock of the Greyhawk Mine is comprised of granite pegmatite and gabbroic rocks. Samples of waste rock and soil were analysed for uranium content utilising both the alpha spectrometry and the neutron activation-delayed neutron counting methods. Also, thorium contents in the samples were determined by the instrumental neutron activation analysis. Results of the analysis are given in Table 6.

Uranium contents in the pegmatite and gabbroic rocks are 31.59 and 2.9 ppm respectively. Morse (1970) noted that U background in the soil of the Bancroft region is less than 1 ppm. Table 6 indicates that soils contain quite high uranium, most samples exhibited about 10 times larger than the background value. It is possible that the dissolved U in the water was being adsorbed on the soils as it passes. During weathering process of the waste rock, U present as uraninite, uran-othorite etc.

Table 6 -- U and Th Contents in Waste Rock and Soil Samples.

Sample #	Depth below ground surface (m)	U (ppm)		* Th (ppm)	234U/238U	
		α-Spect.	NA-DNC		Rock or Soil	water
Pegmatite	-	31.51 ± 0.72	31.97 ± 0.18	22.5	1.02 ± 0.02	-
Gabbro	-	-	2.94 ± 0.05	1.0	1.07 ± 0.02	-
GR9-I	0.00-0.30	-	8.92 ± 0.30	-	-	not measured (above water table)
GR2-II	0.39-0.79	-	1.42 ± 0.04	10.0	+0.99 ± 0.005	-
GR3-III	0.80-1.20	10.27 ± 0.26	10.51 ± 0.10	7.5	0.99 ± 0.007	-
GR4-IV	1.00-1.34	3.32 ± 0.08	3.89 ± 0.06	14.5	1.02 ± 0.02	1.03 ± 0.03
K8-30	8.30	-	15.84 ± 0.14	13.0	-	not measured
G5-80	5.80	24.40 ± 0.54	26.32 ± 0.20	40.33	1.05 ± 0.08	1.07 ± 0.03

+ Unspiked run

* Th detection limit ± 1.0 ppm.

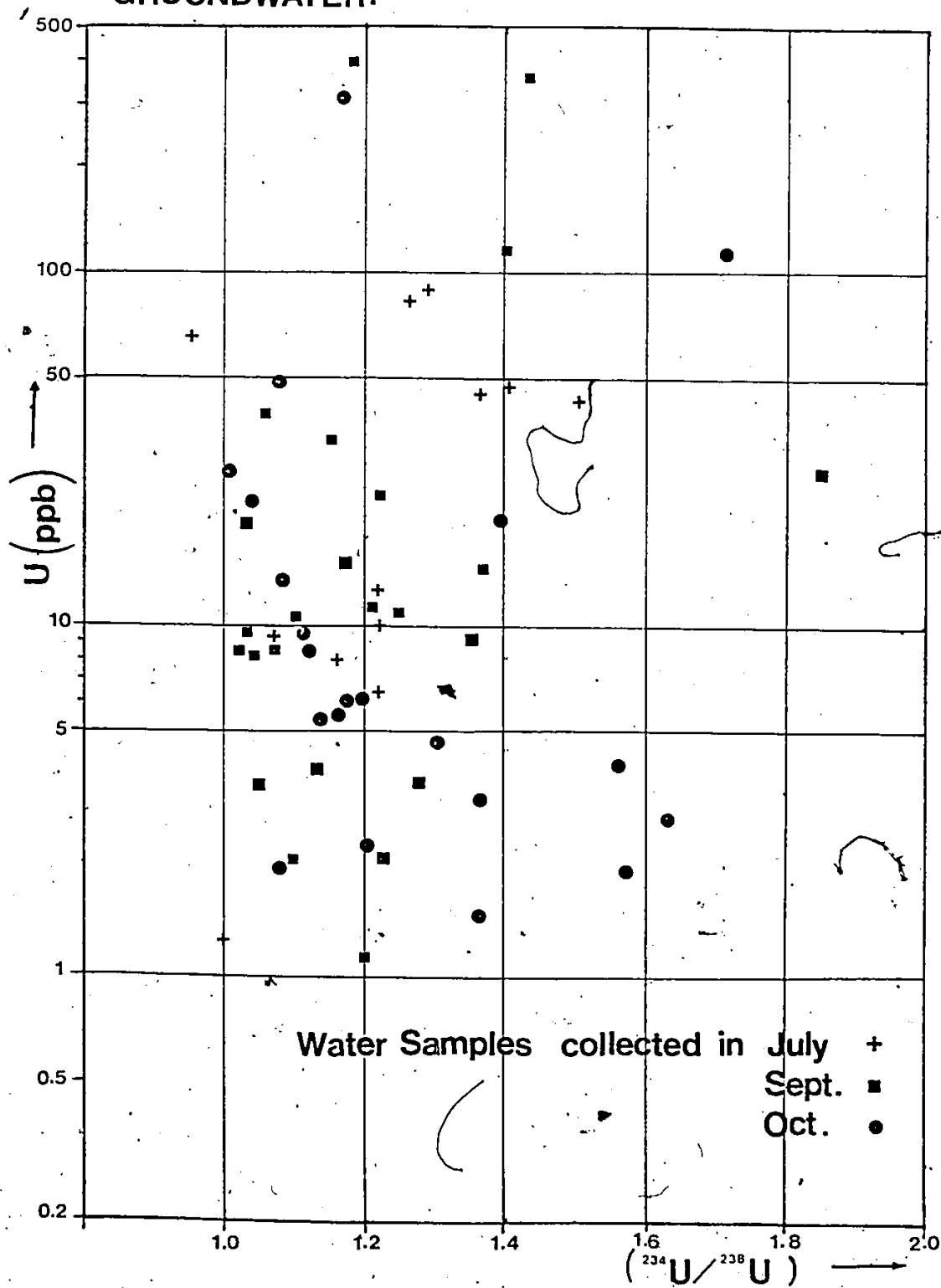
Sample #	Description of Sample	Environment
GR2-II	brown coarse sand	oxidising (undersaturated zone)
GR3-III	"	"
GR4-IV	"	"
GR9-I	"	"
K 8,30	greyish silty sand	reducing ?
G 5,80	"	" ?

oxidised to the comparatively soluble uranyl ions, whereas Th minerals which are relatively insoluble are concentrated in resistant minerals and weathered rocks. Thorium content measured in a few soil samples (see Table 6) may represent a background value, as was shown by Hansen (1968) that Th concentrations in soils varied mainly in the range of 7 to 12 ppm. Furthermore, concentration of Th determined in a few water samples was very low (avg. 0.005 ppb, determined by E. Veska, University of Waterloo) and therefore it probably was left with the waste rock. Uranium appears to be extracted from the ground water as it flows through the aquifer. As a consequence, the concentration of U in the water may be reduced and may also cause the advance rate of the contaminant front to be retarded.

4.2.3 Uranium Isotopes in Water

The activity ratio ($^{234}\text{U}/^{238}\text{U}$) of the ground water samples ranged from 0.95 to 1.85. The deep waters usually contain between 35 and 85% excess of ^{234}U , except sites U-11.80 (18% excess ^{234}U) and K-8.30 (5% excess ^{234}U). Generally, most of the water samples have uranium activity ratios between 1.00 and 1.30 (Fig. 31), with only one sample exhibiting less than unity (site K 3.72). The data of U content and U isotopic ratio from this study were compared with the diagram (Fig. 32) of Osmond and Cowart (1976). Their data represent the U content and U isotopic ratio of ore bearing waters originating from sandstone-type uranium deposits in the U.S.; area A indicates waters close to the ore deposits while area B depicts waters that are farther away from the ore bodies. It appears that the data of U in the Greyhawk ground waters fall in area A of the plot of Osmond and Cowart. Ore-bearing waters from the sandstone-type U deposit may contain quite high U isotopic ratio. However,

FIG. 31. A PLOT OF URANIUM CONCENTRATION VERSUS ACTIVITY RATIO IN THE GREYHAWK GROUNDWATER.



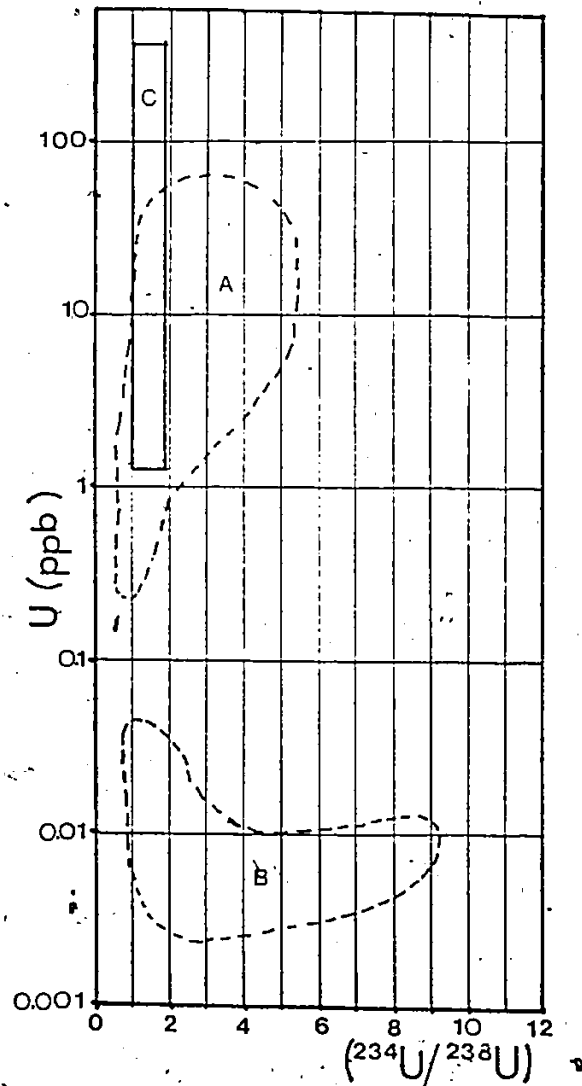


FIG. 32 DISTRIBUTION OF URANIUM CONCENTRATION AND $^{234}\text{U}/^{238}\text{U}$ RATIO OF ORE BEARING GROUNDWATER (AFTER OSMOND AND COWART 1976)

- A - WATER SAMPLES CLOSEST TO ORE BODIES
- B - " " FURTHER AWAY FROM ORE BODIES
- C - " " OF THIS STUDY

the U isotopic ratios of the Greyhawk ground waters show a relatively small range (1.00 to 1.85); this probably represents a typical U-bearing water originating from the leaching of a pegmatitic dike U deposit.

The relative enrichment of ^{234}U isotope in the water samples may have resulted from alpha recoil or selective leaching or a combination of both (Coward and Osmond, 1978). High activity ratios exhibited at the deep sampling sites may be due to leaching of radiation-damaged sites in the bedrock by the acid waters of the waste dump. Additionally, slightly acid water can seemingly allow this to take place (J. Andrews, pers. Commun.). This probability of dissolution of ^{234}U will be especially favoured when the ^{234}U is available close to solid/liquid interfaces (Osmond and Cowart, 1976).

Figure 33 illustrates the distribution pattern of uranium isotopic ratios along the cross-section of B-Q. The data were contoured to visualise the situation more clearly. Figure 33 clearly shows the U isotopic ratio changes from the source of recharge (i.e. waste rock source) into the aquifer. Migration of high U isotopic ratio ($^{234}\text{U}/^{238}\text{U}$) water was observed at intermediate and bottom depths. It is felt that changes in the U isotopic ratio may be related to the flow of the water within the aquifer. This may also indicate the migrating path of the leachate in the aquifer emanating from the waste rock source in which excess ^{234}U is considered as a tracer.

A comparison study was made on Figures 28 and 33 to see if there exists any correlation between the distribution of U content and U isotopic ratio in the waters. It can readily be seen that there are volumes of U-enriched water migrating in the intermediate and deeper zone

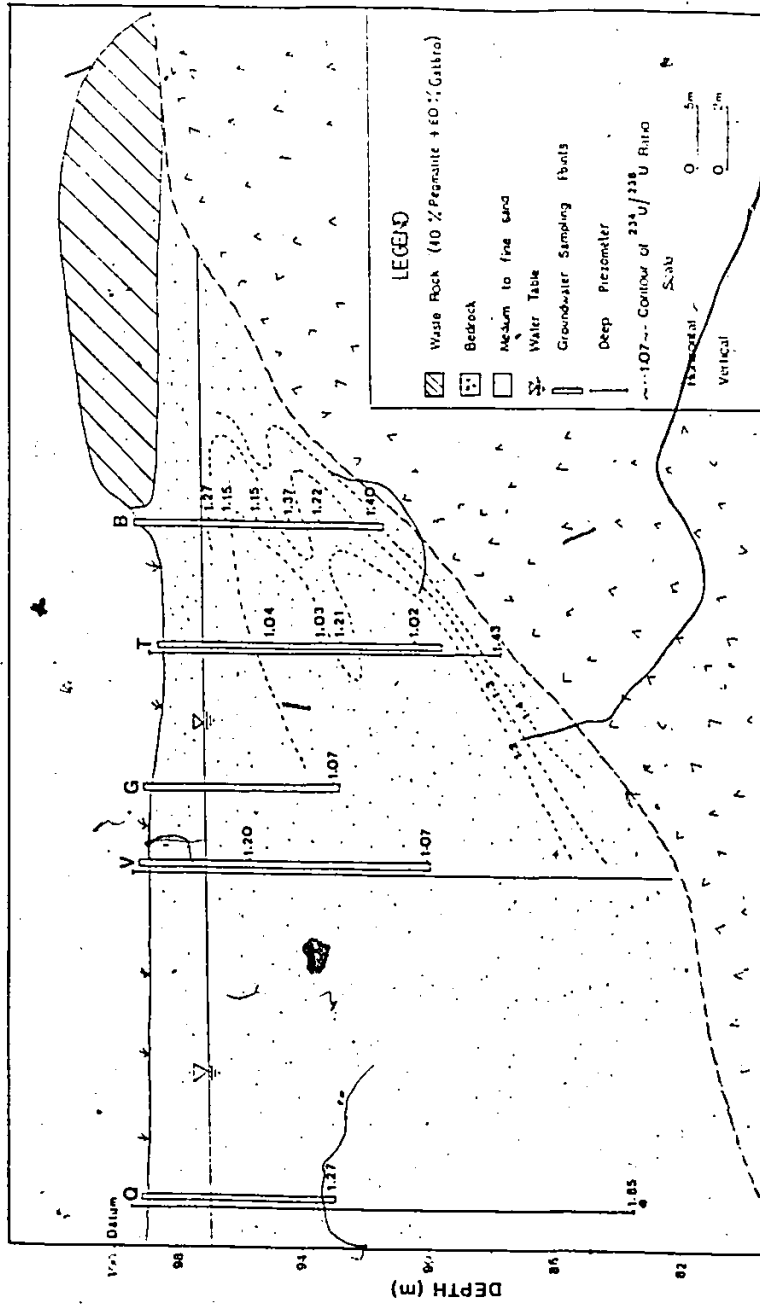


FIG.33. DISTRIBUTION OF URANIUM ISOTOPES ($^{234}\text{U}/^{238}\text{U}$) IN GROUNDWATERS SAMPLED ALONG THE B-Q CROSS-SECTION.

of the aquifer that coincides with the zones of ^{234}U -enriched water. Thus contours of ^{234}U and U concentration possibly represent the flow pattern of contaminants in the aquifer derived from the leaching of the overlying waste rock.

4.2.4 Uranium Isotopes in Waste Rock and Soil Samples

The results of determination of $^{234}\text{U}/^{238}\text{U}$ ratio in the waste rock and soil samples are shown in Table 6. The activity ratio of the waste rock, with pegmatite and gabbro are 1.02 ± 0.02 and 1.07 ± 0.02 , respectively.

The U in the sands of the aquifer was presumably adsorbed from the dissolved U in the water. Therefore, a number of soil samples were analysed for their U isotopic ratio ($^{234}\text{U}/^{238}\text{U}$). It can be seen that the leaching of soils with conc. HNO_3 yields U activity ratios that are similar to that found in the water from the same site. For instance, sites GR4-IV and G 5.80 have uranium ratios of 1.02 ± 0.02 and 1.05 ± 0.08 in soils and 1.03 ± 0.03 and 1.07 ± 0.03 in waters, respectively. With these isotopic characteristics shown in the soils and water at sites GR4-IV and G 5.80, it may be concluded that part of dissolved U in water is probably being deposited on the sands. Unfortunately, no soil samples from the deep sampling points were available for isotopic analyses, particularly from site V16.59 at which U has supposedly been precipitated due to the existing reducing conditions.

The soil samples at sites GR2-II, GR3-III and GR9-I are located in the unsaturated zone. The samples from sites GR2-II and GR3-III have uranium ratios slightly less than unity (see Table 6). The result for GR2-II which contains only 1.42 ppm U may be due to greater

leachability of ^{234}U over ^{238}U (Rosholt et al., 1966). ^{234}U may be preferentially leached compared to the parent ^{238}U by the infiltration water. However, sample GR3-III yielded 10.51 ppm of U on leaching with hot HNO_3 ; this excess U was adsorbed from percolating water. The site of GR3-III may actually reside below the water table at some times of the year. The $^{234}\text{U}/^{238}\text{U}$ of ground water at this site is not known, but is presumably close to 1.00 by analogy with nearby water sample GR4-IV. Uranium content of the soil sample at site GR9-I is quite high (8.92 ppm); this sample may be contaminated with fragments of the overlying waste rock.

4.3 Neutron Activation-Delayed Neutron Counting Technique (NA-DNC)

Thirty-eight ground water samples were determined for their uranium content utilizing the NA-DNC technique. The results of analyses are given in Tables 1, 2 and 3. It can be seen that the uranium content may be obtained to a precision of less than 5% at the levels of uranium concentration in the water samples. At these concentration levels a single irradiation may be adequate (E. Hoffman, pers. comm.). The errors shown with each analysis are from the counting statistics of the individual counting experiments. For example, in one of the determinations for a standard irradiation/delay/counting sequence (30-10-30 sec.) with a neutron flux of about $5.0 \times 10^{12} \text{ n/cm}^2/\text{sec.}$, the system sensitivity is 318.71 ± 3.29 counts per ug of uranium. The calibration factor is thus $0.003138 \text{ ug/count}$ with an error of $\pm 0.000032 \text{ ug/count}$. The background signal for an empty capsule irradiated under the same conditions is 63.3 ± 7.9 counts; and the signal given by a blank sample ($\text{Fe}(\text{OH})_3$) is 68 ± 8.2 counts.

From the analyses carried out by the NA-DNC technique the efficiency of coprecipitation of uranium with $\text{Fe}(\text{OH})_3$ are tested. The results of measurement of uranium by the NA-DNC technique were compared with those from the alpha-spectrometry method (see Tables 1, 2 and 3). Here, it was assumed that the results obtained by the alpha spectrometry method represent a true value of uranium content in the water samples (since a known ^{232}U spike was added to the sample measured by the α -spectrometry method). A histogram of frequency versus percentage yield of uranium was made (Fig. 34) to visualise the situation more clearly and also for qualitative interpretation. This histogram is based on 38 analyses. It can be seen that 88% of the analyses indicate an efficiency of greater than 50%. Also, it indicates that about 60% of the analyses ranged between 80 to 100% efficiency. The data of Tables 1, 2 and 3, in general, indicate that the efficiency increases with increasing uranium content in the samples. Generally, the results showed that the coprecipitation of uranium with $\text{Fe}(\text{OH})_3$ was quite promising, considering the complex conditions that may exist in the natural waters.

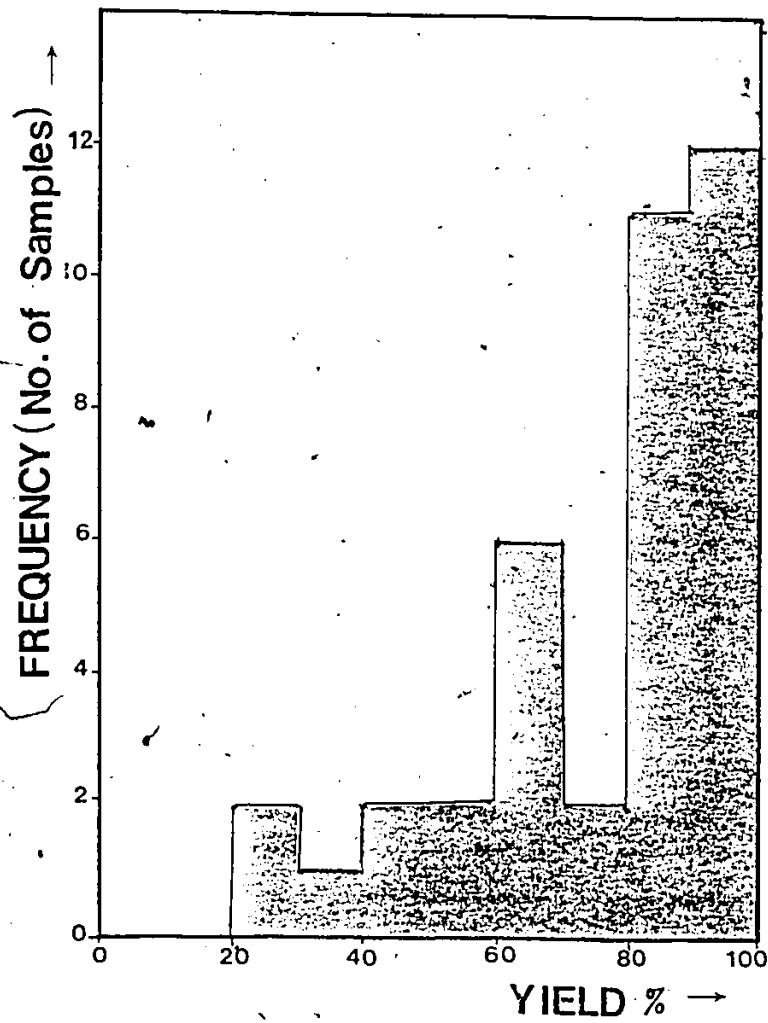
A major factor contributing to the poor efficiency (hence, yields of the chemical collection) of the coprecipitation of uranium with $\text{Fe}(\text{OH})_3$ is incomplete expulsion of CO_2 from the water samples. As mentioned earlier the presence of CO_2 (as carbonate ions) could form soluble uranyl carbonate complexes.

4.4 Determination of $^{234}\text{U}/^{238}\text{U}$ Ratio by Combined Fission Track and Alpha Track Counting (FATC)

4.4.1 Theory

The determination of uranium activity ratio ($^{234}\text{U}/^{238}\text{U}$) by combined

Fig.34.A Histogram of Frequency
Versus % Yield.



fission-track and alpha-track counting is based on the following theory:

For uranium electrodeposited on a planchet, we get:

- (i) fission-track counting records -- ^{235}U fission, and
 (ii) alpha-track counting records -- $^{234}\text{U} + ^{235}\text{U} + ^{238}\text{U}$
 (α -disintegration).

(a) From fission-track measurements:

$$N_f = \gamma_f \phi t \sigma_{235} N_{235} \quad (4.15)$$

But $N_{235} = 0.007 N_{238}$

$$\therefore N_f = \gamma_f \phi t \sigma_{235} (0.007 N_{238}) \quad (4.16)$$

where,

N_f = Number of fission tracks

γ_f = Geometrical factor of fission track production

ϕ = Neutron flux ($\text{n}/\text{cm}^2/\text{sec.}$)

t = Irradiation time (sec.)

σ_{235} = Cross section for uranium fission ($584 \times 10^{-24} \text{cm}^2$)

N_{238} = Number of ^{238}U atoms in sample

N_{235} = Number of ^{235}U atoms in sample.

(b) From alpha-track measurements:

$$N_a = T \gamma_a \left\{ \lambda_{234} N_{234} + \lambda_{235} N_{235} + \lambda_{238} N_{238} \right\} \quad (4.17)$$

where,

N_a = Number of alpha tracks

T = Alpha exposure time (year^{-1})

γ_a = Geometrical factor of alpha track production.

λ_i = Decay constant of respective U isotopes (year^{-1})

N_i = Number of atoms of respective U isotopes

Let A be the activity ratio of $^{234}\text{U}/^{238}\text{U}$.

$$\text{So } A = \frac{a_{234}}{a_{238}} \text{ where } \begin{matrix} a_{234} = \text{activity of } ^{234}\text{U}, \\ a_{238} = \text{activity of } ^{238}\text{U}. \end{matrix}$$

$$\text{Hence } A = \frac{\lambda_{234} N_{234}}{\lambda_{238} N_{238}}$$

$$\text{And, } \frac{N_{234}}{N_{238}} = \frac{\lambda_{238}}{\lambda_{234}} A$$

$$\text{So, } N_{234} = A \left(\frac{\lambda_{238} N_{238}}{\lambda_{234}} \right)$$

Taking $N_{235} = 0.007 N_{238}$, $\lambda_{235} = 6.285 \lambda_{238}$ and

$$N_{234} = A \frac{\lambda_{238} N_{238}}{\lambda_{234}}$$

and substituting in equation 4.17, we get,

$$N_a = T \gamma_a \{ A \lambda_{238} N_{238} + 0.044 \lambda_{238} N_{238} + \lambda_{238} N_{238} \}$$

$$= T \gamma_a \lambda_{238} N_{238} \{ A + 1.044 \}$$

$$\therefore N_a = T \gamma_a \{ A + 1.044 \} \lambda_{238} N_{238} \quad (4.18)$$

Dividing equation (4.18) by equation (4.16)

$$\text{Track ratio, } R = \frac{N_a}{N_f} = \frac{T \gamma_a \{ A + 1.044 \} \lambda_{238} N_{238}}{\gamma_f \rho t \sigma_{235} (0.007 N_{238})}$$

$$= \frac{\gamma_a}{\gamma_f} \cdot \frac{T}{\rho t} \cdot \frac{\lambda_{238}}{\sigma_{235}} \{ A + 1.044 \} \cdot \frac{1}{0.007}$$

$$\text{So, } R = k \{ A + 1.044 \}$$

$$\text{where } k = \text{constant} = \frac{\gamma_a T \lambda_{238}}{0.007 \gamma_f \rho t \sigma_{235}}$$

$$\therefore R = kA + 1.044k \quad (4.19)$$

Equation 5 is a first order equation with slope (k) and intercept (1.044k).

$$(i) \text{ slope } k = \frac{\gamma_a \lambda_{238}}{0.007 \gamma_f \sigma_{235}} \cdot \frac{T}{\phi t}$$

Assuming that $\gamma_a = 0.5$, and

$\gamma_f = 1.0$ (100% fission detected since there are 2 fission products/fission).

$$\text{Thus } k = \frac{0.5 \lambda_{238}}{0.007 \times 1.0 \times \sigma_{235}} \cdot \frac{T}{\phi t}$$

Substituting $\lambda_{238} = 1.54 \times 10^{-10} \text{ yr}^{-1}$ and

$\sigma_{235} = 584 \times 10^{-24} \text{ cm}^2$ in eqn. above

$$\therefore k = 1.889 \times 10^{13} \cdot \frac{T}{\phi t} \quad (4.20)$$

(ii) From the two experiments, the slopes k_1 (set J) and k_2 (set K) may be combined.

$$\text{Relative slopes, } \frac{k_2}{k_1} = \frac{T_2}{T_1} \cdot \frac{\phi_1 t_1}{\phi_2 t_2} \quad (4.21)$$

(iii) Intercept, $I = 1.044 k$

Substituting $k = 1.889 \times 10^{13} \cdot \frac{T}{\phi t}$ in eqn. above

$$\therefore I = 1.972 \times 10^{13} \cdot \frac{T}{\phi t} \quad (4.22)$$

4.4.2 Fission Track and Alpha Track Results

The determinations presented here are the results of two separate irradiations with different integrated fluxes set J ($8 \times 10^{11} \text{ n/cm}^2$)

and set $K(8 \times 10^{12} \text{ n/cm}^2)$. It was found that fission tracks in muscovite etched in 49% HF for 20 minutes at room temperature give well-defined projections on a TV screen. The tracks can be counted on the screen without any appreciable introduction of error. The projections clearly showed the fission source distribution. Similarly, alpha tracks in cellulose nitrate film etched with 6.25N NaOH at $30.00 \pm 1.0^\circ\text{C}$ also showed well-defined tracks. Alpha and fission tracks are approximately the same size in the etched films (15 to 20 μ).

In this study, homogeneous track (both fission and alpha) distributions were obtained. Plate 3 shows an example of fission track distribution; these tracks were made by fission fragments from the induced fission of ^{235}U . On the other hand, plate 5 shows an example of alpha track; these tracks were made by alpha particles emitted from uranium isotopes (^{234}U , ^{235}U and ^{238}U) that imparted on the cellulose nitrate film. The resulting fission fragments and α -particles enter the detector at all angles with a certain fraction penetrating the detector. After etching, the particle paths become enlarged holes.

Hashimoto (1972) and many others noted that, the counting of tracks may give erroneous results mainly because of heterogeneous distribution of uranium in the samples. Tracks distribution however can be improved by electroplating the uranium on a stainless steel planchet. This resulted in a uniform distribution (Plates 3 and 5).

However, it must be emphasised that a reasonable integrated flux (n/cm^2) must be used in order to obtain a convenient number of fission tracks for counting. If the integrated neutron flux value were too high, it may cause considerable overlapping of the tracks (Plate 4), thus

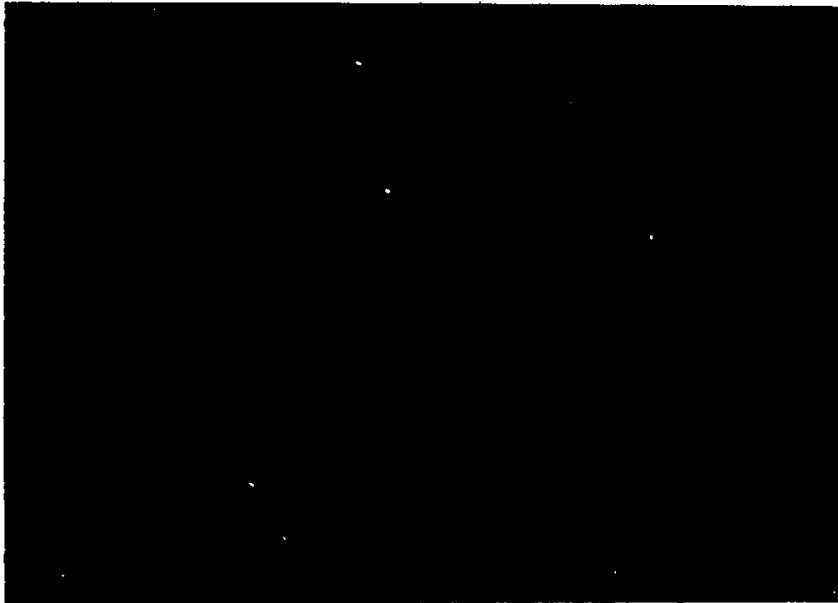


Plate 3. Photomicrograph showing fission tracks distribution in etched muscovite (sample Q 4.15).



Plate 4. Photomicrograph showing cluster of fission tracks in etched CN85 film (sample U-11.80).

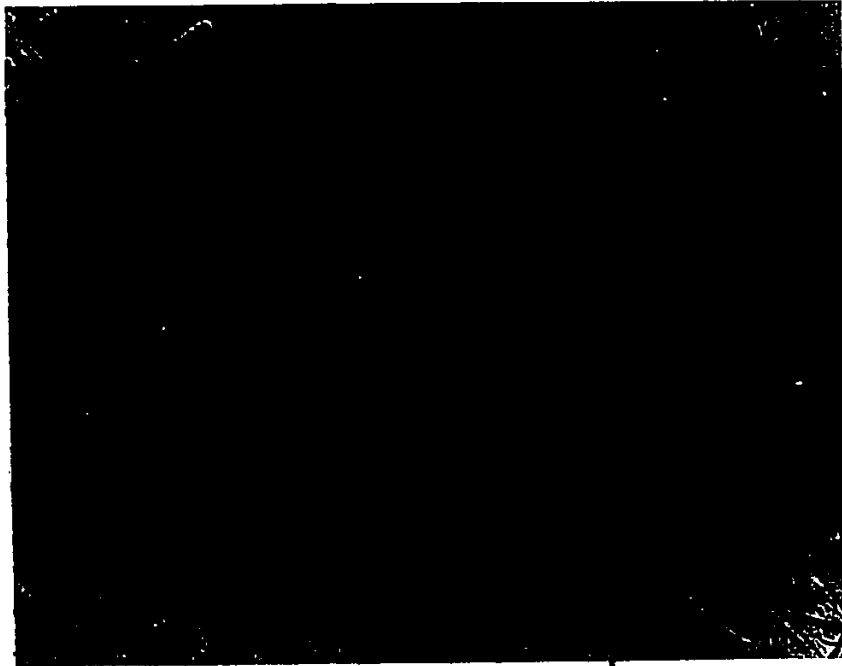


Plate 5. Photomicrograph showing alpha tracks distributed in etched CN 85 film (sample B-5.7 July).

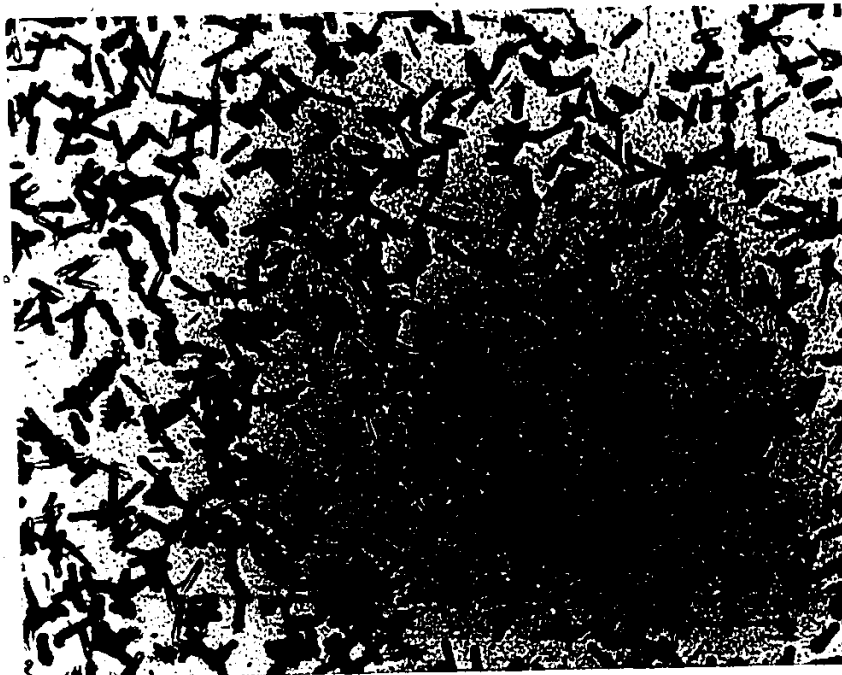


Plate 6. Photomicrograph showing cluster of alpha tracks in etched CN 85 film (sample U-11.80).

it becomes very difficult to count. Conversely, a very low neutron flux would give very low fission track density. However, in this study, after the second irradiation a suitable neutron flux value can normally be estimated, thus a reasonable distribution of fission track distribution was obtained (Plate 3). Similarly, a suitable amount of time for α -particle detection is chosen for each set of samples to get a reasonable distribution of α -track (Plate 5); overlapping of alpha tracks may occur if the exposure time were too long (Plate 6) which leads to results not suitable for counting purposes. Fortunately, in general, no serious difficulty was encountered in counting projected tracks from the detectors; on projection, the tracks can easily be distinguished from the dirt or noise.

The number of fission-track and alpha-track counted from each set of samples are given in Table 7 (set J) and Table 8 (set K). The major factors contributing to the error in the fission and alpha tracks are the efficiency of calibration curve, neutron dose, geometrical factor, of both fission and alpha tracks and track recognition. All except track recognition are relative errors for the same irradiation. Thus, the counting errors are the only source of error that can be expressed qualitatively in this research. The standard deviation is taken as the square root of the number of tracks counted.

Since the uranium activity ratio ($^{234}\text{U}/^{238}\text{U}$) of all samples measured by combined fission track and alpha track counting are also determined on an alpha spectrometer, therefore a regression curve of $\sum N_\alpha / \sum N_f$ against $^{234}\text{U}/^{238}\text{U}$ ratio can be made. The data of sets J and K are computed separately using a standard computer programme; $\sum N_\alpha / \sum N_f$ is

Table 7 -- Comparison of the results of f- α track and α -spectrometry analyses for set J.

Sample #	No. of track (N)				Mean	ΣN	$\Sigma N_e / N_f$	$(^{234}\text{U}/^{238}\text{U})$		
	A	B	C	D				α -Spect.	Exptl.	
STD.										
A 1.0	a	3316	3000	3263	3103	3170 \pm 56	12682 \pm 112	0.950 \pm	1.00 \pm	1.07
	f	3426	3175	3550	3195	3336 \pm 58	13346 \pm 115	0.011	0.02	
STD.										
A 0.5	a	1250	1206	1133	1180	1192 \pm 35	4769 \pm 69	0.844 \pm	1.00 \pm	0.92
	f	1226	1650	1500	1275	1412 \pm 38	5651 \pm 75	0.016	0.02	
STD.										
J 5.75	a	3765	3373	3160	2585	3220 \pm 57	12883 \pm 113	1.234 \pm	1.44 \pm	1.49
	f	2740	2720	2435	2540	2608 \pm 51	10435 \pm 102	0.016	0.03	
B 5.7 (July)	a	4156	4525	4500	4433	4403 \pm 66	17614 \pm 133	1.107 \pm	1.30 \pm	1.30
	f	3954	4103	3785	4068	3977 \pm 63	15910 \pm 126	0.012	0.05	
O 7.7	a	5778	6016	6157	5607	5889 \pm 77	23558 \pm 153	1.154 \pm	1.43 \pm	1.37
	f	5560	5005	4950	4884	5099 \pm 71	20399 \pm 142	0.011	0.04	
C 8.6	a	2510	2934	2896	2747	2771 \pm 53	11087 \pm 105	1.082 \pm	1.16 \pm	1.26
	f	2196	2859	2940	2250	2561 \pm 51	10245 \pm 101	0.015	0.08	
Q 4.15	a	5194	4600	4050	4750	4626 \pm 68	18504 \pm 136	0.815 \pm	1.00 \pm	0.88
	f	6200	5592	6278	4622	5673 \pm 75	22692 \pm 150	0.008	0.11	
B 4.7	a	2104	2466	2209	2393	2293 \pm 48	9172 \pm 96	1.058 \pm	1.37 \pm	1.23
	f	1786	2216	2315	2350	2166 \pm 47	8667 \pm 93	0.016	0.04	
B 2.2	a	1901	1866	1800	1872	1859 \pm 43	7349 \pm 86	1.089 \pm	1.27 \pm	1.28
	f	1692	1725	1705	1709	1707 \pm 41	6829 \pm 83	0.018	0.05	
B 5.7 (Sept.)	a	1057	1083	1005	1050	1048 \pm 32	4193 \pm 65	1.145 \pm	1.22 \pm	1.36
	f	818	975	900	968	915 \pm 30	3661 \pm 60	0.025	0.05	

a - alpha track

f - fission track

Table 7 -- Comparison of the results of f- α -track and α -spectrometry analyses for set K

Sample #	No. of track (N)				E	Mean	ΣN	$\Sigma N_e / \Sigma N_f$	R =	$(^{234}\text{U}/^{238}\text{U})$ α -Spect. Exptl.
	A	B	C	D						
STD.										
A 0.2	a	1546	1721	1563	1448	1560	1568 \pm 50	7838 \pm 88	0.428 \pm 0.005	1.00 \pm 1.1
	f	3605	3315	3800	3685	3900	3661 \pm 60	18305 \pm 135		0.02
STD.										
A 0.1	a	762	1065	1023	1090	869	962 \pm 31	4809 \pm 69	0.349 \pm 0.006	1.00 \pm 0.88
	f	2562	2352	2972	3080	2711	2755 \pm 52	13777 \pm 117		0.02
Q 2.65	a	588	798	713	635		684 \pm 26	2734 \pm 52	1.416 \pm 0.008	1.21 \pm 1.13
	f	1365	1440	1954	1804		1640 \pm	6563 \pm 84		0.10
J 1.15	a	891	1022	1084	982		995 \pm 32	3979 \pm 63	0.440 \pm 0.008	1.28 \pm 1.23
	f	2137	2013	2529	2359		2260 \pm 48	9038 \pm 95		0.13
Q 15.43	a	1305	1142	1606	1243		1349 \pm 37	5396 \pm 73	0.600 \pm 0.010	1.62 \pm 1.85
	f	1892	2580	2424	2100		2249 \pm 47	8996 \pm 95		0.04
K 1.72	a	1033	1102	1004	1100		1084 \pm 33	4339 \pm 66	0.369 \pm 0.006	1.07 \pm 0.96
	f	2880	2888	2746	2944		2892 \pm 54	11458 \pm 107		0.06
T 4.86	a	804	767	834	766		792 \pm 28	3171 \pm 56	0.424 \pm 0.009	1.03 \pm 1.17
	f	1616	1830	1992	2030		1867 \pm 43	7468 \pm 86		0.04
GR4- 1.14	a	1266	1278	1264	1280		1247 \pm 35	4988 \pm 71	0.346 \pm 0.005	0.95 \pm 0.87
	f	3264	3404	3255	3670		3598 \pm 60	14393 \pm 120		0.02
K 8.03	a	1834	1840	1746	1860		1820 \pm 43	7280 \pm 85	0.424 \pm 0.006	1.05 \pm 1.17
	f	4324	4320	4485	4012		4285 \pm 66	17141 \pm 130		0.03
V 8.89	a	1236	1250	1135	1350		1242 \pm 35	4971 \pm 71	0.391 \pm 0.006	1.07 \pm 1.04
	f	3015	3024	3160	3501		3175 \pm 56	12700 \pm 112		0.02
STD.										
B 3.7	a	1020	1063	1008	1180		1067 \pm 33	4271 \pm 65	0.418 \pm 0.007	1.15 \pm 1.15
	f	2350	2300	3000	2560		2552 \pm 51	10200 \pm 101		0.06

a - alpha track
f - fission track

considered as a dependent variable. The two sets give a linear regression as follows:

$$\text{Set J: } y = (0.69 \pm 0.13)x + (0.21 \pm 0.16) \quad (4.23)$$

$$\begin{aligned} \text{corr. coeff. 'r'} &= 0.88 \\ \text{variance} &= 0.07 \end{aligned}$$

$$\begin{aligned} \text{where, slope} &= 0.69 \pm 0.13 \\ \text{intercept} &= 0.21 \pm 0.16 \end{aligned}$$

$$\text{substituting } y = \frac{\sum N_x}{\sum N_f} \text{ and } x = A = {}^{234}\text{U}/{}^{238}\text{U ratio}$$

$$\text{thus: } \frac{\sum N_x}{\sum N_f} = 0.69 A + 0.21$$

$$\therefore A = 1.45 \left(\frac{\sum N_x}{\sum N_f} \right) - 0.304 \quad (4.24)$$

$$\text{Similarly; Set K: } y = (0.26 \pm 0.04)x + (0.12 \pm 0.05) \quad (4.25)$$

$$\begin{aligned} \text{corr. coeff. 'r'} &= 0.90 \\ \text{variance} &= 0.03 \end{aligned}$$

$$\begin{aligned} \text{where, slope} &= 0.26 \pm 0.04 \\ \text{intercept} &= 0.12 \pm 0.05 \end{aligned}$$

$$\text{substituting } y = \frac{\sum N_x}{\sum N_f} \text{ and } x = A = {}^{234}\text{U}/{}^{238}\text{U ratio}$$

$$\text{thus, } \frac{\sum N_x}{\sum N_f} = 0.26 A + 0.12$$

$$\therefore A = 3.85 \left(\frac{\sum N_x}{\sum N_f} \right) - 0.46 \quad (4.26)$$

From the two regression curves shown in Figures 35 and 36 (i.e. experimental data) the values of slope, relative slope and intercept are compared with those obtained by calculation (eqns. 4.20, 4.21 and 4.22).

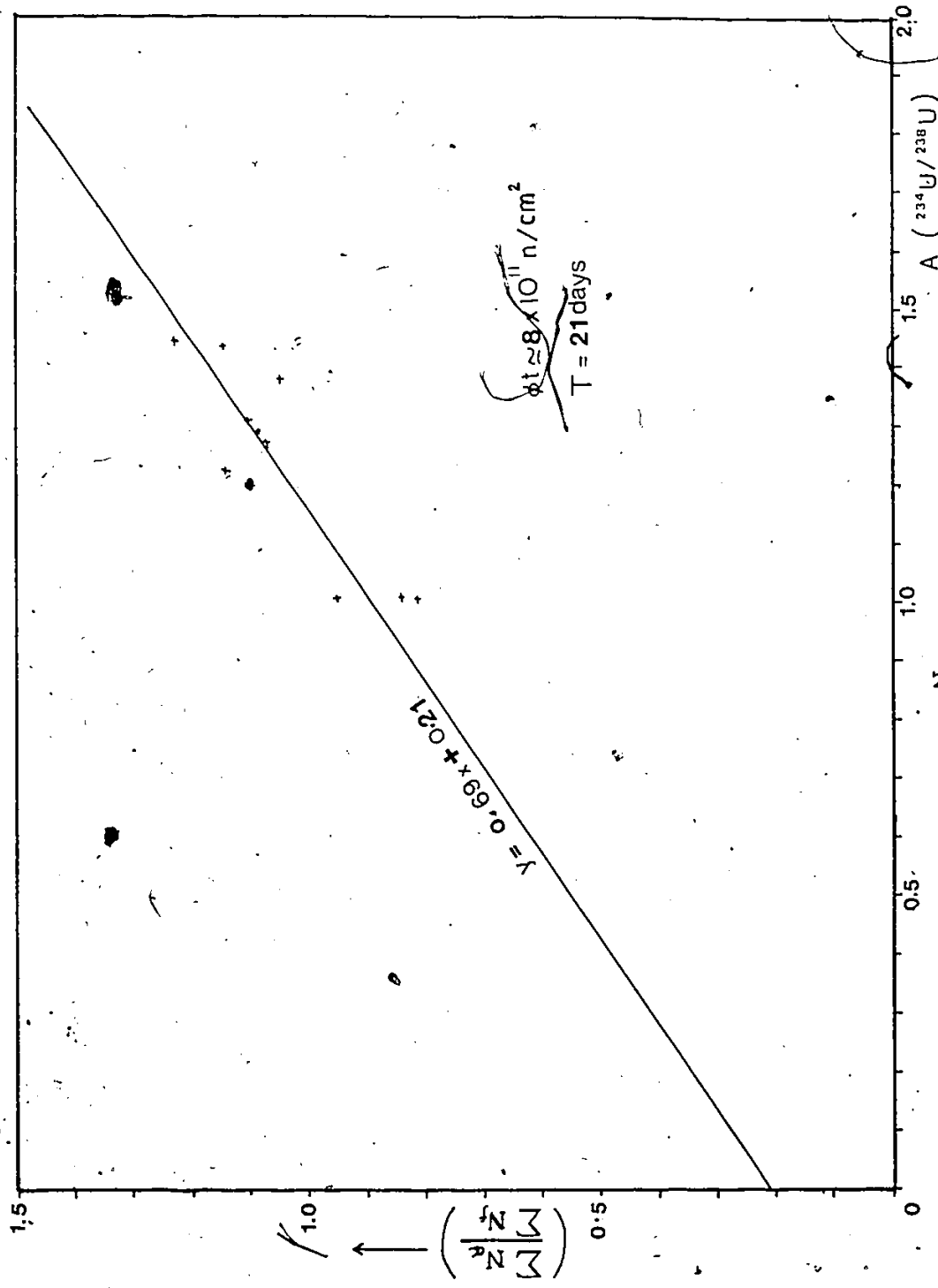


Fig. 35. A Regression Curve of $\sum \frac{N_f}{N_r}$ versus Uranium Activity Ratio for Set J.

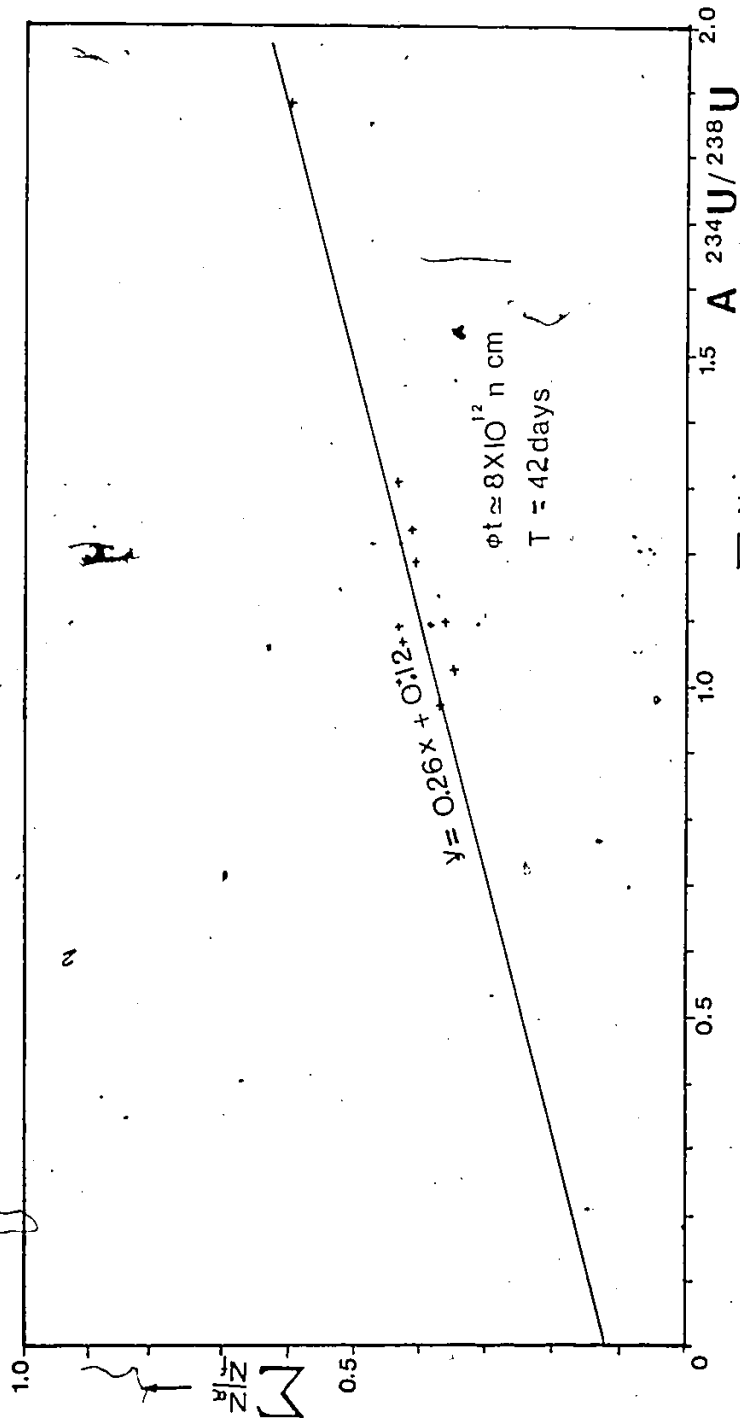


FIG. 36. A REGRESSION CURVE OF: $\sum_{N_i}^{N_i}$ VERSUS URANIUM ACTIVITY RATIO FOR SET K.

The comparison results are given in Table 9. It can be seen that all calculated values except slopes for set K show discrepancy with that of the experimental values. This disagreement may be attributed to possible error of estimated ϕt value which cannot be accurately controlled; the calculated values are dependent of the neutron fluxes used. Presumably the measured ϕt value for set K is true (i.e. based on slope agreement), hence, ϕt for set J may be corrected. Taking the relative slope to be 2.65 (i.e. experimental data), therefore the corrected ϕt for set J should be 1.51×10^{12} n/cm²; if so, the calculated slope and intercept would be 0.69 and 0.72, respectively. However, it appears that the calculated intercepts for both sets are still larger than that found experimentally. The reason for this is not known.

Table 9 -- Experimental and Calculated Values of Slope, Relative Slope and Intercept.

Sample #	T/ ϕt	Relative Slope ($\frac{k_1}{k_2}$)		Slope (k)		Intercept (I)	
		Exptl.	Calc.	Exptl.	Calc.	Exptl.	Calc.
set K	1.44×10^{-14}	2.65	5.04	0.26	0.27	0.12	0.28
set J	7.19×10^{-14}			0.69	1.36	0.21	1.42

Set J: $T_1 = 5.75 \times 10^{-2}$ year;

$\phi_1 t_1 = 8 \times 10^{11}$ n/cm² \pm an order of magnitude

Set K: $T_2 = 1.15 \times 10^{-1}$ year;

$\phi_2 t_2 = 8 \times 10^{12}$ n/cm² \pm an order of magnitude

The uranium activity ratio ($^{234}\text{U}/^{238}\text{U}$) can be obtained by substituting $\Sigma N / \Sigma N_f$ value of each sample from sets J and K in equations (4.24) and (4.26), respectively. The results are given in Tables 7 and 8. From the comparative study made in Tables 7 and 8, it shows that the method based on combined fission track and alpha track counting in the determination of uranium activity ratio ($^{234}\text{U}/^{238}\text{U}$) is generally in good agreement with that of the alpha spectrometry method. The results exhibited reasonable differences (± 0.20) within the interval of activity ratios considered. The average errors are 3% and 7% for sets K and J respectively. From this study it may be concluded that the technique may have a great potential to be applied for determination of uranium activity ratios in water and perhaps, also be applicable for other geological materials.

However, one of the main drawbacks of the present study is that the tracks have to be counted by eye. Counting the tracks manually is a time-consuming process, averaging about 3 hours per sample for counting about 10000 tracks. Furthermore, there is a factor of operator fatigue when counting large quantities of tracks. Also, the efficiency may differ from one track observer to another because of the subjective criteria employed in track recognition. However, when an automatic counting system is available it can greatly reduce the time for counting. The system can count in a matter of a few minutes for an analysis. The auto-counting system is now widely used, particularly for fission track counting (Gold and Cohen, 1972; Khan and Durrani, 1972; Gross and Tommasino, 1970; Cogel et al., 1972 and others). Automatic counting equipment would be a more objective means of track counting; the efficiency for counting

would be different than for manual counting with an optical microscope.

In summary, the combined fission track and alpha track counting can give a good estimate of uranium activity ratio ($^{234}\text{U}/^{238}\text{U}$) in water samples. This method may be useful for determining $^{234}\text{U}/^{238}\text{U}$ ratio in water samples of very low uranium concentration because it only requires very small quantity of water sample for an analysis. At very low uranium concentration it may be difficult to analyse by the α -spectrometry method. Furthermore, the technique does not need specialised electronic equipment. If a nuclear reactor is available, the cost per sample is fairly low. Moreover, this method is simple, direct and may be rapid provided an auto-counting system is available. However, for good reproducibility, the experimental conditions have to be strictly controlled such as etching condition and particularly the total thermal neutron flux (n/cm^2) must be determined with accuracy. Unfortunately, the integrated neutron flux was not determined accurately in this work. Also, a standard calibration should be performed to determine for both alpha- and fission-track detection efficiency. Nevertheless, further refinements of the technique are necessary to make it reliable and quantitative.

CHAPTER V

SUMMARY

The plutonic rocks that outcrop at the Greyhawk Uranium Mine area consist mainly of pegmatitic granite and intruding metagabbro. The uranium ore is found in porphyroblastic leucogranite. As a result of mining operations the waste rocks (pegmatite and gabbro) were piled up at the site. These waste rocks have undergone weathering processes and consequently introduce leachate to the aquifer.

The ground water system in the area is quite complex and is largely controlled by the free-water elevation in the swamp. The surface water drainage is towards the south-west, draining into Bentley Lake and Bow Lake.

The preliminary evaluation of the Greyhawk ground waters suggests that they can generally be divided into two types with respect to their geochemical constituents:

(i) The shallow ground water zone which has low total dissolved solids, and

(ii) the deeper ground water zone which has a much higher total dissolved solids. The principal constituents of the leachate are calcium, sulphate and bicarbonate. These were produced during rock weathering process where pyrite (FeS_2), calcite (CaCO_3), dolomite ($\text{CaMg}(\text{CO}_3)_2$) and anorthite ($\text{CaAl}_2\text{Si}_2\text{O}_8$) are assumed to be the main source of major ion weathering products.

The Greyhawk ground waters generally contained significant concentrations of uranium, with most of samples at deep sampling points usually showing high uranium content than shallower samples. Uranium in these waters formed complexes with carbonate and sulphate ions. Uranium contents in the waters decrease with distance from the waste rock; part of the dissolved U is taken up by the porous medium as it flows through the aquifer.

The Greyhawk ground waters have a relatively low $^{234}\text{U}/^{238}\text{U}$ ratio (0.95 to 1.85); high activity ratio values are usually associated with deep sampling points. The flow pattern of contaminants emanating from the waste rock source was deduced from the ^{234}U -enriched water distribution pattern. It appears that the contaminants is migrating at intermediate and bottom depths of the aquifer.

The determination of uranium content in the samples with the neutron activation-delayed neutron counting technique is promising. The technique indicated that provided an appropriate neutron irradiation is available, the method is rapid, accurate and precise. The technique is capable of handling about 3000 samples per day at the current capacity of the McMaster University Nuclear Research Reactor.

A new technique to determine uranium isotopic ratio ($^{234}\text{U}/^{238}\text{U}$) using combined alpha-track and fission-track was developed. With this technique it was generally feasible to obtain a first estimate value of uranium isotopic ratio ($^{234}\text{U}/^{238}\text{U}$). Considerable improvements on the method are still to be made in order to obtain a better precision; counting of tracks may be done quickly by using the auto-counting system

instead of visual counting; and by counting more tracks the technique would give a higher precision. To the best of the author's knowledge this technique is the first ever initiated and applied in determining $^{234}\text{U}/^{238}\text{U}$ ratio in natural environments. Therefore, naturally the author does not expect a high degree of perfection in this technique particularly at the early stage. However, this study would provide an intriguing insight into near future research possibilities.

APPENDIX I

ELECTROPLATING PROCEDURE FOR URANIUM

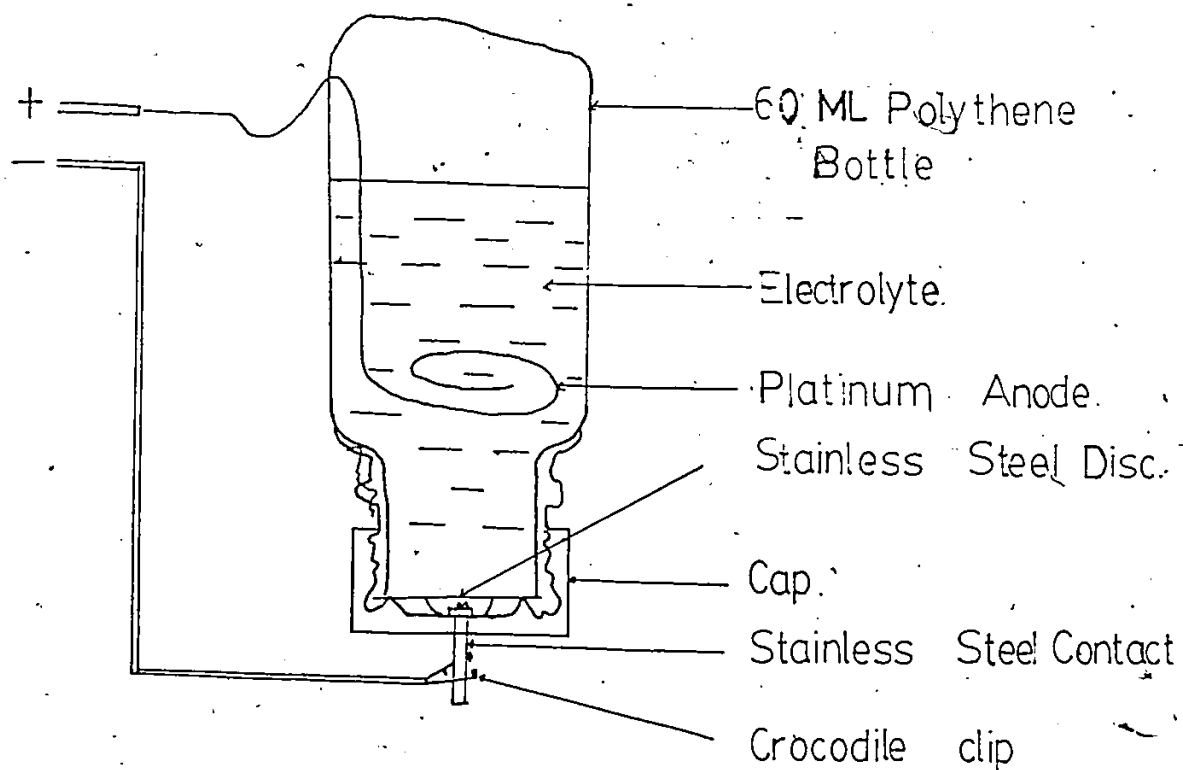
(Modified after A. Latham)

Materials:

- (1) Electrolyte of $\text{HNO}_3 + \text{H}_2\text{SO}_4$ (4 ml of conc. HNO_3 and 0.5 ml of conc. H_2SO_4 added to about 500 mls of deionised (distilled water), adjusted to pH of about 1.5 with NH_4OH .
- (2) A 1-inch diameter stainless steel disc (i.e. the cathode to be electrodeposited).
- (3) An electroplating cell made from a 60 ml polyethylene bottle. The bottom is part removed and is used as a lid. The cap has a stainless steel bolt holding a small stainless steel leaf spring which lightly "spring loads" against the disc when the bottle is screwed against it.
- (4) A platinum wire spiral acts as anode.
- (5) An adjustable d-c power supply to deliver up to several Amps. with an ammeter.
- (6) 0.1N HCl for washing the platinum anode.
- (7) Acetone for cleaning and washing.

The Procedure:

- (1) After the final separation step of U from other interfering elements (as mentioned in the text), take up U again in the electrolyte.
- (2) Wash a stainless steel disc with acetone and place it in the cap of the cell.

FIG. 37 DIAGRAM OF THE APPARATUS

(3) Screw on the bottle tightly and clamp the cell by the cap in the upside down position.

(4) Place the cleaned platinum spiral (anode) into the cell about 1.5 cm from the cleaned disc (i.e. cathode).

(5) Pour the electrolyte containing the U into the cell. Rinse the beaker twice and add more electrolyte into the cell so that the level in the cell is about $\frac{4}{5}$ full. Close the lid.

(6) Connect the cell to a d-c battery. Switch on and adjust the current to about 0.8 Amps. Plate for about 3 to 4 hours.

(7) At the end of deposition do not switch off. Instead, remove the lid and then quickly invert the cell. This prevents the U from going back into solution.

(8) With the cathode crocodile clip now disconnected, keep the cell inverted and squirt the disc with acetone.

(9) Leave the platinum spiral in 0.1N HCl until the next plate out.

Notes:

(i) Efficiency:

Three experiments were carried out for checking the efficiency of electroplating of U with the above procedure using ^{232}U spike solution. Results of the 3 experiments showed that the recovery of ^{232}U are 70, 88 and 90 per cent; 3 to 4 hours plating time yielded 88 and 90% recovery while 2 hours plating time yielded only 70%. Thus, 3 to 4 hours plating time should be sufficient.

(ii) The HNO_3 electrolyte is used to prevent vigorous hydrogen gassing at the cathode but this may occur if a higher current is used (1.0 Amps). Vigorous gassing may result in a poor quality of deposit.

(iii) The deposit, before any flaming should be fairly even over the area and have a metallic sheen.

REFERENCES

- Adams, A. S., J. K. Osmond and J. J. W. Rogers, 1959. The Geochemistry of Th and U; in "Physics and Chemistry of the Earth", V3, L. H. Ahrens et al., 298-348.
- ALPHA-AWWA-WPCF, 1975. Standard Methods. American Public Health Association, Washington, D.C., 1193 pp.
- American Public Health Assn., American Water Work Assn. and Water Pollution Federation, 1975. Standard Methods for the examination of water and waste water. 14th Ed. Washington D.C., U.S.A.
- Amiel, S., 1962. Analytical applications of delayed neutron emission in fissionable elements. Anal. Chem., 34, 1683-1692.
- Amiel, S., J. Gilat and D. Heymann, 1967. Uranium content of chondrites by thermal neutron activation and delayed neutron counting. Geochim. Cosmochim. Acta 31 1498-1504.
- Andrews, J. N. and R. L. F. Kay, 1978. The evolution of enhanced $^{234}\text{U}/^{238}\text{U}$ activity ratios for dissolved uranium and ground water dating. U.S. Geol. Surv., open-file Rpt., 135. 78-701, 11-13.
- Andreyev, P. F. and A. P. Chumachenko, 1964. Reduction of uranium by natural organic substances. Geochem. Intl. 1 3-7.
- Bastle, L. H., 1969. Migration of radionuclides in porous media; in "Health Physics", A. M. F. Duhamel (editor), V2 pt. 1, 707-730.
- Barker, F. B. and R. C. Scott, 1958. Uranium and Radium in the ground water of the Llamo Estacado, Texas and Mexico. Am. Geop. Union, V39(3), pp. 459-466.

- Baturin, G. N., 1968. Geochemistry of uranium in the Baltic. *Geochem. Intl.* 5: 344-348.
- Bertine, K. K., L. H. Chan and K. K. Turekian, 1970. Uranium determinations in deep-sea sediments and natural waters using fission tracks. *Geochim. Cosmochim. Acta* 34: 641-648.
- Boulanger, A., D. J. R. Evans and B. F. Raby, 1976. Uranium analysis by neutron activation delayed neutron counting. Atomic Energy Canada (unpublished).
- Branov, V. I., Y. A. Surkov and V. D. Vilenskii, 1958. Isotopic shifts in natural uranium compounds. *Geochem. Intl.* 5: 591-599.
- Brits, R. J. N., 1979. A routine method for the determination of the $^{234}\text{U}/^{238}\text{U}$ ratio in natural water. *Chem. Geol.* 25: 347-354.
- Burwash, R. A. and G. L. Cumming, 1976. Uranium and thorium in the Precambrian basement of western Canada. I. Abundance and distribution. *Can. J. Earth Sc.*, 13: 284-293.
- Chalov, P. I., 1959. The $^{234}\text{U}/^{238}\text{U}$ ratio in some secondary minerals. *Geochemistry (1959)* 203-210.
- Chalov, P. I., T. V. Tuzava and Y. A. Musin, 1964. Isotopic ratio $^{234}\text{U}/^{238}\text{U}$ in natural waters and its use for nuclear geochronology. *Geochem. Intl.* 1: 402-408.
- Chalov, P. I., K. I. Merkulova and T. V. Tuzova, 1966. The $^{234}\text{U}/^{238}\text{U}$ ratio in the water and bottom sediments of the Aral Sea and the absolute age of the basin. *Geochem. Intl.* 3: 1149-1155.
- Chalov, P. I. and K. I. Merkulova, 1969. Possibility of controlled separation of ^{234}U and ^{238}U by external oxidation of uranium in minerals. *Geochem. Intl.* 6: 159-162.

- Chalov, P. I., N. A. Svetlichnaya and T. V. Tuzova, 1970. ^{234}U and ^{238}U in the waters and bottom sediments of Lake Balkhash and the age of the Lake. *Geochem. Intl.* 7: 604-609.
- Chamberlain, J. A., 1964. Hydrogeochemistry of uranium in the Bancroft-Haliburton region, Ontario. *Geol. Surv. Can., Bull.* 1030-F, 19 pp.
- Chapman, L. J. and D. F. Putman, 1951. The physiography of southern Ontario. Univ. of Toronto Press, 2nd ed., 386 pp.
- Cherdyntsev, V. V., Z. A. Malyshev, I. N. Sokolova, I. V. Kazachevskiy and I. V. Borisov, 1964. Isotopic composition of uranium and thorium in the supergene zone. *Geochem. Intl.* 1: 398-401.
- Cherdyntsev, V. V., I. V. Kazachevskiy and Y. A. Kuz'mina, 1965. Dating of pleistocene carbonate formations by the thorium and uranium isotopes. *Geochem. Intl.* 2: 794-801.
- Cherdyntsev, V. V., 1971. Uranium-234. Israel Program for Scientific Translations, Monson, Jerusalem, 308 pp.
- Cohen, P., 1964. An evaluation of uranium as a tool for studying the hydrogeochemistry of the Truckee Meadows area, Nevada. *Jour. Geop. Res.* 66(12) 4199-4206.
- Congel, F. J., J. H. Roberts, D. Dries, J. Kastner, B. G. Oltman, R. Gold and R. J. Armani, 1972. Automatic system for counting etched holes in thin dielectric plastics. *Nucl. Instr. and Meth.*, 100: 247-252.
- Cowart, J. B. and J. K. Osmond, 1977. Oxidation/Reduction in the Edwards limestone aquifer as indicated by dissolved uranium isotopes. *Geol. Soc. Am., Abs. with Prog.* 7, p. 938.

- Cowart, J. B. and J. K. Osmond, 1977. Uranium isotopes in ground water: their use in prospecting for sandstone-type uranium deposits. *J. Geochem. Expl.* 8: 365-379.
- Cowart, J. B., J. K. Osmond and M. I. Kaufman, 1978. Uranium isotopic variations in groundwater of the Floridan aquifer and Boulder Zone south of Florida. *J. Hydrol.* 36: 161-172.
- Cross, W. G. and L. Tommasino, 1970. A rapid reading technique for nuclear particle damage tracks in thin foils. *Radiation Effects*, 5: 85-89.
- Cumming, C. L., 1974. Determination of uranium and thorium in meteorites by the delayed neutron method. *Chem. Geol.* 13: 257-267.
- Davis, J. C., 1973. *Statistics and Data Analysis in Geology*. John Wiley, Toronto, 550 pp.
- Dement'yev, V. S. and N. G. Syromyatnikov, 1968. Conditions of formation of a sorption barrier to the migration of uranium in an oxidising environment. *Geochem. Intl.* 5: 394-399.
- Doi, K., S. Hirono and Y. Sakamaki, 1975. Uranium mineralization by ground water in sedimentary rocks, Japan. *Econ. Geol.* 70: 628-646.
- Dooley, J. R., M. Tatsumoto and J. N. Rosholt, 1964. Radioactive disequilibrium studies of roll features, Shirley Basin, Wyoming. *Econ. Geol.* 59: 586-595.
- Dooley, J. R., H. C. Granger and J. N. Rosholt, 1966. Uranium-234 fractionation in the sandstone-type uranium deposits of the Ambrosia Lake district, New Mexico. *Econ. Geol.* 61: 1362-1382.
- Faure, G., 1977. *Principles of Isotope Geology*. John Wiley, Toronto, 464 pp.

- Fix, P. F., 1955. Hydrogeochemical exploration for uranium. U.S. Geol. Surv., Prof. Pap., 300: 667-671.
- Fleischer, R. L. and O. G. Raabe, 1978. Recoiling alpha emitting nuclei: Mechanism for uranium-series disequilibrium. Geochim. Cosmochim. Acta 7: 973-978.
- Freeze, R. A. and J. A. Cheery, 1979. Ground water. Prentice Hall, New Jersey, 604 pp.
- Gascoyne, M., 1977. Uranium series dating of speleothems: An investigation of technique, data processing and precision. Tech-Memo 77-4 Geol. Dept., McMaster University (unpublished).
- Gascoyne, M., 1979. Isotope and geochronologic studies of speleothem. Ph.D. Thesis, McMaster University, Hamilton, Ontario.
- Geraldo, L. P., M. F. Cesar, O. Y. Mafra and E. M. Tanaka, 1979. Determination of uranium concentration in water samples by the fission track registration technique. J. Radioanal. Chem., 49(1): 115-126.
- Gillham, R. W., J. A. Cherry and H. D. Sharma, 1979. Hydrogeologic, hydrogeochemical and model studies of ground water contaminant migration from waste rock at an abandoned uranium mine near Bancroft, Ontario. Office of Research Administration, University of Waterloo, Progress Rept., 16 pp.
- Gold, R. and C. E. Cohn, 1972. Analysis of automatic fission track scanning in solid-state nuclear track recorders. Rev. Sc. Inst. 43(1): 18-28.
- Goldhaber, M. B., R. L. Reynolds and R. O. Rye, 1978. Origin of a South Texas roll-type uranium deposit: II sulfide petrology and sulfur isotope studies. Econ. Geol. 73: 1690-1705.

- Griffith, J. W., 1967. The uranium industry--its history, technology and prospects.
- Grisak, G. E. and R. E. Jackson, 1978. Geochemical retardation processes; in "An appraisal of the hydrogeological process involved in shallow subsurface radioactive waste management in Canadian terrain". Inland Water Resources. Fisheries and Environment Canada, 84: 36-74.
- Hanson, R. O. and P. R. Stout, 1968. Isotopic distributions of uranium and thorium in soils. Soil Sc. 105(1): 44-50.
- Hashimoto, T., 1971. Determination of the uranium content in sea water by a fission track method with condensed aqueous solution. Geochim. Cosmochim. Acta 56: 347-354.
- Hewitt, D. F., 1957. Cardiff and Faraday townships, Ont. Dept. Mines, Map 1957-1.
- Hewitt, D. F., 1959. Geology of Cardiff and Faraday Townships, Ont. Dept. Mines, 66th Ann. Rept. 3.
- Hostetler, P. B. and R. M. Garrels, 1962. Transportation and precipitation of uranium and vanadium at low temperatures, with special reference to sandstone type uranium deposits. Econ. Geol. 57(2): 137-167.
- Huang, W. H. and R. M. Walker, 1967. Fossil alpha particle tracks: A new method of age determination. Science, 155: 1103-1106.
- Kaufman, M. I., R. S. Rydell and J. K. Osmond, 1969. $^{234}\text{U}/^{238}\text{U}$ disequilibrium as an aid to hydrologic study of the Floridan aquifer. J. Hydrol. 2: 374-386.

- Khan, H. A. and Durrani, S. A., 1972. Electronic counting and projection of etched tracks in solid state nuclear track detectors. Nuclear Inst. and Method 101: 583-587.
- Kigoshi, K., 1971. Alpha recoil Th-234: Dissolution into water and the $^{234}\text{U}/^{238}\text{U}$ disequilibrium in nature. Science, 173: 47-48.
- Kobashi, A; J. Sato, and N. Saito, 1979. Radioactive disequilibrium with uranium, thorium, and radium isotopes leached from euxenite. Radiochim. Acta 26: 107-111.
- Koide, M. and E. O. Goldberg, 1965. $^{234}\text{U}/^{238}\text{U}$ ratios in sea water: in Progress in Oceanography, V3, Pergamon Press, London, 173-177.
- Kronfeld, J., 1972. Hydrologic investigation of the ground water of central Texas using U-234/U-238 disequilibrium. Ph.D. Thesis, Rice University.
- Kronfeld, J. and J. A. S. Adams, 1974. Hydrologic investigations of the ground waters of central Texas using $^{234}\text{U}/^{238}\text{U}$ disequilibrium J. Hydrol. 22: 77-88.
- Kronfeld, J., 1974. Uranium deposition and Th-234 alpha-recoil: An explanation for extreme $^{234}\text{U}/^{238}\text{U}$ fractionation within the Trinity aquifer. Earth Plan. Sci., Lett. 21: 327-330.
- Kronfeld, J., E. Gradsztajn, N. W. Muller, J. Radin, A. Yaniv and R. Zach, 1975. Excess ^{234}U : An aging effect in confined waters. Earth Plan. Sci. Lett., 27: 342-345.
- Kronfeld, J., E. Gradsztajn and A. Yaniv, 1979. A flow pattern deduced from uranium disequilibrium studies for the Cenomanian carbonate aquifer of the Beersheva region, Israel. J. Hydrol. 44: 305-310.
- Lang, A. H., J. W. Griffith and H. R. Steacy, 1962. Canadian deposits of the uranium and thorium. Geol. Surv. Can., Econ. Geol. 16.

- Langmuir, D., 1978. Uranium solution-mineral equilibria at low temperatures with applications to sedimentary ore deposits. *Geochim. Cosmochim. Acta* 42: 547-569.
- Lisitsin, A. K., 1962. Form of occurrence of uranium in ground waters and conditions of its precipitation as UO_2 . *Geochemistry Vol. 1962*: 876-884.
- Lively, R. S., R. S. Harmon, A. A. Levinson and C. J. Bland, 1979. Disequilibrium in the uranium-238 series in samples from Yeelirrie, Western Australia. *J. Geochem. Expl.* 12: 57-65.
- Lopathina, A. P., 1964. Characteristics of migration of uranium in the natural waters of humid regions and their use in the determination of the geochemical background for uranium. *Geochem. Intl.* 1: 788-794.
- Millard, H. T. Jr., 1974. Determination of uranium and thorium in USGS standard rocks by the delayed neutron technique; in "Description and Analysis of seven new USGS standards. U.S. Geol. Surv., Prof. Pap. 840: 61-65.
- Morse, R. H., 1969. Radium geochemistry applied to prospecting for uranium. *Can. Min. Jour.*, May, 75-76.
- Morse, R. H., 1970. The surficial geochemistry of radium, radon and uranium near Bancroft, Ontario, with application to prospecting for uranium. Ph.D. Thesis, Queen's University, Kingston, Ontario.
- Morse, R. H., 1971. Comparison of geochemical prospecting methods using Ra with those Rn and U. *Geochem. Expl. CIM Spec.* V2: 215-230.

- Nordemann, L. M. M., 1980. Use of $^{234}\text{U}/^{238}\text{U}$ disequilibrium in measuring chemical weathering rate of rocks. *Geochim. Cosmochim. Acta* 44: 103-108.
- Ontario Water Resources, 1965. Radiological Water pollution in the Elliot Lake and Bancroft areas. *Ont. Wat. Res.*, 48 pp.
- Osmond, J. K., H. S. Rydell and M. I. Kaufman, 1968. Uranium disequilibrium in ground water: An isotopic dilution approach in hydrologic investigations. *Science*, 162: 997-999.
- Osmond, J. K., M. I. Kaufman and J. B. Cowart, 1974. Mixing volume calculations, sources and aging trends of Floridan aquifer water by uranium isotopic methods. *Geochim. Cosmochim. Acta* 38: 1083-1100.
- Osmond, J. K. and J. B. Cowart, 1976. The theory and uses of natural uranium isotopic variations in hydrology. *Atomic Energy Review*, 14(4).
- Picken, J. F., J. A. Cherry, G. E. Grisak, W. F. Merritt and B. A. Risto, 1978. A multilevel device for ground water sampling and piezometer monitoring. *Ground water* 16(5): 322-327.
- Price, P. B. and R. M. Walker, 1963. A simple method of measuring low uranium concentration in natural crystals. *App. Phys. Lett.*, 2: 23-25.
- Reynolds, R. L. and M. B. Goldhaber, 1978. Origin of a South Texas roll-type uranium deposit: I. Alteration of iron-titanium oxide minerals. *Econ. Geol.* 73: pp. 1677-1689.
- Robertson, D. E., 1968. The adsorption of trace elements in sea water on various container surfaces. *Analytica Chimica Acta*. 42: 533-536.

- Rogers, J. J. W. and J. A. S. Adams, 1969. Uranium. In: Handbook of Geochemistry, (editors, K. H. Wedepohl et al., II/1, Springer-Verlag, Berlin.)
- Rosholt, J. N., W. R. Shields and E. L. Garner, 1963. Isotopic fractionation of uranium in sandstone. *Science* 139: 224-226.
- Rosholt, J. N., A. P. Butler, E. L. Garner and W. R. Shields, 1965. Isotopic fractionation of uranium in sandstone, Powder River Basin, Wyoming, and Slick Rock District, Colorado. *Econ. Geol.* 60: 199-213.
- Scatterly, J., 1956. Radioactive mineral occurrences in the Bancroft area. Ont. Dept. Mines, Ann. Rept. 65; pt. 6: 117-121.
- Schwarcz, H. P., 1978. Dating methods of Pleistocene deposits and their problems II. Uranium-series disequilibrium dating. *Geosc. Can.* 5(4): 184-188.
- Stumm, W. and J. J. Morgan, 1970. Aquatic chemistry. John Wiley, New York.
- Swanson, V. E., 1961. Geology and geochemistry of uranium in marine black shales. U.S. Geol. Surv., Prof. Pap., 356-C: 90-100.
- Thode, H. G., H. Klearskoper and D. McElcheran, 1951. Isotope fractionation in the bacterial reduction of sulphate. *Research (London)*, 4: 581-582.
- Thompson, P., 1973a. Speleochronology and late Pleistocene climates inferred from O, C, H, U and Th isotopic abundances in speleothems. Ph.D. Thesis, McMaster University, Hamilton, Ontario.
- Thompson, 1973b. Procedures for extraction and isotopic analysis of uranium and thorium from speleothem. Tech. Memo. 73-9, Dept. of Geology, McMaster University.

- Thompson, P., D. C. Ford, and H. P. Schwarcz, 1975. $^{234}\text{U}/^{238}\text{U}$ ratios in limestone cave seepage waters and speleothem from West Virginia. *Geochim. Cosmochim. Acta* 39: 661-669.
- Thurber, D. L., 1962. Anomalous $^{234}\text{U}/^{238}\text{U}$ in nature. *J. Geophys. Res.* 67(11): 4518-4520.
- Thurber, D. L., 1965. The concentrations of some natural radioelements in the waters of the Great Basin. *Bull. Volcanol.*, 28: 195-201.
- Titayeva, N. A. and T. I. Veksler, 1977. The state of radioactive equilibrium in the uranium and thorium series as an indicator of migration of radioactive elements and active interaction between phases under natural conditions. *Geochem. Intl.* 14(4): 99-107.
- Umemoto, S., 1965. $^{234}\text{U}/^{238}\text{U}$ in seawater from the Kuroshio region. *J. Geophys. Res.* 70: 5326-5327.
- Veselsky, J., 1974. An improved method for the determination of the ratio $^{234}\text{U}/^{238}\text{U}$ in natural water. *Radiochim. Acta* 21: 151-154.
- Veska, E., R. W. Gillham, J. A. Cherry and H. D. Sharma, 1979. An evaluation of the Greyhawk Mine area for conducting detailed investigations of the migration of Ra-226 and associated contaminant in unconsolidated geological materials. Offices of Research Administration, University of Waterloo, Progress Rept., 36 pp. (Unpublished).
- Vinogradov, A. P., 1959. The geochemistry of rare and dispersed chemical elements in soils. Consultants Bureau Inc., New York.

Wakshal, E. and F. Yaron, 1974. $^{234}\text{U}/^{238}\text{U}$ disequilibrium in waters of the Judea Group aquifer in Galilee, Northern Israel; in "Isotope Techniques in Ground water Hydrology", V2, IAEA, 151-177.

Zaichik, V. E., 1973. Instrument for counting tracks on the surface of solid track detectors. Instr. and Exptl. Techniques 15: 1669-1671.